UNIVERSITÀ
DEGLI STUDI
DI PADOVA

Administrative unit: **Università degli Studi di Padova**

Department: **Territorio e Sistemi Agro-Forestali (TESAF)**

PhD Program: **Land, Environment, Resources, Health (LERH)**

Batch: XXIX

Thesis title: Suspended sediment fluxes in an Alpine torrent basin

PhD Program Coordinator: Prof. Davide Matteo Pettenella

Supervisor: Prof. Mario Aristide Lenzi

PhD candidate : Adriana García-Rama Ocaña

Suspended sediment fluxes in an Alpine torrent basin

Ph.D thesis

Adriana García-Rama Ocaña

CONTENTS

LIST OF FIGURES

LIST OF TABLES

ABSTRACT

Suspended sediment transport regards the finer material present in the channel and can be defined as the mobilization of particles suspended in water columns. This process is highly influenced by several factors, especially in mountainous areas, where it depends upon the size, morphology and lithology of the catchment, the stability of the coarse surface layer, the vegetation cover, the soil moisture and the characteristics of the precipitation, among others. Due to the many factors controlling it, suspended sediment transport in mountainous streams features greater variability than in low-land rivers. The assessment of suspended sediment transport, which can contribute up to the 100% of the total sediment load in mountainous areas, becomes necessary for the study of the solid transport in this kind of watersheds. In this context, intensive monitoring and long data series are a basic key in understanding the dynamics of the fine sediment fluxes interpreting the interactions of the factors influencing them and predicting the suspended sediment loads. Even so, studies of the suspended sediment transport in mountain catchments with an extended monitoring period are rare in literature.

This thesis aims to analyze the suspended transport dynamics occurring in the Rio Cordon catchment, located in the eastern Italian Alps (Dolomites). The general objectives are to investigate the quantity and effectiveness of the fine sediment delivered by the sources present in the basin area, to assess the main factors affecting the suspended sediment fluxes in both long- and short-term, and to identify hydrological thresholds that control the response of suspended sediments to the water inputs. The Rio Cordon is a small catchment of 5 km^2, characterized by step-pool and riffle-pool morphology and by a mean slope equal to 13%. It features the typical Alpine climatic conditions, due to which the runoff shows a nivo-pluvial regime dominated by snowmelt between May and June and characterized by significant floods due to persistent rainfall in summer and early autumn. A continuous monitoring station located at the outlet of the basin provides us with data since 1986. Three decades of monitoring of fine sediment fluxes have been analyzed at different time scales, ranging from long- (30 years) to short- term analysis (single event). The assessment of the annual sediment budget through the whole study period has shown that during the three decades, 79% of the total load registered in Rio Cordon was suspended load (11962 t). Nonetheless, this contribution was heterogeneously distributed both seasonally and through the years. The study of the seasonal behavior throughout the whole study period permits to appreciate substantial differences among years. Before 2001 the years showing higher loads from snowmelt events than from rainfall events were rare (only 5 cases out of 15), while from 2001 to 2015, snowmelt was the main suspended sediment contributor of the year in 10 cases.

The analysis of the single events included the study of several parameters, such as the water discharge, the suspended sediment concentration, the runoff volumes, the total suspended sediment load, the characteristics of the precipitation, and the previous rainfall conditions. Hysteresis relationship between water discharge (Q) and suspended sediment concentration (SSC) at the event scale was described by analyzing the SSC/Q ratios of the rising and descending limbs of hydrograph and sedigraph. The barycenters of the sedigraph and hydrograph were calculated using Varignon's theorem of moments in aims to add information about the way SSC and Q change within the event. Once assessed the sediment transport characteristics of the single events occurring during the study period, the sediment entrainment conditions were investigated. In this context, an exhaustive comparison with the flood events occurring in the Carapelle torrent was performed. The Carapelle is a medium-sized catchment of 50 km^2 located in the Apulia Region, characterized by a Mediterranean climate and geomorphologic conditions. The analysis of the flood events occurred in both catchments permitted to assess the differences between them and the common factors that control the transport dynamics. Whilst 67.6% of the events analyzed in the Rio Cordon showed a clockwise behavior, 88% of the events showed a counter-clockwise behavior in the Carapelle torrent. Antecedent precipitations had greater influence in the transport dynamics in the Carapelle, whilst the rainfall characteristics during the event were more relevant in the Cordon. Differences in the catchment size and in the coupling explained the main differencesbetween catchments. Statistical analyses suggested that the main factors affecting suspended sediment transport are related to the flood properties and to the precipitation characteristics in both catchments.

Field campaigns developed in 2014 and 2015 in the Rio Cordon catchment highlighted different responses to the water input at different reaches of the main channel that have a role in the transport dynamics.

The results of this long-term analysis in the Rio Cordon have highlighted the temporal heterogeneity of the transport dynamics in this catchment, as well as the unpredictability that characterizes them. The catchment shows a stability trend, which can be interrupted if a high intensity flood event takes place. In this case, some source areas remain active for some time after the event, and the following events (both rainfall and snowmelt) show higher supply conditions. The sediment sources that contribute to the suspended sediment budget are usually located in the surroundings of the lower part of the main channel, thus indicating low coupling between the hillslopes from the upper areas of the catchment and the stream main channel.

RIASSUNTO

Il trasporto di sedimenti in sospensione riguarda il materiale fine presente nel corso d'acqua, e può essere descritto come la mobilizzazione delle particelle sospese nella colonna d'acqua. Nelle aree montane questo processo è definito da molteplici fattori, tali come la dimensione, morfologia e litologia del bacino, la stabilità dello stratto superficiale grossolano del letto fluviale, la copertura vegetale, il contenuto idrico del suolo e le caratteristiche delle precipitazioni. Dati i numerosi fattori che ne condizionano le dinamiche, il trasporto di sedimenti in sospensione in torrenti montani presenta una maggiore variabilità rispetto ai fiumi di pianura. Negli ambienti montani, il contributo del materiale fine alla quantità totale di sedimento trasportato può arrivare fino al 100%, perciò l'analisi e la quantificazione di questo tipo di trasporto è di fondamentale importanza. A tal fine, il monitoraggio continuo e ripetuto nel lungo periodo risulta indispensabile per lo studio delle dinamiche dei flussi di sedimenti fini, nonché per l'interpretazione delle interazioni fra i fattori che influiscono in esse e per la predizione delle produzioni solide. Nonostante ciò, i lavori che analizzano il trasporto in sospensione sulla base di a una lunga serie di dati sono particolarmente rari.

L'obiettivo di questa tesi consiste nello studio delle dinamiche di trasporto del materiale sospeso nel bacino del Rio Cordon situato nelle Alpi Italiane. Il lavoro punta ad analizzare la quantità del materiale rilasciato dalle sorgenti di sedimento presenti nel bacino e l'effettività del trasporto, studiare i fattori principali che hanno un ruolo nel deflusso dei sedimenti sia nel breve che nel lungo termine, ed identificare le soglie idrologiche che controllano la risposta dei solidi ai contributi liquidi. Il bacino del Rio Cordon è un bacino dolomitico di piccole dimensioni (5 km^2) il cui collettore principale è caratterizzato da morfologie a *step-pool* e a *riffle-pool* e da una pendenza media pari al 13%. Il bacino presenta le condizioni climatiche tipiche delle zone alpine, per le quali il regime nivo-pluviologico controlla il comportamento idrologico. Lo scioglimento nivale controlla i deflussi liquidi durante Maggio e Giugno, mentre durante l'estate e l'atunno il bacino è dominato da eventi di pioggia di alta intensità. Il monitoraggio continuo del bacino è stato permesso grazie ad una stazione sperimentale installata nel 1986 in corrispondenza della sezione di chiusura. Questo lavoro analizza tre decadi di dati di trasporto in sospensione in diverse scale temporali, partendo dal lungo periodo (studio interannuale) fino al breve periodo (studio di eventi singoli).

Grazie alle serie di dati disponibili, sono state studiate le produzioni annuali.In tre decadi di monitoraggio sono state trasportate 11962 t di solidi sospesi, il 79% del materiale solido totale trasportato. Tuttavia, sia il contributo annuale che quello stagionale mostrano delle variazioni notevoli.

Lo studio delle tendenze stagionali permette di aprezzare delle differenze fra i diversi anni. Prima del 2001, il contributo dello scioglimento nivale al trasporto in sospensione era molto limitato. Successivamente, tra il 2001 ed il 2015 si è visto come in undici eventi il contributo maggiore di solidi sospesi sia stato rappresentato dallo scioglimento nivale.

Lo studio dei singoli eventi prevede l'analisi di diversi parametri, come le portate liquide, la concentrazione di sedimenti in sospensione, i volumi di deflusso, il trasporto totale di sedimenti fini, le caratteristiche delle precipitazioni e le condizioni di pioggia precedenti l'evento. Il rapporto d'isteresi fra la portata (Q) e la concentrazione di sedimenti in sospensione (SSC) a scala di evento è stato analizzato attraverso i valori di SSC/Q nel ramo ascendente e discendente dell'idrogramma e del sedimentogramma. I baricentri di queste due curve sono stati calcolati con il teorema dei momenti di Varignon con l'obiettivo di ottenere nuove informazioni sui cambiamenti di Q e SSC all'interno dell'evento. Questa procedura ha permesso di valutare la variabilità del trasporto in sospensione e di analizzare le condizioni di soglia per la mobilizzazione del materiale fine. È stato poi sviluppato un confronto tra questi risultati e quelli ottenuti dall'analisi degli eventi singoli registrati nel torrente Carapelle, un bacino di medie dimensioni (50 km^2) situato nel nord della Puglia e caratterizzato da condizioni climatiche e geomorfologiche tipiche dei bacini mediterranei. Dal confronto tra le due aree di studio, è stato possibile individuare le differenze nel comportamento ed analizzare i fattori che ne controllano il trasporto di sedimenti. Il 67.6% degli eventi osservati nel Rio Cordon ha mostrato un'isteresi oraria, mentre nel Carapelle l'88% degli eventi ha presentato un ciclo antiorario. Inoltre, il Carapelle è più influenziato dalle pioggie antecedenti del Rio Cordon, mentre che quest'ultimo mostra una risposta leggermente alle charatteristiche della precipitazione durante l'evento. I motivi principali di tali differenze possono essere riconducibili alle diverse dimensioni dei bacini e alla diversità di connettività riscontrata in ogni bacino. Diverse analisi statistiche hanno rivelato che i fattori che più influenzano il trasporto di sedimenti in sospensione in entrambi i bacini sono le caratteristiche dei deflussi e le precipitazioni.

I dati ottenuti dai lavori in campo sviluppati nel 2014 e 2015 nel Rio Cordon hanno sottolineato una risposta eterogenea ai deflussi da parte delle diverse aree del bacino. Questo ha delle conseguenze nelle dinamiche di trasporto.

I risultati di questa analisi di lungo termine hanno sottolineato la grande eterogeneità temporale che caratterizza le dinamiche di trasporto all'interno di questo bacino, così come l'imprevedibilità delle produzioni solide. Nonostante il bacino tenda alla stabilità, questa tendenza può venire interrotta da

eventi di alta intensità. In questo caso, l'attivazione di alcune aree sorgenti può causare il rilascio continuo di materiale anche durante gli eventi sucessivi (sia eventi di scioglimento che di pioggia), i quali mostrano dunque alte condizioni di disponibilità. Le aree sorgenti di sedimento che contribuiscono alla produzione totale misurata nella sezione di chiusura si trovano prevalentemente nelle vicinanze (oppure in prossimità) del collettore principale, a causa della disconnettività che caratterizza la parte intermedia del bacino.

1. CHAPTER ONE- BACKGROUND

1.1. State of the art

1.1.1. Mountain streams

Mountain streams are characterized by high slope (higher than 3-5%), sinuosity value close to 1 and high erosion capacity (Billi, 1994). Their geomorphic features and particular dynamics determine the characteristics of the solid material delivered to downstream channels, influencing on the quantity, timing and size of sediment transported by lowland rivers. Montgomery and Buffington (1997) defined five types of streambed morphology that can be found in alluvial mountainous channels: cascade, step-pool, plane bed, riffle pool and dune-ripple (Figure 1). Criteria for this division feature bedform pattern, dominant roughness elements, dominant sediment sources, sediment storage elements, grain ize, confinement and slope. The theoretical structure of an alluvial mountain channel would show all five types of bed morphology, starting from the cascade type at the top and finishing with the dune-ripple morphology at the lower part of the stream. Nevertheless, as slope does not usually show a regular decrease it is not easy to find the complete succession in nature and therefore a channel of this type unlikely contains all possible streambed morphologies. While pool riffle and dune ripple are more common with moderate slopes, the cascade, step-pool and plane bed configurations are the principal morphologies detectable in the high gradient channels.

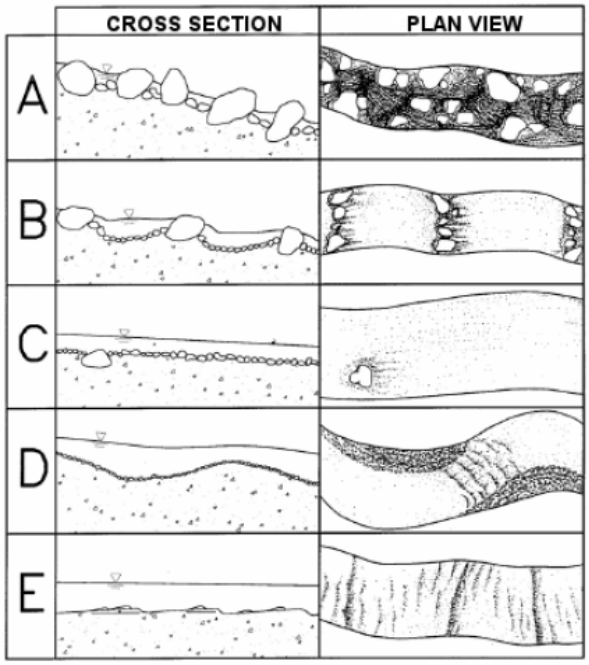

Figure 1: Channel bed morphology for alluvial channels (after Montgomery and Buffington, 1997).

Cascade morphology occurs on channels characterized by steep slopes that are narrowly confined. Cobbles and large boulders form its streambed, and it features feature high ratios of transport capacity to sediment supply and resiliency to changes in the sediment supply (Montgomery and Buffington, 1997). This morphology exhibits high stability with the larger elements becoming mobile only during infrequent events of recurrence interval (RI) greater than 50-100 years (Montgomery and Buffington, 1997). The main sources of roughness are the grains and banks.

Step-pool (Fig. 2) is the most common morphological structure of mountain streams (Billi et al. 1998; Lenzi, 2001). This structure can be found in narrower sections with a slope between 5 and 15%. It shows pools separated by boulders and cobbles, and large wood in some cases, organized into discrete channel-spanning accumulations (Montgomery and Buffington, 1997). It is usually associated with steep gradients, small width to depth ratios, elevated confinement and high ratios of transport capacity to sediment supply (Montgomery and Buffington, 1997). The flow shows critical and subcritical conditions over the steps and subcritical flow in the pools. As the cascade, this structure shows high resiliency to changes in the sediment supply and discharge. In fact, it takes form during extraordinary events and is very stable in case of ordinary events due to armoring processes (Whittaker and Jaeggi, 1982; Whittaker; 1987).

Figure 2: Step-pool structure in Rio Cordon

The plane bed morphology (Fig. 3) occurs in straight channels with moderate-high slopes, low width to depth ratios and large values of relative roughness, caused mainly by grains and banks

(Montgomery and Buffington, 1997). It features armored bed surfaces that that require near-bankfull conditions for the entrainment of sediment. Due to this armoring, sediment supply is commonly limited.

Figure 3: Plane bed morphology in Rio Cordon

Low-gradient alluvial channels (pool-riffle and dune ripple) have lower ratios of transport capacity to sediment supply, and a greater response to changes in sediment supply. Their streambed, composed gravels and sands features higher sinuosity than the previous types, and their dominant sediment sources are the banks and the channel.

The geomorphic characteristics of the mountainous streams affect considerably their sediment transport processes, which differ significantly from those occurring in lowland channels (Lenzi et al., 2003; Gomi, 2003; Comiti and Mao, 2012).

1.1.2. Sediment transport in mountainous catchments

Sediment transport, in hydrology, is the process of mobilization of the material from the hillslopes to the channel and throughout the channel. There are different ways of motion that can occur contemporaneously inside a stream. Molecules and ions, as well as the very fine particles, are mainly transported as dissolved load. In mountain fluvial systems, the transport processes occur mainly as suspended transport and bedload transport during floods, but also as debris and mudflows. The factors that determine the type and magnitude of the transport are several and have been highlighted by many

authors. Among others, some of the controlling factors are the coupling with source areas (Cavalli et al., 2013), the origin of runoff generating the transport, the hydraulic conditions (Lenzi et al., 1997, 1999, 2006a; Recking et al., 2012), the grain size distribution, (Mao et al., 2008; Yager et al., 2012), the presence of in-channel wood (Wilcox and Wohl, 2006; Rigon et al., 2012) and the channel morphology (Lenzi 2001; Mao et al., 2009).

In order to understand the transport processes that take place along a stream, it is important to differentiate between suspended sediment transport, which affects the finer material, and bedload transport, which acts on the coarser material. It is not easy to establish the threshold between bedload transport and suspended sediment transport but we can say that generally suspended sediment transport affects particles with diameter below 1 μm if the regime is laminar. If the flow is turbulent, it affects particles with diameter below 2 mm, but it can affect particles up to 64 mm in cases of high turbulence (Lenzi and Marchi, 2000; Lenzi et al., 2003; Mao, 2004). However, when studying sediment transport it is important to take into consideration this difficulty to establish a threshold between both kinds of sediment transport, due to which a variable fraction of the suspended load will probably remain unsampled (Fig. 4), as well as suspended sediment discharge may include some of the bed-material load component (Diplas et al., 2008).

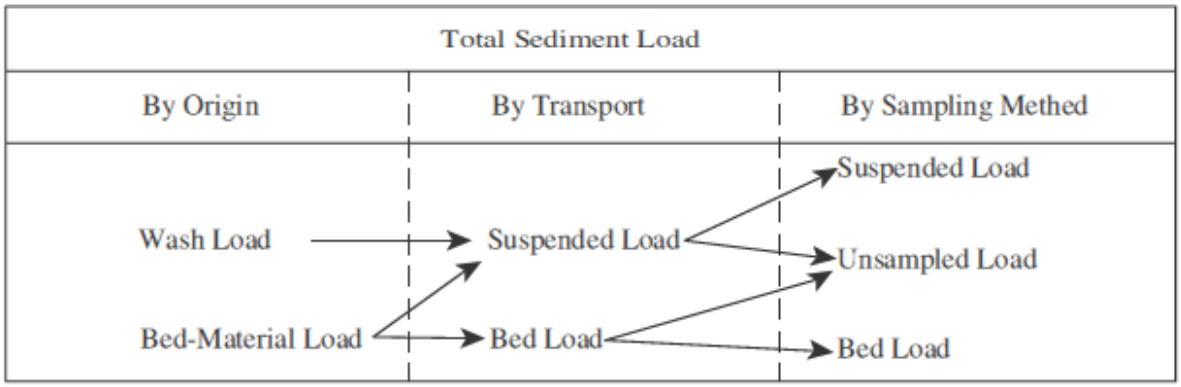

[1]That part of the sediment load that is not collected by the depth-integrating suspended-sediment and pressure-difference bedload samplers used, depending on the type and size of the sampler(s). Unsampled-load sediment can occur in one or more of the following categories: a) sediment that passes under the nozzle of the suspended-sediment sampler when the sampler is touching the streambed and no bedload sampler is used; b) sediment small enough to pass through the bedload sampler's mesh bag; c) sediment in transport above the bedload sampler that is too large to be sampled reliably by the suspended-sediment sampler; and d) material too large to enter the bedload-sampler nozzle.

Figure 4: Components of total-sediment load considered by origin, by transport, and by sampling method. Source: Diplas et al., 2008.

Non-impacted mountainous streams can be characterized by having a seasonal behavior that includes periods of sediment supply limitation, due to winter colluvial accumulation or inactive hillslope processes (Mao et al., 2008; Recking, 2012). Their sediment delivery processes differ significantly from those occurring in lowland channels (Lenzi et al., 2003; Gomi, 2003). This is because they are affected by many factors such as slope erosion processes, particle size distribution, stream hydrodynamics, channel and bedform morphology (Lenzi et al., 1999; Mao et al., 2008), as well as the presence of sediment sources and their connectivity or disconnectivity with downstream areas (Borselli et al., 2008; Heckmann & Schwanghart, 2012; Cavalli et al., 2013; Fryirs, 2013). Because of all these affecting factors, sediment transport in mountainous streams shows a high variability from event to event and within events.

Bedload transport regards coarser material and occurs when it moves along the channel bed rolling, sliding or by saltation. This phenomenon presents higher spatial and temporal discontinuity than suspended transport (Mao, 2004). In mountain environments, the analysis and quantification of bedload transport is of fundamental importance for hazard assessment, understanding the morphodynamics of higher order channels, planning and designing reservoir sedimentation (Rickenmann, 1999; Nitsche et al., 2011). The importance of this phenomenon contrasts with the fact that it is difficult to monitor, especially in small streams, due to its high-energy and impulsive nature. In most streams, flows are competent for transporting sand and fine gravels while only large floods can transport coarser material (Recking, 2012). Therefore, during a long period lacking large floods, armoring processes in the surface layer can take place in the bed and mountain streams can subsequently be considered supply-limited (Lenzi et al., 1999, 2004; Bathurst, 2007). Occasionally if a large flood takes place, the armor layer can be destroyed and sand and fine gravels stored in the bed can consequently be released until new lag formations contribute to reducing bedload transport (Brummer & Montgomery, 2006; Lenzi et al., 2006a, 2006b). Bedload transport in mountain streams can hence be characterized by successive inactive and active periods dependent on the supply (Lenzi, 2004; Mao, 2004; Rainato et al., 2016).

Suspended sediment transport is the mobilization of finer particles suspended in water columns. It differs from bedload transport in high-gradient streams because it has its origin not only in streambank erosion but also in hillslope activities. Consequently, its variability depends on different factors. Despite it is commonly considered less important than bedload transport (Lenzi et al., 2003), it deserves attention because it is fundamental for the study of sediment yield and budget and water

quality and can be an indicator of hillslope erosion (Benkhaled et al., 2013; Rainato et al., 2016). Moreover, its contribution to the total sediment load can range from 10% to 100% in high-gradient streams (Bathurst et al., 1987; Barsch et al., 1994; Billi et al., 1998; Mao, 2004). Even if it does not show such a marked succession of active and inactive periods as bedload, suspended sediment production is characterized by a significant variability and is highly dependent upon the stability of the coarse surface layer of the channel bed in high-gradient courses. If the armor layer of the bed is broken, a high quantity of fine sediment from the subsurface layer can become available (Diplas and Parker, 1992). In this case, a higher suspended sediment supply is observed in the subsequent floods.

1.1.3. Sediment supply

Sediment supply conditions can produce a wide variety of situations in headwater streams. The local sediment availability is the main controlling factor of the sediment transport in this kind of channels (Recking, 2012). Suspended sediment delivery is temporally heterogeneous in non-impacted headwater streams, including supply limitation periods following the rapid evacuation downstream (Turowski et al., 2011). This alternation of conditions frequently shows a seasonal behavior: Collins (1990) showed significant variations of suspended sediment transport on a seasonal scale in Swiss glaciated basins. Bogen (1995) found considerable differences in suspended sediment concentration between the beginning and the last days of the snowmelt in Norwegian rivers. Lenzi et al. (2003) defined the relation between suspended sediment concentration (SSC) and water discharge (Q) according to the seasons in a small alpine catchment.

Moreover, sediment supply is also affected by the recent hydrological regime (Turowski et al., 2011). In fact, large flood events can destroy the bed stability and therefore increase the sediment availability (Lenzi and Marchi, 2000; Lenzi, 2001; Rainato et al., 2016). The availability of the fine sediments once stored in the channel bed can be enhanced for prolonged periods following the event (Lenzi et al., 2004; Rainato et al., 2016). Sediment supply is determined mostly by hillslope activities and bank erosion (Recking, 2012). Hence, sediment supply is closely linked to the hillslope and channel stability. If the sediment supply of a mountain fluvial system is balanced with its transport capacity, the system is under equilibrium conditions. Unstable conditions appear when one of these two factors prevails. If the transport capacity is greater than the sediment supply, the system features erosion processes due to the deficit of available material. If the sediment supply is greater than the transport capacity of the system, deposition of material takes place along the channels, thus changing the bed morphology and the slope conditions.

1.1.4. Sediment sources and coupling

Sediment transport in mountains streams is closely dependent on hillslope processes (Recking, 2012). Identification of the sediment contributing areas of a catchment permits to know the amount of solid material that is susceptible to move towards the channel network when a rainfall event or a snowmelt event takes place (Cavalli, 2009). Many works (Buffington & Montgomery, 1997; Dalla Fontana & Marchi, 2003; Bathurst, 2007; Yu et al., 2009) have highlighted the importance of assessing the sediment sources when studying the transport dynamics within a catchment. This can be developed through field survey, with the use of digital terrain models (DTMs) or with a combination of both things. Airbone LiDAR-derived high resolution DTMs give a reliable morphological representation of the studied area, thus permitting a high accuracy in the study of the sediment dynamics (Marks & Bates, 2000; McKean & Roering J., 2004; Cavalli, 2009).

Channel sediment supply depends not only on the quantity, location and activation of the sediment sources, but also on the capability of the solid material to move downstream from the source and reach the channel network (Cavalli et al., 2013). Usually, sediment is not transported directly from a source to the channel network but to various storage land forms that are themselves filled and depleted (Heckmann and Schwargart, 2013). In fact, a discrepancy between erosion within the catchment and sediment yield at its outlet is often noted, and can be explained by the decoupling effect (Wainwright et al., 2010, Fryirs, 2013). This decoupling or disconnectivity is described as the degree to which any limiting factor restrains the efficiency of sediment transfer processes. Recking (2012) showed that higher transport rates are present in channels that are defined as “connected” to an active source. Even so, an efficient coupling between hillslopes and channel network does not always ensure an effective downstream transfer of sediment (Cavalli et al., 2013). Many qualitative approaches have been developed in order to understand more about connectivity between sediment sources and the fluvial system. Based on morphological and grain size field observations, Hooke (2003) established five categories (fully, partially or potentially connected, un- and disconnected) to describe river reaches. Korup (2005) introduced a nominal classification scheme for the coupling interface between landslides and the fluvial system (area, linear, point, indirect, nil). Faulkner (2008) studied connectivity changes and their role in badland evolution. Quantitative approaches towards sediment connectivity can be also useful. Many works introduce empirical equations and geomorphic and topographic indices, based on GIS applications, as a tool for the assessment of sediment transfer possibility (Mitasova et al., 1996; Dalla Fontana & Marchi, 2003; Borselli et al., 2008; Gao and Puckett, 2012; Heckmann and

Schwargart, 2013). Even so, it is important to bear in mind that an efficient connection between hillslopes and channel network does not always ensure an effective downstream transfer of sediment along the channel (Cavalli et al., 2013).

1.1.5. Suspended sediment transport

Finer particles move through the channel suspended in water columns. Suspended sediment concentration SSC shows a spatial variability across a channel section. The vertical sediment flux at a specific height z is defined as the mass passing a unit cross-sectional area in unit time. This flux can be obtained from the following equation if the corresponding particle concentration SSC(z) and the water velocity v(z) are known.

$$F_{susp}(z) = SSC(z) \cdot v(z)$$

(Equation 1)

When considering a section S of the channel, the suspended solid discharge can be obtained if the mean SSC(S) and the water discharge Q(S) are known.

$$Q_{susp}(S) = SSC(S) \cdot Q(S)$$

(Equation 2)

The variability of SSC depends upon the velocity of the fluid, the position of the particles in the water column and the size and shape of the particles. One of the most diffused methods for calculating the average concentration in a water column is the one proposed by Straub (1936). Using simplified laws of velocity and sediment distribution, he showed that the mean concentration of suspended sediment in a column can be calculated as:

$$SSC_m = \frac{3}{8} SSC_{0.2D} + \frac{5}{8} SSC_{0.8D}$$

(Equation 3)

Were SSCm is the mean suspended sediment concentration of the considered column, $SSC_{0.2D}$ is the concentration at a height of 0.2 of the total height of the column, and $SSC_{0.8D}$ is the concentration at a height of 0.8.

Total suspended sediment present in a channel consists mostly of material eroded from the hillslopes or streambank, but also of sediment deposited on the riverbed that is available for resuspension (Eder et al. 2010; Eder et al. 2014). In fact, multiple-peak sedigraphs accompanying a single-peak hydrographs are often noted in small watersheds. These multiple peaks may be related to the activation of different sediment sources such as the streambed itself, where deposited sediments from previous events may become re-suspended when flow increases (Eder et al., 2010). Deposition and resuspension dynamics are among the factors that explain the decoupling of the finer material. Some studies (Duijings, 1986; Walling et al., 1998; Navratil et al., 2010) have determined that the sediment stored in the channel can range from 2% to 10% of the total suspended sediment load. The calculation of the sediment delivery ratio shows that the scale of the basin affects the efficiency of the sediment displacement (Walling, 1983). Small basins (<0,1 km^2) show a delivery ratio close to 100%, while bigger basins (100-1000 km^2) show delivery ratios lower than 10% (López-Tarazón et al., 2012). This can be explained because, given concrete geomorphic conditions, the probabilities of the sediment getting trapped by any kind of obstacle are higher in a bigger basin, while the erosion rate is not influenced by the dimension of the catchment.

Suspended sediment transport in high-gradient streams features a greater variability than in low-land rivers. Moreover, its contribution to the total sediment load is also highly variable, ranging from 10% to 100% (Bathurst et al., 1987; Barsch et al., 1994; Billi et al., 1998; Mao, 2004), whilst suspended transport in low-land rivers shows a contribution from 70% to 95% (Simons and Senturk, 1977; Walling and Webb, 1981). The controlling factors of the suspended sediment transport in headwater streams has been described by many previous works. Size, morphology and lithology of the catchment, stability of the coarse surface layer, presence of decoupling features, land uses, soil moisture, amount, duration, intensity and spatial extent of precipitations are, among others, some of the parameters influencing the suspended transport dynamics (Klein 1984; DeBoer and Campbell 1989; Lenzi et al. 2003; Seeger et al. 2004; Soler et al. 2008; Gentile et al. 2010a; De Girolamo et al. 2015). Because of the many different factor affecting suspended sediment transport and the heterogeneous distribution of the fine sediment sources, it is not easy to create formulas to predict suspended sediment production in relation to precipitation (Banasik and Bley, 1994; He and Owens, 1995). Some authors have proposed formulas to predict the long-term fractions in mountainous Alpine water courses as a function of the basin area (Schlunegger and Hinderer, 2003; Turowsky et al., 2010). Even so, the high variability hinders this task.

1.1.6. Hysteresis

The relationship between Q and SSC is heterogeneous not only between seasons and events but also within a single event (Williams, 1989; Mao, 2004; Seeger et al., 2004). In fact, these two variables show a hysteretic relationship. Many authors have studied the Q-SSC relationship during single hydrologic events (Axelsson, 1967; Arnborg et al., 1967; Walling, 1974; Wood, 1977; Paustian & Beschta, 1979; Burt & Gardiner, 1984; Jeje et al., 1991).Williams (1989) wrote one of the first works in which the most common classes of hysteretic loops between water discharge and suspended sediment concentration were described. He defined the main characteristics of each model of loop and gave field examples for each of them. This classification includes single line, circular clockwise loop, circular counter-clockwise loop, and eight-shaped loop (Table 1, Figure 5). If the sediment peak and the water discharge peak arrive contemporaneously and the rising and falling limbs of respective graphs are parallel, the event shows a linear loop. If the sediment peak SSC_p occurs before the water discharge peak Q_p, or if the SSC/Q ratios on the rising limb of the hydrograph are greater than those on the falling limb, the events show a clockwise loop. Instead, if the sediment peak SSC_p occurs later than the water discharge peak Q_p, or if SSC/Q ratios on the rising limb of the hydrograph are lower than those on the falling limb, the loops have a counter-clockwise direction. A mixed loop occurs when a combination of circular and single line characteristics takes place. The eight-shaped loop occurs when a combination of a clockwise loop and a counter-clockwise loop takes place, usually because discharge and/or sediment concentration present more than one peak. The patterns of suspended sediment concentration and water discharge result from complex interactions between the processes that determine discharge and sediment transport during an event (Fang et al., 2015). Its analysis is helpful for the understanding of sediment transport processes (Aich et al., 2014), but their interpretation is often complicated. They can be an indicator of different runoff and sediment transport processes (Eder et al., 2010). More recently, many authors have developed different studies in order to understand more about this phenomenon. Lenzi & Marchi (2000) studied the sediment sources of several floods in a small Alpine catchment basing their analysis in the Q-SSC relationship. Zabaleta et al. (2007) assessed hysteretic differences between three small catchments of the Basche Country (Spain). Soler et al. (2008) analyzed the responses of two Pyrenean catchments in order to identify the role of their characteristics in the hysteresis phenomena.

Table 1: Williams (1989) classification for SSC-Q relationships.

Classes of C-Q relations

Class	Relation	C/Q criteria	Sample reference
I	Single-valued line	$(C/Q)_1=(C/Q)_2$	
	A. Straight line	A. Slopes of two subsections of the overall relation are equal	Wood (1977)
	B. Curve, slope of which increases with increasing values of Q	B. Slopes of two subsections of the overall relation are unequal-steeper for larger values of Q	Wood (1977)
	C. Curve, slope of which decreases with increasing values of Q	C. Slopes of two subsections of the overall relation are unequal- flatter for larger values of Q	-
II	Clockwise loop	$(C/Q)_1>(C/Q)_2$ for all values of Q	Paustian & Beschta (1979)
III	Counterclockwise loop	$(C/Q)_1<(C/Q)_2$ for all values of Q	Axelsson (1967)
IV	Single line plus a loop	$(C/Q)_1=(C/Q)_2$ for one range of Q values	-
V		$(C/Q)_1<>(C/Q)_2$ for other range of Q values	
	Figure eight	$(C/Q)_1>(C/Q)_2$ for one range of Q values	
		$(C/Q)_1<(C/Q)_2$ for other range of Q values	Arnborg *et al.* (1967)

$(C/Q)_1=(C/Q)$ on Q-graph's rising limb, for a selected discharge; $(C/Q)_2=(C/Q)$ on Q-graph's falling limb, paired to a particular $(C/Q)_1$ by being calculated at same value of Q. Dashes mean no reference available.

One of the main questions most of the researchers ask to themselves is what are the parameters affecting hysteresis behavior. The size of the catchment, the sediment yield, the rainfall amount and the soil moisture seem to be the main variables that control it (Klein, 1984; DeBoer & Campbell, 1989). Seeger et al. (2004) associated antecedent soil moisture and rainfall characteristics with the type of loop that a single event shows in a small catchment in the Spanish Pyrenees, demonstrating that the sediment sources contributing sediment yield depend on these antecedent weather variables, and not only on the characteristics of rainfall and soil moisture during the event. Alexandrov et al. (2007) assumed that in semi-arid environments intense rainfalls produce clockwise hysteresis, while low rainfall intensity causes counterclockwise hysteresis or a univocal relationship between both variables. Also Soler et al. (2010) correlated weather variables with the Q-SSC characteristics. They showed that kinetic energy, peak discharge, rainfall intensity, and antecedent baseflow and runoff coefficients are some of the factors that determine the hysteresis shape in a mountainous Mediterranean catchment. However, the analysis of the hysteresis can be a helpful approach in the transport processes study. For example, it can become a tool in the suspended load calculation. In fact, some authors (Krueger et al., 2009; Eder et al., 2010) have developed different approaches to calculate the suspended sediment load in single hydrologic events from the hysteresis relationship. This can be very useful because, as sediment sources are not homogeneously distributed within the basin, it is not easy to predict the sediment yield in relation to rainfall or water discharge data. Moreover, hysteresis analysis is a

common approach for linking sediment sources to downstream sediment loads. Asselman (1999) used hysteresis analysis to describe a seasonal pattern for the sources that were activated during single events in the large basin of the River Rhine. Lenzi & Marchi (2000) showed that the type of hysteretic loop of a single event explained the distance of the active sediment source to the outlet in a small Alpine catchment. Jansson (2002) determined the sediment source of four hydrologic events in a small river basin in Costa Rica thanks to the study of the sedigraph and the hydrograph of each one of them. However, SSC-Q hysteresis behavior is difficult to assess and usually typical patterns such as clockwise or counter-clockwise loops can be attributed to different causes, depending on the size of the catchment as well as its geomorphic and climatic characteristics (Smith and Dragovich 2009).

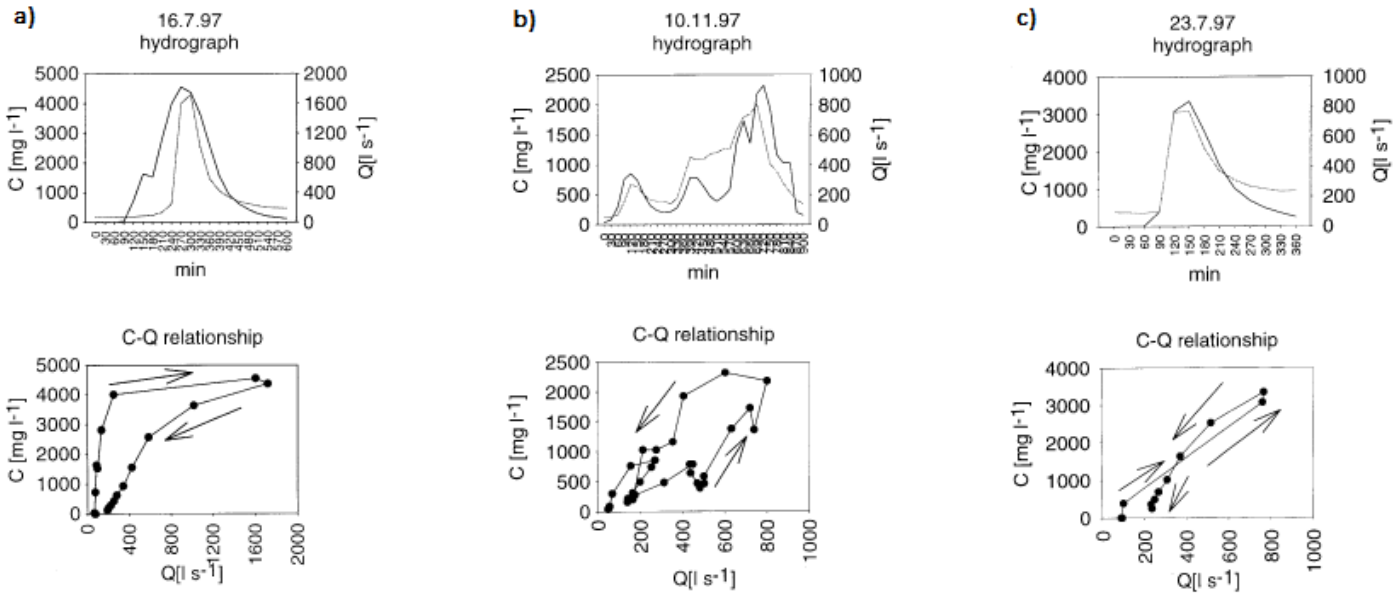

Figure 5: Examples of a) Clockwise hysteretic loop, b) counter-clockwise hysteretic loop, and c)eight-shaped hysteretic loop elaborated from different flood events. Upper figures are hydrograph (thinner line) and sedigraph (thicker line). Lower figures are the Q-SSC relationship during the flood events. Source: Seeger et al., 2004.

1.1.7. Suspended sediment measurement

Interpreting the interactions of the factors influencing suspended sediment transport through catchments usually requires intensive monitoring; yet it is not easy to find a commercially available, cost-effective monitoring method for suspended sediment transport. Sampling systems for collecting suspended-sediment data have evolved considerably in the last decades. They can be divided in point-integrated systems, depth-integrated systems and continuous sampling systems. Because the particles

show a heterogeneous distribution within the water column, samples from multiple vertical sections should be taken using point or depth-integrating samplers (Woods, 2014). Point-integrated systems take one sample at one established point of the vertical that is usually considered representative of the vertical studied, while depth-integrated systems move along the vertical taking two or more samples. Some sampling technologies include rigid-bottle samplers and bag samplers. These samplers are designed to collect a representative velocity-weighted sample of the water-sediment mixture, but are likely to present bias (Gray et al., 2010). They can be used as punctual, manual samplers or, with the previous required installation, continuous samplers. The great advantage of the continuous sampling is the possibility of studying continuous data from long periods.

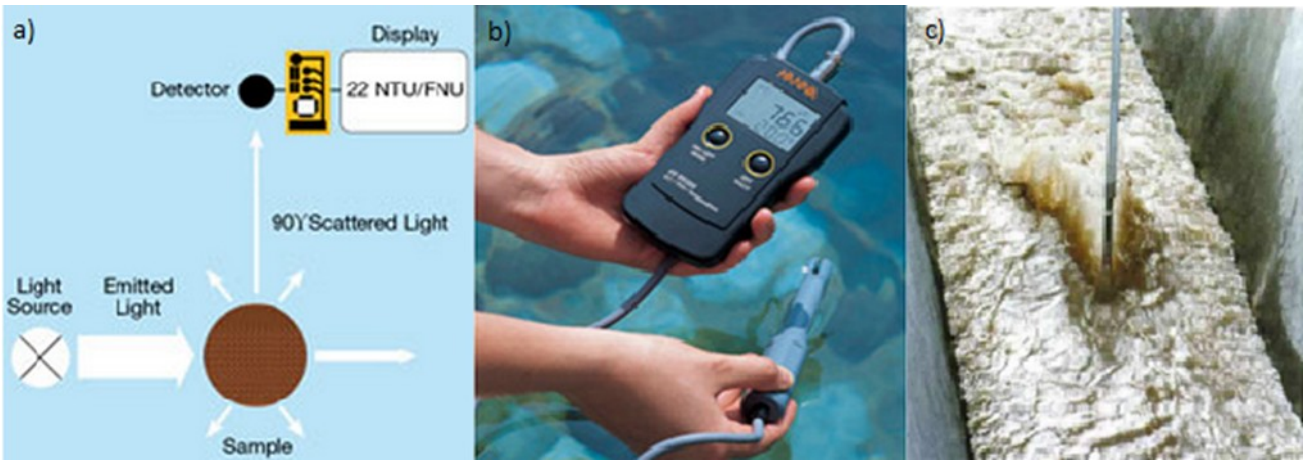

Figure 6: a) Mechanism of a turbidity meter (Source: http://en.aqualytic.de/). b) Manual turbidity meter (Source: http://www.geoscientific.com/). c) Continuous turbidity meter in the Rio Cordon monitoring station.

Measurements of turbidity are the most widespread method for the suspended sediment analysis, despite some authors such as Lewis (2002) proclaim that it is virtually impossible to collect perfect turbidity data. Turbidity is an expression of the optical properties of a liquid that cause light rays to be scattered and absorbed rather than transmitted in straights lines through the sample (Anderson, 2005). Turbidity measuring instruments usually work with visible or infrared light. Some systems work as punctual samplers (point-integrated or depth-integrated) while others can measure continuously. A regression model (SSC vs. turbidity) is required to calculate SSC from turbidity data. Nevertheless, different errors in turbidity-SSC transformation due to mineralogy differences, particle size variations and water color can be done (Jansson, 1992; Lenzi & Marchi, 2000). Besides, in most streams the relation between turbidity and SSC varies significantly between events (Lewis, 2002).

Consequently, numerous samples should be analyzed to correctly assess the turbidity-SSC regression relation. Nevertheless, a regression model to compute SSC should never been considered static, but rather to represent a set period in a dynamic system (Gray and Gartner, 2010). Hence, further data will help verify changes in the turbidity-SSC relationship. An additional possible bias in the suspended sediment study can have its origin in data quality. It is necessary to take into account possible errors in the sampling derived from biological fouling (Lewis, 2002), samplers altering the water velocity (Gray et al., 2008), or differences of concentration within the water column (Gray et al., 2010), among others.

However, turbidity measurement is not the only method for the suspended sediment transport analysis. Other suspended solids analysis methods are the Digital Optical Imaging, which does not require routine calibration and can quantify SSCs and size and shape characteristics of the sediments (Gray et al., 2010) or the pressure-difference technique, which measures the changes of pressure of a sample water column (Gray et al., 2010). The acoustic backscatter techniques have recently shown great potential for estimating suspended-sediment concentrations accurately and cost-effectively (Wood, 2014). Backscatter (Figure 7) is often used to assure the quality of velocity data, but it can also be used as an indicator of the concentration of sediment in the meter's measurement volume. It holds several advantages over turbidity meters, because they are not as susceptible to biological fouling as turbidity sensors and they provide information on grain size if multiple acoustic frequencies are used (Gray et al., 2010; Wood, 2014).

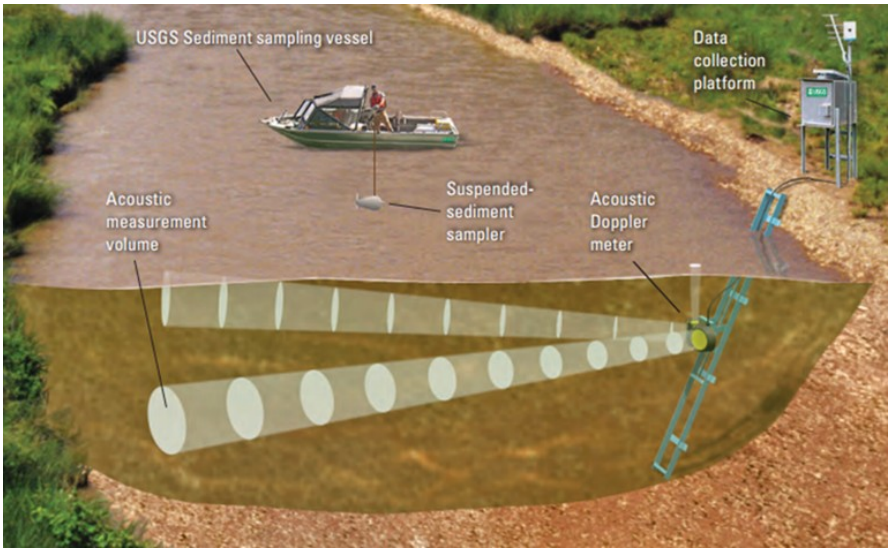

Figure 7: Example of a sediment acoustic backscatter (Source: Wood, 2014).

Whatever the chosen estimating method, it is important to keep in mind that the accuracy of estimates is more dependent on sampling design and data quality than on the measuring method (Eads, 2002).

1.1.8. Hydrograph separation technique

The hydrograph separation technique, based on the chemical changes suffered by the water in its pathway from the source to the main channel, is widely used to determine the changing proportions of pre-event and event water in small size catchments. Despite its uncertainties and limitations have been described in different works (Taylor et al., 2002; Penna et al., 2010; Klaus & McDonnell, 2013), its efficiency in tracing the origin and the paths of water in mountainous basins has been clearly demonstrated (Dunne & Black, 1970; McNamara et al., 1997; Huth et al., 2004; Penna et al., 2013; Mouri et al., 2014). Naturally present tracers, such as ^{18}O, ^{2}H, Silicate or the electrical conductivity (EC) are the most commonly used in this technique. The main requisite is that the tracer signatures must be conservative; that is, they must not change through the studied hydrological event. Otherwise, it must be feasible to correct the possible changes. Tracer-based hydrograph separation has brought important advances in the understanding of runoff generation processes since the late 1960's. Pinder and Jones (1969) published one of the first hydrograph separation using isotopes as tracers. In this work, the different ^{18}O signature in the water permitted to separate the storm hydrograph in a direct flow and groundwater flow component. They introduced the concept still used today of the complete mixing of old water (i.e. pre-event water) with new water (i.e. event water) in the channel during the storm hydrograph event.

The stormflow hydrograph can be separated in the contributions of new and old water with the following mass approach (Klauss & McDonnell, 2013) When using two runoff components (event water or new water and pre-event water or old water) and one observed tracer, the following linear mixing equation can be written:

$$Q_s = Q_o + Q_n$$

(Equation 4)

$$C_s Q_S = C_O Q_O + C_n Q_n$$

(Equation 5)

$$F_O = \frac{C_s - C_n}{C_o - C_n}$$

(Equation 6)

Where Q_s is the streamflow, Q_o is the contribution of old water and Q_n is the contribution of new water, C_s, C_o and C_n are the abundance of the tracer (EC, isotopes, Si, among others) in the streamflow, pre-event water and event water, respectively.

When facing two-component hydrograph separations, some assumptions are usually taken (Moore, 1989; Buttle, 1994; Klauss & McDonnell, 2014):

1. The abundance of the tracer in the new water and the old water (event and pre-event water, respectively) are significantly different.

2. The new water maintains a constant tracer signature in space and time.

3. The tracer signature of the old water is constant in space and time.

4. The tracer signature of the soil water must be similar to that of groundwater, or contributions from the unsaturated zone are negligible.

5. Surface storage contributions to the streamflow are negligible.

Because ^{18}O and ^{2}H are part of the water molecule, their use as tracers has been widely chosen in hydrograph separation studies (Fritz et al., 1976; Herrmann and Stichler, 1980). Their addition to the channel water occurs naturally during the precipitation events, and, if they are not exposed to evaporation, the only factor inducing changes in their proportions is the water mixing (Kendall and McDonnell, 1998; Klaus and McDonnell, 2013).They are the most common tracer when facing hydrograph separation studies, but in some specific situations, the use of electrical conductivity (EC) can be a better option. Even though this tracer is not entirely conservative due to the rainwater dissolving solutes as it passes through the soil (McNamara et al., 1997), its use in hydrograph separation has several advantages. The difference in the electrical conductivity of event and pre-event water can be very large (usually two orders of magnitudes but sometimes even three), whereas the difference in isotopic composition of event and pre-event water can be very small or even negligible (Klaus and McDonnell, 2013). Thus, the uncertainty from the measurement is smaller in EC-based estimates of the event water contributions to streamflow components (Genereux, 1998). Furthermore,

electrical conductivity is often chosen as tracer because it is cheap to measure and permits continuous field monitoring without the need to take water samples (Caissie et al., 1996) and with relatively little maintenance (Penna et al., 2015).

The use of other tracers such as Silicates (Uhlenbrook & Hoeg, 2003; Williams et al., 2009) or ions (Sueker et al., 2000; McHale et al., 2002; Liu et al., 2011) has been chosen by several studies. Anyway, combining more than one type of tracer can help overcoming the difficulties, and the integration of stable isotopes of water with other geochemical tracers seems to be an optimal solution (Mc Namara et al., 1997; Hangen et al., 2001; Maurya et al., 2011; Muñoz-Villers and McDonnell, 2012; Penna et al., 2013).

1.1.9. Permanent measuring structures

Permanent measuring structures installed in mountain streams are a valuable tool in the sediment transport studies, because their constant monitoring provides the opportunity to analyze long-term data of water discharge and sediment load, useful for analyzing sediment transport. Because their installation requires a considerable investment and they need additional continuous maintenance, they are not a widely extended solution. Even so, since the beginning of the 20th century some installations were settled in Europe, such as the two experimental hydrologic catchments established by the Swiss Forest Research Institute. The Rappengraben and the Sperbelgraben catchments, designed to study runoff, were equipped with a stream gauging station, sand traps and sediment retention basins (Rickenmann, 1997). Since then, many experimental catchments with regular measurements on sediment volume have been established in different Swiss mountainous regions (Engler, 1919; Burger, 1945; Keller, 1965; Rickenmann, 1997). The Erlembach experimental catchment and instrumented sediment transport station is working since 1985 and is one of the most important installations having a long time series of bedload and suspended sediment transport data (Keller, 1965; Fattorelli et al., 1986; Rickenman, 1997).

Figure 8: Initial Sperbelgraben runoff measuring station (after Engler, 1919).

In Austria, some monitored catchments can be found, such as the Pitzbach catchment, where the Tyrolean Water Power Company maintains a gauging station. There, bedload data from acoustic impulse measurements have been studied (Turowski & Rickenmann, 2009). Another example is the Petzenkirchen creek, where discharge, suspended sediment concentration and turbidity are continuously monitored since 2005 (Eder et al., 2010). In Spain, the CEDEX (Public Works Study and Experimentation Center) manages a net of more than 1200 gauging stations distributed throughout the country that automatically record the water discharge in the most significant catchments. Besides, sediment transport is studied in some watersheds, like Aixola, Barrendiola and Añarbe catchments, whose turbidity and discharge are continuously measured since 2003 (Zabaleta et al., 2007). In the United States of America, the U. S. Geological Survey (U. S. G. S.) has established since the beginnings of the last century a high number of stations in catchments of the whole country measuring daily or instantaneously water discharge and sediment transport (1593 stations to date). This had permitted thorough analysis of the sediment transport dynamics (Wolman & Miller, 1960; Nolan et al., 1987; Buchanan & Schoellhamer, 1998; Gray et al., 2000; Uhrich & Bragg., 2003). In Italy, the best example is probably Rio Cordon monitoring station (Fig. 9), built by TeSAF Department of Padua University in collaboration with ARPA Veneto. In this installation, an inlet flume, an inclined grid for coarser material separation and conductivity and turbidity sensors are working continuously since 1986 (Fattorelli et al., 1988; Billi et al., 1998; Lenzi et al., 2003).

Figure 9: Rio Cordon permanent monitoring station.

Other operative Italian experimental stations and instrumental high-gradient streams for suspended sediment, bedload transport and debris flow monitoring are the Boris torrent (Iovino and Puglisi, 1989) and the Moscardo torrent (Marchi et al., 2002; Mao et al., 2009).

1.2. Aims

This work aims to be a contribution in the knowledge about dynamics of the sediment transport in mountainous catchments, focusing particularly on the suspended sediments. The nature and dynamics of the mountain headwaters affect the features of sediment delivered to downstream channels, determining the quantity, timing and size of material transported by lowland rivers. The assessment of suspended sediment transport, which can contribute up to the 100% of the total sediment load in mountainous areas, becomes necessary for the study of the solid transport in this kind of watersheds. In this context, intensive monitoring of the parameters affecting this process is a very useful tool for interpreting the interactions of the factors influencing this process. This thesis aims to study the suspended transport dynamics occurring in the Rio Cordon catchment, located in the eastern Italian Alps (Dolomites), during the last three decades. This basin features a continuous monitoring station located at the outlet that provides us with data since 1986, and is characterized by the typical Alpine climatic conditions, due to which the runoff shows a nivo-pluvial regime dominated by snowmelt between May and June and with significant floods that are due to persistent rainfall in summer and

early autumn. The objectives are to investigate the quantity and effectiveness of the fine sediment delivered by the sediment sources of the catchment through the study period, to assess the main factors that affect suspended sediment transport in both long- and short-term, and to identify the hydrological thresholds controlling the response of suspended sediments to the water inputs. In this context, nearly three decades of monitoring of fine sediment fluxes are analyzed at different time scales, ranging from short-term (single event), middle-term (seasonal, annual) and long-term (30 years). Annual and seasonal suspended sediment loads are assessed, and the effective runoff volumes associated to them are analyzed. Once assessed the sediment transport characteristics of the single events occurring during the study period, the suspended sediment motion conditions are investigated. In this context, an exhaustive comparison with the events occurring in a Mediterranean catchment, the Carapelle torrent, permits to assess the factors that control the transport dynamics in both catchments. These study areas were chosen because of their differences in terms of extent, geology, morphology, climatic regime, land use, and flow regime. Finally, some field campaigns from the latest years of the study period in the Rio Cordon are analyzed, in order to understand the factors influencing the suspended sediment dynamics within flood events.

Overall, not many studies of the suspended sediment transport in mountain catchments with such an extended monitoring period are available in literature. Understanding the factors affecting the dynamics of the fine sediment fluxes in mountainous environments can be essential for predicting the suspended sediment dynamics through events and long-term periods, as well as to assess their relative loads.

2. CHAPTER TWO- MATERIALS AND METHODS

2.1. Study areas

2.1.1. Rio Cordon Catchment

The Rio Cordon torrent can be considered a representative Alpine stream. It is a tributary of the Fiorentina Torrent, which is, in turn, tributary of the Piave River. The basin (Figure 10), located in the Eastern Dolomites, in the Italian Alps, has a dimension of 7.68 km^2, but the measuring station is installed at 1763 m a.s.l., delimiting a sub-basin area of 5.02 km^2. The elevations range from 2763 to 1763 m a.s.l, and the main channel is 2.84 km long, with a main slope of 17%. This torrent presents the typical characteristics of a small mountainous stream (Table 2), with frequent floods originated both by snowmelt or rainfall events. No urbanized area or roads are present within the basin area.

Table 2: Main characteristics of the Rio Cordon catchment.

Area (km^2)	5.07
Perimeter (km)	10.3
Minimum elevation (m a.s.l.)	1763
Maximum elevation (m a.s.l.)	2748
Gravelius Index	1.28
Catchment average slope (%)	52
Qmax ($m^3 s^{-1}$)	10.41
Qaverage ($m^3 s^{-1}$)	0.26
Length of the main channel (km)	2.84
Average width of the main	5.7
Average slope of the main	13.6
Average annual precipitation	1100
Snowfall (%)	35
Mean annual temperature (°C)	-2

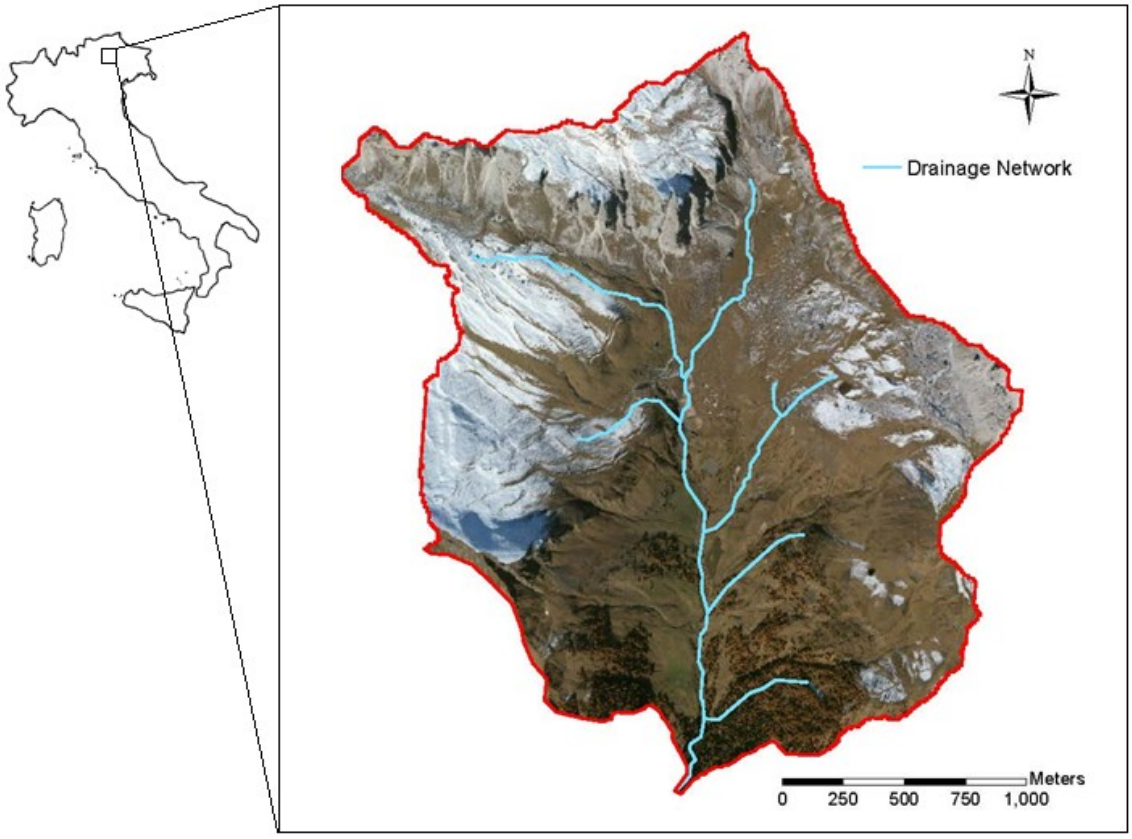

Figure 10: The Rio Cordon catchment area.

Geologic characterization

The Rio Cordon catchment is geologically characterized by morrenic debris that have its origin in dolomitic material, but also sandy marble rocks from the Wengen group and sandy siliceous tuff stones from the Buchenstein group. The presence of three different geomorphologic elements divides the catchment area in three morphologic units with different physiographic characteristics (Fritz et al., 1992).

The first one is situated in the Eastern zone of the watershed. Dolomitic rocks and material from the Wengen group constitute this unit. Here, the hydrographic network presents an ephemeral tendency because of the high permeability of the soils. Hence, it is activated only during snowmelt or during high intensity storms. Occasional falls from the dolomitic cliffs create sediment fans that can originate debris flows.

The second morphologic unit occupies the Northern area of the basin (Figure 11). The rocky substrate is exclusively constituted by material from the Wengen group. The hydrographic network presents a permanent dynamic here, due to the hydrological reservoirs formed by dolomitic rocks. The alluvial fans where sediment deposition processes take place downstream these rocks represent the main sediment source in this area.

Figure 11: Alluvial fans from the Northern part of the catchment area.

The third morphologic unit, located in the lower part of the basin, is characterized by a younger topography and it is hence exposed to frequent morphodynamic processes that change the characteristics of the surface. The material is mostly from the Wengen group, but close to the outlet appear some small areas of calcareous tuff stones from the Buchenstein group. The channel network is strongly defined, showing perennial water courses. The unsteadiness of the rocks and the Quaternary surface lead into several erosion processes. These usually affect the superficial layer of the ground and induce into debris accumulations at the bottom of the rock cliffs.

Soils are generally thin and can be classified in three typologies:

- Soils from the high slope zones that present discontinuous vegetation cover: These soils show a developed skeleton and a medium organic content;
- Soils from the forested areas: High organic content can be found in those zones where a continuous and fit vegetation is present;
- Brown soils, which show a high iron compounds content because of the chemical alteration of the rock.

Fitoclimatic characterization

The basin presents the typical climatic characteristics of the Alpine areas. According to the Thornwaite classification (Figure 12), the Rio Cordon area belongs to a microthermic, humid region, with a positive hydrologic balance. The main fitoclimatic classification is Alpinetum, with transition to Picetum in the lower zones of the catchment. The mean annual precipitations are 1100 mm. About 35% of the annual precipitations fall as snow from December to April. Mean annual temperature is 2 °C, while the maximum and minimum annual temperatures are around 20 °C and -8 °C, respectively.

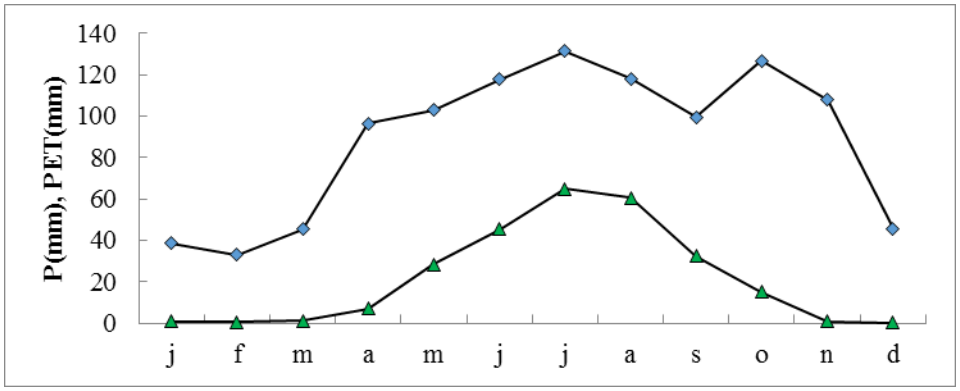

Figure 12: Thornwaite hydroclimatic balance of the Rio Cordon catchment. Precipitation (P) is represented in blue while potential evapotranspiration (PET) is represented in grey.

Flood events present different characteristics according to the year period in which they take place, as Figure 13 shows. In the latest days of April, May and the beginning of June, flood events correlated to snowmelt processes take place within the basin (Dalla Fontana, 1992). During these events, the registered sediment transport consists mainly of suspended material transport. During July and August, the catchment features brief and intense summer storms. During September, October and November, long rainfall events are recorded. During these events, precipitation intensity can reach high levels, inducing sometimes into high bedload transport rates. Water discharge is limited during the winter months due to the snow cover and the absence of liquid precipitations.

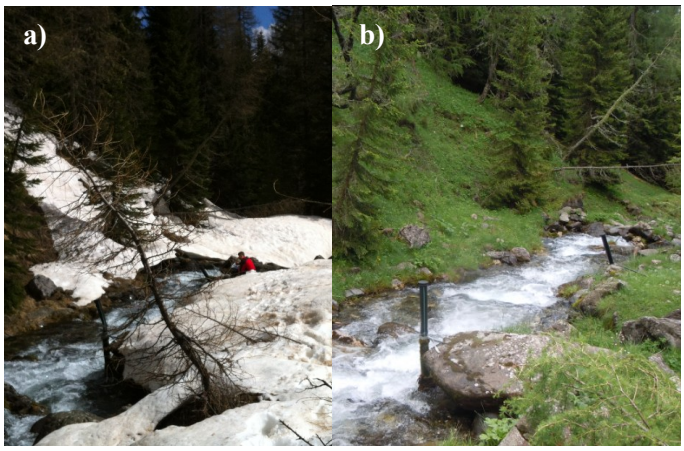

Figure 13: A low reach of the main channel during snowmelt (a) and during a rainfall event (b).

Due to the high elevations, forests (*Larix decidua* Mill. and *Picea abies* (L.) Karst) are located in the lower part of the catchment area and cover just the 7% of it. Alpine grasslands and shrubs cover the major part of the catchment (60% and 15% respectively), as can be noted in Figure 14. The remaining 14% of the basin area features bare land (Fattorelli et al., 1988; Trevisani et al., 2010).

Figure 14: Upper grasslands from the upper part of the catchment and small forested areas downstream.

Sediment sources

There is a high sediment availability in the Rio Cordon catchment area (Figure 15). Source areas were surveyed after the major floods of September 1994. The estimation was that sediment sources covered 5.2% of the total basin (Dalla Fontana and Marchi, 1994). More recent surveys (Figure 16) estimated that sediment sources areas cover about 13% of the catchment (Cavalli, 2009). They are mainly

constituted by talus slopes, shallow landslides, eroded streambanks and debris flow channels (Dalla Fontana and Marchi, 1994; Lenzi et al., 2003). An inventory of the source areas carried out in 2006 determined that landslides and surficial erosion represent about the 62% of total sediment source areas (Cavalli et al., 2016). The rest of the source areas are mainly covered by active talus (32.4%) and debrisflow related areas (11.6%).

The characteristics of the morphologic units and the sediment sources typology permit to understand some of the transport dynamics that are present in the basin. The upper geomorphologic unit features debris fans from the erosion processes affecting the dolomitic riffs. Pluvio-colluvial depositions characterize the low-gradient hills of the second unit, located in the medial zone of the catchment. The lower unit presents abundant debris material due to the erosion processes affecting the Quaternary surface.

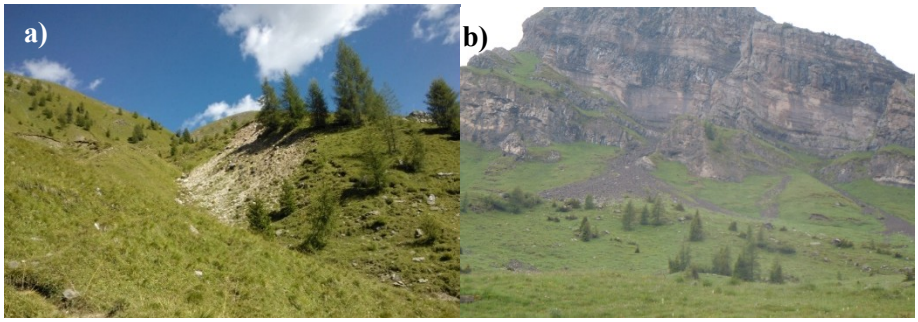

Figure 15: Talus slope in the medial part of the basin (a) and alluvial fans in the upper part (b).

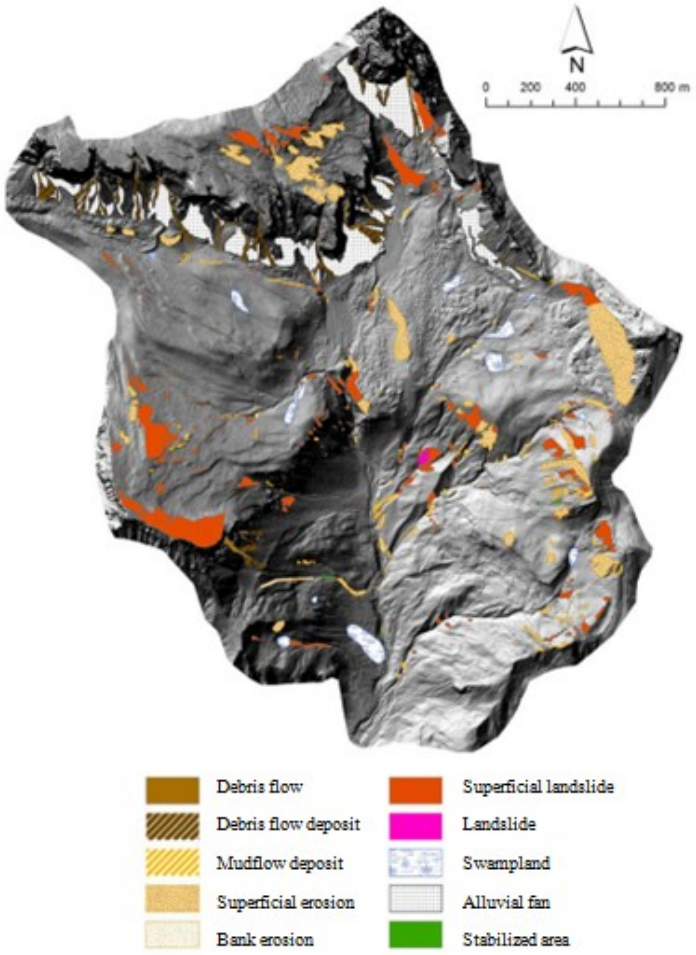

Figure 16: Sediment sources in the Rio Cordon catchment (after Cavalli, 2009).

Despite sediment is available within the whole catchment area, this condition does not lead into high sediment supply conditions (Cavalli, 2009). A peculiarity of this catchment is that about 50% of the total sediment source area is located upstream of a low gradient moraine belt where sediment deposition is induced. The basin headwaters therefore provide a minor contribution to the total sediment yield, independently of the local intensity of erosion processes (Dalla Fontana & Marchi, 2003). In addition, scree deposits on talus slopes are usually far and disconnected from the main channel. As a result, the basin headwaters provide a minor contribution to the total sediment yield, independently from the local intensity of erosion processes, because the sediment that actually arrives to the outlet of the basin has its origin only in the lower half of the basin. Besides, the sediment eroded from rock cliffs is temporarily stored as scree deposits on talus slopes, and there exists a decoupling between them and the stream channel. For these reasons, the stream has a low to moderate sediment supply condition (Mao et al., 2009).

Figure 17: Examples of the material deposited.

Morphology and grain size distribution of the main channel

The main channel is developed over Quaternary moraine deposits and its bed shows a complex morphology. According to the Montgomery and Buffington (1997) classification for the mountainous water courses, it features cascade, step-pool and riffle-pool structures. Cascade reaches can be found in the upper part of the channel (Fig. 18). Riffle-pool structures are present in both upper and medium reaches. Step-pool, sometimes mixed with riffle-pool, is the dominant morphology of the main channel (Lenzi, 2001). This structure, in which steps are mainly formed by boulders, is significantly stable and may undergo substantial modifications only during remarkably high floods of recurrence interval (RI) of around 30 years. Also cascades, riffle-pool and mixed reaches formed by step-pool sequences irregularly punctuated by small heaps of coarse material can be found in the stream channel.

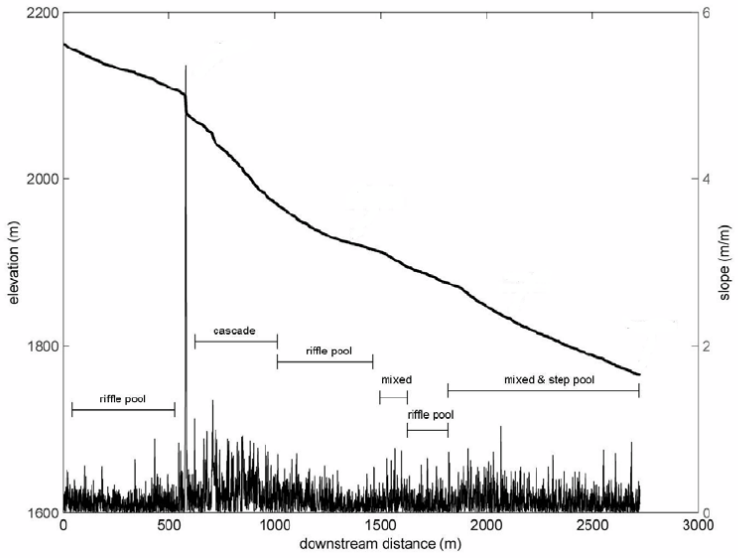

Figure 18: Longitudinal profile of the Rio Cordon main channel (after Cavalli, 2009)

The grain size analyses carried out on the streambed during 2004 estimated the following grain size distribution: D_{16} was equal to 37 mm, while D_{50} =119 mm and D_{84} =357 mm (Mao, 2004). Moreover, the field surveys highlighted a strong degree of surface armoring, finding that the subsurface grain size distribution is finer than at the surface (D_{50} /D_{50ss} ~ 3) (Mao et al., 2010). This analysis was developed again during August 2014, and the grain size distribution (Fig. 19) obtained from the 326 particles measured showed the following results: D_{16}= 29 mm, D_{50} = 114 mm, and D_{84}=358 mm (Rainato, 2016). Such percentiles appear roughly consistent with the GSD evaluated by Mao (2004). A reduction equal to 26.1% and 4.6% was be observed in D_{16} and D_{50} , respectively (Rainato, 2016).

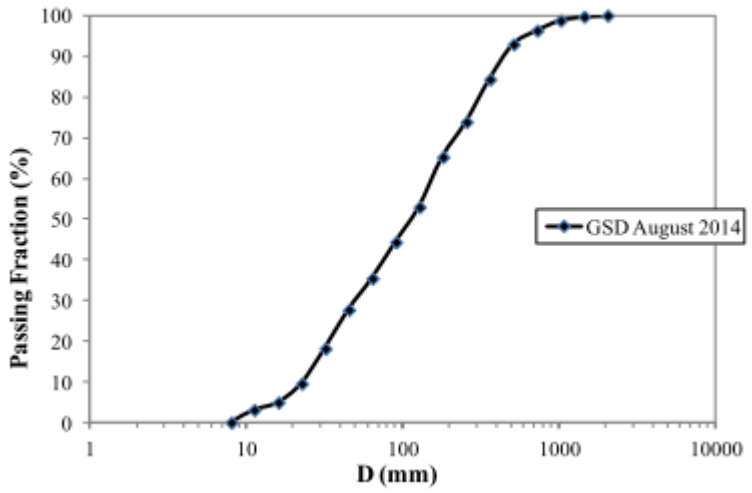

Figure 19: Grain size distribution in the Rio Cordon main channel (after Rainato, 2016).

2.1.2. Measuring station in the Rio Cordon

The monitoring station of Rio Cordon (Fig. 20) was built in 1986, at an altitude of 1763 m a.s.l. (Fattorelli et al., 1988). It consists of an inlet flume, an inclined grid, a storage area and an outlet flume. The inlet flume, where the flow gets channelized, features a longitudinal slope equal to 3%. The first water level and turbidity measures take place in this flume. Subsequently it runs into the inclined grid. This grid, with a longitudinal slope and a transversal slope equal to 60% and 27% respectively, separates the coarse material (>20 mm), that falls subsequently in the storage area. There, 24 ultrasonic sensors fixed in a rigid frame measure the volume increase. Once separated from the coarse sediment, the flow runs into a flume where the second turbidity and water level measures take place and then flows into a settling basin where the fine sediment is stored. The water goes out from the monitoring station downstream the settling basin through an outlet flume. The monitoring station is actually managed by the Regional Land Safety Department of ARPAV.

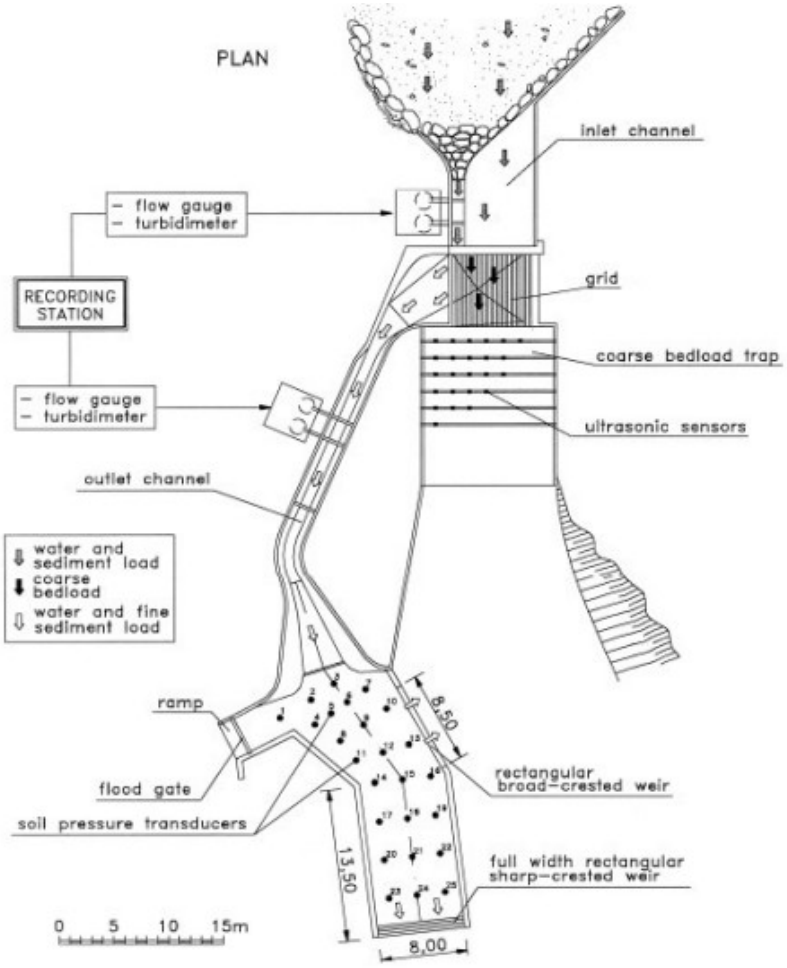

Figure 20: Plan of the Rio Cordon measuring station

As said, the suspended sediment is measured by two turbidity meters: the first one is a light scattered instrument (Hach SS6), installed in 1994 in the inlet channel, while the second one is a light absorption device (model Partech SDM-10) installed in the outlet channel since the beginnings of the station. Both are fixed in correspondence of the water level gauges in order to simultaneously measure the water level and the turbidity. Moreover, if the discharge exceeds a specified threshold, flow samples are gathered automatically using a Sigma pumping sampler, placed along the inlet flume (Lenzi and Marchi, 2000). Collected data are radio transmitted to the Arabba Centre of ARPAV.

Figure 21: Turbidity meter at the outlet channel of the Rio Cordon Monitoring station.

A complete and more detailed description of the measuring station is also available in several previous papers (Fattorelli et al., 1988; Lenzi et al., 1999; Lenzi et al., 2004; Picco et al., 2012). The continuous monitoring permitted to analyze the flood events taken place in the catchment from 1986 to the present, characterized by bedload and suspended sediment transport, as well as the seasonal and annual variations. Most of the important floods occurred during the study period are described in detail in previous works (Lenzi et al., 1999; Lenzi and Marchi, 2000; Lenzi, 2001; Mao, 2004; Rainato et al., 2013, 2016).

Figure 22: Monitoring station of Rio Cordon.

Some of the floods registered by the monitoring station deserve a special mention, the first of them taking place on September 1994. This flood is considered the most important event occurred since the installation of the station. It was originated by high intensity rainfall characterized by maximum rainfall rates of 7.2 mm, 16.4 mm and 25.3 mm for 5 min, 15 min and 30 min respectively (Lenzi and Marchi, 2000) which caused the highest discharge ever recorded by the Rio Cordon measuring station,

with a value of 10.4 m^3 s^{-1} (recurrence interval of more than 100 years). Unlimited sediment supply conditions were created due to this flood because the bed armor layer formed over years was destroyed, and the streambed became consequently the main source of sediment. In fact, subsequent ordinary floods showed higher levels of sediment load rates than the pre-1994 registered events (Lenzi et al., 2004; Mao et al., 2010). The same trend is observable regarding the mean annual sediment yield (Lenzi et al., 2003): in the period 1986-1993 this values reaches 77.7 t km^{-2} $year^{-1}$, while in the period 1995-2001, after the 1994 flood, the value increases up to 130.6 t km^{-2} $year^{-1}$. Several minor bank erosion and bank failures were observed during the surveys after the event, both along the main channel and along some tributaries (Billi et al., 1998). Besides, the step-pool morphology was altered during this flood, and it was restored only after the slow action of pool scouring of several ordinary floods (Lenzi, 2001; Lenzi et al., 2004; Mao, 2004).Therefore the September 1994 flood can be considered a moment of considerable change for the channel, from both the morphology and the sediment availability points of view (Mao et al., 2010).

A second event occurred in October 7, 1998, caused by moderate but persistent autumn rainfall of 101 mm in 24 hours (Mao, 2004). More than 3900 t of fine and coarse sediment were transported during this event. A limited number of active sediment source areas was observed in the basin after the event (Lenzi, 2000), suggesting that the material could have been supplied by the destabilized channel-bed.

The event of the 11th of May 2001 was a quasi-unlimited sediment supply condition. It occurred at the end of the snowmelt period, as a consequence of a mud flow: a shallow landslide moved into a small tributary because of the soil saturation (Lenzi et al., 2004). As a consequence of this, a debris fan of 4176 m^3 formed on the main stream, providing fine sediment easily transportable downstream to the main channel. Most of the material transported during this event was suspended load (1017.6 t).

Two smaller, but still significant, events occurred recently, in 2012 and 2014. The one during November 2012 took place during a persistent autumn rainfall that generated a water discharge peak of 2.10 m^3 s^{-1} (Rainato et al., 2013). Bedload and suspended load were 24.4 t and 60.8 t, respectively. Field surveys developed after the flood showed that the main sediment source was a debris flow channel located just upstream the monitoring station. The event occurred in June 2014 can be classified as a mixed snowmelt-rainfall event. It showed a flood peak of 2.06 m^3 s^{-1}. The main source area was a

debris flow channel located in the median part of the basin. The material provided by debris flow reached the channel bed approximately 1300 m upstream the station.

2.1.3. Carapelle catchment

The Carapelle Torrent is one of the main torrents in northern Apulia. The area closed at the monitoring station has an extension of 499.4 km^2 (Table 3). The stream comes from the Apennines in Campania and, after crossing areas of the Subappennino, runs along the flood plain of the Tavoliere to its natural mouth at the south-central Gulf of Manfredonia into the Adriatic sea. The basin lithology is predominantly of clayey-sandy Plio–Pleistocene sediments in the alluvial fan and flyschoid formations in the mountainous areas, which are subject to erosion (Gentile et al., 2010a). Land use is mainly agricultural, with plains and low hills used for wheat and olive groves while at higher altitudes there are predominantly woodland and pasturing activities. A typical Mediterranean climate characterizes the catchment area. In relation to the different gauges in the watershed, annual precipitations are between 450 and 800 mm, while average annual temperatures range between 10 and 16 °C. Snowfall is not significant. The rainfall distribution shows a great spatial and temporal heterogeneity, producing significant events throughout the year.

Table 3: Main characteristics of the Carapelle catchment.

Area (km^2)	499.4
Perimeter (km)	141.7
Minimum elevation (m a.s.l.)	112
Maximum elevation (m a.s.l.)	1094
Gravelius Index	1.78
Catchment average slope (%)	15
Qmax ($m^3\ s^{-1}$)	159.5
Qaverage ($m^3\ s^{-1}$)	108.07
Length of the main channel (km)	65.98
Average width of the main channel (m)	9.6
Average slope of the main channel (%)	12.1
Average annual precipitation (mm)	450÷800
Snowfall (%)	0
Mean annual temperature (°C)	10÷16

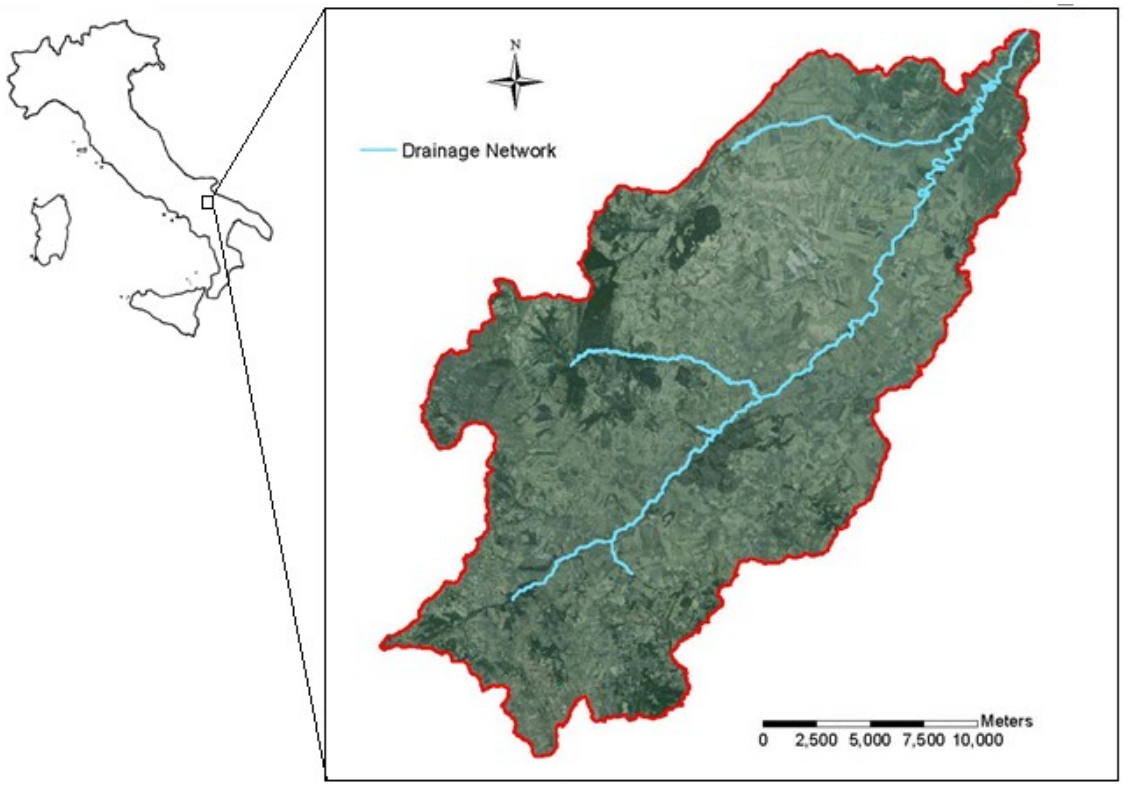

Figure 23: The Carapelle catchment area.

A monitoring station is located at Ordona-Castelluccio dei Sauri bridge, equipped with an ultrasound stage meter that transmits data in telemetry, a traditional electro-mechanical stage meter and a cableway (Gentile et al., 2010a). For the continuous measurement of the turbidity, the station is equipped with an optical infrared probe, installed in 2006 by the DISAAT Department of Bari University. Solar panels and a cabin for housing the data acquisition system complete the equipment. Laboratory and field tests were used to link suspended sediment concentration and turbidity (Gentile et al., 2008). The instrument is housed in a perforated pipe to protect it from the impact of the coarse material carried by the flow and to prevent measurement errors caused by natural radiation in the infrared range (Orwin & Smart, 2005). Flow data and suspended solid concentrations have been used to study the sediment dynamics at the event scale (Gentile et al., 2010a) and also to model erosion and transport processes in the watershed (Gentile et al., 2010b; Abdelwahab et al., 2013; Abdelwahab et al., 2014; Bisantino et al., 2015).

2.2. Research methodology

2.2.1. Continuous monitoring 1986-2015

The Rio Cordon catchment area features two meteorological stations and one monitoring station at the main channel. The continuous maintenance of the devices installed and the periodic data downloading made by the Regional Land Safety Department of ARPA Veneto has permitted to build up a solid database. This database has been used in many previous works (D'Agostino et al., 1994; Lenzi et al., 1997, 1999, 2003, 2004; Lenzi & Marchi, 2000; Lenzi & Mao, 2003; Mao, 2004; Mao et al., 2008; Picco et al., 2012; Rainato et al., 2013; García-Rama et al., 2016; Rainato, 2016).

Rainfall volume and air temperature have been registered continuously by the two meteorological stations, settled in the outlet section and in the upper part of the catchment, respectively.

Since the installation of the monitoring station in 1986, water level, bedload volumes and water turbidity, among other parameters, have been collected continuously at the outlet section. These parameters are usually measured at 1 hour interval. When the water discharge reaches the flood threshold (0.9 $m^3 s^{-1}$), turbidity and water level data are collected every 5 min. The collaboration with the Regional Land Safety Department of ARPA Veneto permits us to use and analyze these data. The first step is to control and filter the data in order to obtain reliable datasets. Subsequently, data are analyzed. In terms of water discharge measure, despite data from the three water level gauges are available, the water level gauge situated in the inlet channel is the one giving more reliable data. In fact, the other two water gauges require more calibration and maintenance work. In terms of suspended sediment data, values from the inlet flume turbidity meter are more reliable than the ones from the outlet flume instrument, because of the same reasons as invoked in the water level devices. Moreover using the upstream sensors, the analyses appear consistent with the previous works carried out in Rio Cordon basin (Lenzi et al., 2001; Mao, 2004).

2.2.2. Annual data validation and data base updating

A general updating of the three decades series of data was necessary even though a considerable amount of data had already been elaborated by previous authors. Especially between 1986 and 2004, many water level and turbidity recordings from the Rio Cordon monitoring station were used for suspended sediment transport analysis (Lenzi and Marchi, 2000; Lenzi et al., 2003; Mao, 2004). From 2004 to the present, most part of the available data was still unconverted (not checked or without scientific treatment), because all the analysis performed in this period regarded mostly bedload

transport or single events with particular characteristics (Lenzi et al., 2006a,b; Mao and Lenzi, 2007; Picco et al., 2012; Rainato et al., 2016). A literature review was necessary for the whole study period, in aims of checking the concordance between the conversion and interpretation methods used in past and the ones used now, as well as finding eventual information gaps and filling them with the appropriate conversion of the original data. The methods performed in this work are in concordance with the methods that deal with data registered in the measuring station of the Rio Cordon applied in previous works.

Data registered by the thermometers of the meteorological stations located at the bridge of the outlet section and at Mondeval di Sora was collected. 60-min data was organized and elaborated, and then mean daily temperature was calculated for the whole study period. The same procedure was made with data from the two pluviometers, located in the same points. Daily rainfall and daily temperature data were used to stablish the duration of the snowmelt season and whether a flood event registered was a rainfall event, a snowmelt event or a mixed event. The criteria for stablishing the the beginning of the snowmelt period was to register mean daily temperatures above 5ºC and minimum daily temperatures above 0ºC for several days, followed by a significant increasing of the water discharge values, and/or a significant increasing of the water discharge values during days without any precipitation. The end of the snowmelt was identified by a significant decrease of the hydrograph happened during days showing mean daily temperatures above 5ºC and minimum daily temperatures above 0ºC.

Because available information of the water discharge and the suspended sediment concentration released by previous works regarded mostly significant events, a conversion of most part of the original data of the whole study period was needed. In the case of the water discharge, the upstream water level gauge has demonstrated to be more reliable because of its good state of maintenance and calibration. Besides, using the upstream sensor, the analyses appear consistent with the previous works carried out in Rio Cordon basin (Lenzi et al., 2006b; Mao et al., 2009). Hence, we primarily chose the data produced by this device, whilst data from the other water level gauges have been used only when data from the in-channel gauge was not available. After organizing and elaborating the 60-min data of every year, we could stablish the monthly, annual and seasonal behavior of Q. Runoff volumes (Ru, 10^3 m^3) were calculated from the hourly values of Q. Daily, monthly, seasonal and annual values of Ru were subsequently assessed. Flood events were identified within each year from the hourly values of Q, and 5-min data from the days of the events were isolated and studied in order to develop a more detailed analysis of every event. The assessment of the water discharge (Q) measured every 5 minutes allows to

better evaluate the hydrograph of floods, permitting to estimate the peak discharge (Q_p) and the initial value of Q, as well as the duration of the event. In case of sediment transport, the effective runoff (Ru, 10^3 m^3) is estimated for each flood. The effective runoff is defined here as the portion of the hydrograph volume that contributes to the transport, exceeding the detected threshold discharges. In the Rio Cordon, the determination of thresholds is possible thanks to the data produced by the turbidity meters and by the recorded timing of initiation and ending of the coarse bedload separated and accumulated on the storage area.

Also in the case of the turbidity measurements, the upstream sensor was used primarily because of its major reliability. After organizing and elaborating the 60-min data of every year, we could stablish the monthly, annual and seasonal behavior of SSC and assess the days or periods in which suspended sediment transport occurrs. Hourly suspended sediment loads of these periods were calculated from Q and SSC hourly values. Daily, monthly, seasonal and annual values of suspended loads were subsequently assessed. Once the flood events are isolated, the assessment of the suspended sediment concentration every 5 minutes permits to construct the detailed sedigraph, to identify the peak (SSC_p) and to calculate an accurate value of the total suspended load during the flood (SSL). In case of unreliable data or malfunction of the sensors, three formulas are available to calculate suspended sediment concentration values from water discharge values according to the season. This SSC-Q relationship was proposed by Mao (2004) and has been used since then for periods lacking data (Rainato et al., 2016). The approach is based on the different runoff generation processes depending on the season. Runoff is dominated by snowmelt from 1 April to 15 June, by brief, intense storms from 16 June to 31 August, and by extended rainfall events from 1 September to 31 November. The SSC-Q formulas reflect the different relationships between the water discharge and the suspended sediment transport that these runoff-generation conditions cause. After organizing and elaborating the 60-min data of every year, we could stablish the monthly, annual and seasonal behavior of SSC and assess the days or periods in which suspended sediment transport occurrs. Hourly suspended sediment loads of these periods were calculated from Q and SSC hourly values. Daily, monthly, seasonal and annual values of SSL were subsequently assessed.

2.2.3. Conversion values H-Q, NTU-SSC

Water level values (H, in meters) from the water gauges installed in the monitoring station are converted to water discharge values (Q, m^3s^{-1}) thanks to the formulas established for those sensors. Despite some Q values from the studied events were already converted for previous works, hourly

values for the whole years of the 1986-2015 period were needed for this study and hence they were calculated. A new conversion formula was needed for the gauge installed in SST3 (upstream sampling station, explained in chapter 2.2.4.) in order to calculate the water discharge from the registered water level values in this section. The points of this new H-Q regression curve (R^2=0.92) were obtained by repeated water discharge observations at different water levels with the saline solution method.

The turbidity values (NTU, Nephelometric Turbidity Units) are converted into suspended sediment concentration values (SSC, g l^{-1}). This conversion is based on laboratory tests and its reliability has already been stated in previous works (Lenzi & Marchi, 2000; Mao, 2004). As with the H-Q data, a new NTU-SSC conversion was needed in this work for the samples collected at the SST3 section. Water samples were collected at different flow conditions. After their turbidity was assessed, samples were filtrated through glass fiber filter paper. The filter was subsequently dried in oven and weighted. The NTU-SSC regression curve obtained (R^2=0.96) permitted to assess the suspended sediment concentration of the water samples collected in the upstream sampling station.

2.2.4. Field research and analysis

Data collected in consecutive gauging stations provide detailed information on suspended sediment transport processes and permits to analyze changes in the hysteresis patterns along the water course (Aich et al., 2014). Field campaigns were developed in 2014 and 2015, with the aim of studying the spatial variations featured by the suspended sediment transport within single flow events. The hypothesis was that taking account of the hydrograph and sedigraph occurring several points, not ony in the outlet section, would permit us to localize the main sediment source during the event. One of the challenges of this task was to deal with the unpredictability of the weather in the catchment's surrounding areas. Besides, 2015 lacked a proper snowmelt period in the catchment, due both to the low quantity of solid precipitations accumulated during the winter and the unusual slow melting during the spring. For this reason, the only snowmelt studied was the one from 2014. The parameters studied were isotopic content, electrical conductivity (EC), suspended sediment content of the in-channel and discharge values. We monitor these parameters hourly in different sections of the main channel. The sections, called SST3 (upstream station) and SST1 (downstream station), were selected following morphological criteria (Figure 24). During the first campaigns, a third sampling station, SST2, was placed between SST1 and SST3, but 2014 analysis demonstrated that conductivity values and isotopic

content values from water sampled in SST2 and SST1 did not show particular differences (ANOVA test, Kruskall-Wallis test). From the statistical point of view, water samples from SST2 belonged to the same population than SST1, and hence the sampling station SST2 was removed from the analysis. Therefore, this work reports only the results obtained from SST1 and SST3.

Sampling campaigns were performed during single events occurring in the Rio Cordon catchment. The beginning of the event was defined as the beginning of the rainfall or the snowmelt process that caused the rising of the water discharge values. Measurements of electrical conductivity (EC), SSC and q were taken through the event. EC was measured in rain water or snowmelt water, stream water, groundwater and soil water. The underground water sampling was possible thanks to a well installed besides the SST3 section. Turbidity was measured in stream water and subsequently converted into SSC values by the regression formulas. The piezometers installed in the stream channel measured the water level at 15-min intervals. Conversion from water level to water discharge values was calculated thanks to the regression curve assessed for each section. All the in-channel measurements were developed in SST1 and SST3 contemporaneously from the beginning to the end of the flood event.

Besides, samples of event water, pre-event water and old water were taken during the reported events in order to perform a HS (Hydrograph Separation). The tracer used for this technique was the electrical conductivity of the water, even though the first idea was to perform the HS using stable water isotopes as tracers. Hence, the ^{2}H and ^{18}O isotopic composition of the water samples was determined by an off-axis integrated cavity output spectroscope (model DLT-100 908-0008, Los Gatos Research Inc., United States of America). The analysis procedure and method to mitigate possible carry over effects followed the ones reported in Penna et al. (2010; 2012). The typical instrumental precision (average standard deviation of 1490 samples) was 0.5 ‰ for $\delta^{2}H$ and 0.10 ‰ for $\delta^{18}O$. However, this technique did not give good results, because the difference in isotopic composition of event and pre-event water was very small in most cases, or even negligible. For this reason, only EC was taken into account for the hydrograph separation, and this work reports results considering this tracer. Due to the spatial heterogeneity of soil water chemistry, it is difficult to obtain an accurate chemical signature of the old water component. Some studies used the tracer value in the stream prior to rainfall to characterize old water (Heppell and Chapman, 2005; Pellerin et al., 2007). Another common method for estimating the old water component is to assume that the stream water during the low flow periods between storms represents an integrated sample of the old water in the basin (McNamara et al., 1997).

The value of electrical conductivity in baseflow was adjusted following this methodology. The event-based average EC of rainfall was obtained from direct measurement of field samples. The event-based average electrical conductivity of snowmelt was obtained from direct samples through the entire snowmelt period. The EC of rain water, snowmelt water, groundwater and stream water was measured in the field using several portable conductivity meters (WTW GmbH, Germany) with precision of ± 1 μScm^{-1}. The EC data was converted to specific conductance (EC of water at 25°C).

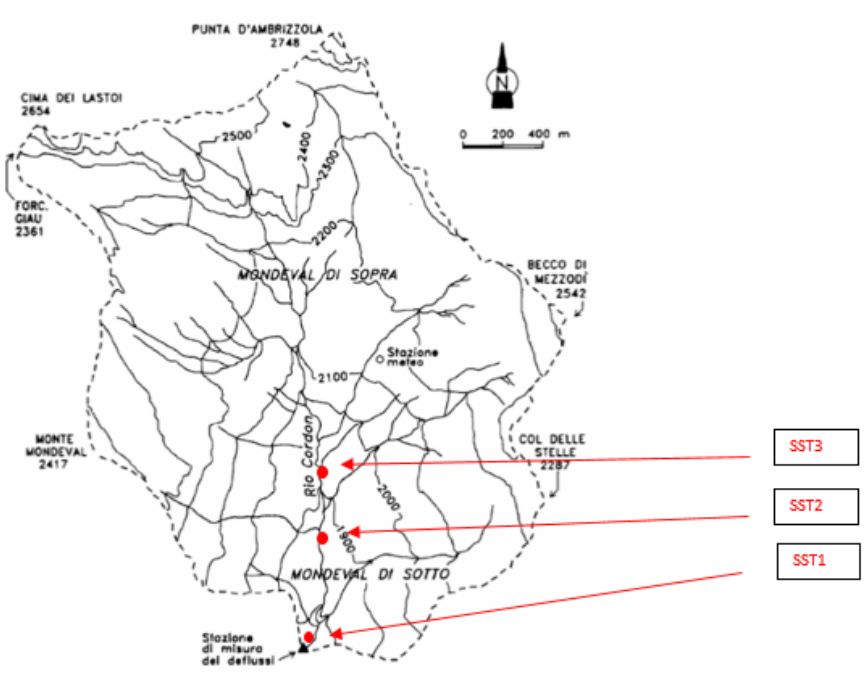

Figure 24: Location of the sampling stations in the catchment.

3. CHAPTER THREE- ANALYSIS AND RESULTS

3.1. 30 years of suspended sediment fluxes: 1986-2015.

3.1.1. Annual sediment budget and suspended fraction

In the Rio Cordon, the total sediment yield is considered as the sum of bedload and suspended load. Bedload data was obtained from the ultrasonic sensors located in the deposition basin of the monitoring station. Suspended sediment load data were obtained from the turbidity meters and the water gauges located in the inlet and outlet flumes. The total annual sediment loads (TSL) for the period 1986-2015 were calculated (Figures 26 and 27). During this study period, 15100 t of sediment were mobilized. The mean annual specific yield of the three decades of study was calculated as 100.7 t km^{-2} y^{-1}; however, Figure 27 shows that the cumulated curve does not increase homogeneously but presents two considerably steep steps. In fact, the years 1994 and 2001 show high loads, due to the extraordinary events that have been mentioned before. These years break dramatically the general trend and suggest a division of the 30 years in three periods: the 1986-1993 period, the 1995-2000 period and the 2002-2015 period. The annual sediment budget registered through the 2002-2015 period shows lower values than the previous periods. In fact, during the period after the mud flow of the 2001 snowmelt period, which originated 1017.6 t of fine sediment, the annual sediment yield has been less than 500 t y^{-1}, with the only exception of 2002 and 2009. The sediment supply released after the 2001 determined the higher loads of 2002, while the high volumes of water from snowmelt registered in 2009 were the main factor that induced into a higher load. Apart from these two cases, the main annual specific yield during the third period has been less than 100 t km^{-2} y^{-1}, and its mean annual specific yield is 47.9 t km^{-2} y^{-1}, whilst the period 1986-1993 and 1995-2000 show a mean value of 77.7 t km^{-2} y^{-1} and 94.2 t km^{-2} y^{-1} respectively.

Figure 25: Coarse material deposited at the monitoring station after 14 September 1994 event (left) and alluvial fun originated by a mud flow coming from a tributary on 11 May 2001 event (right).

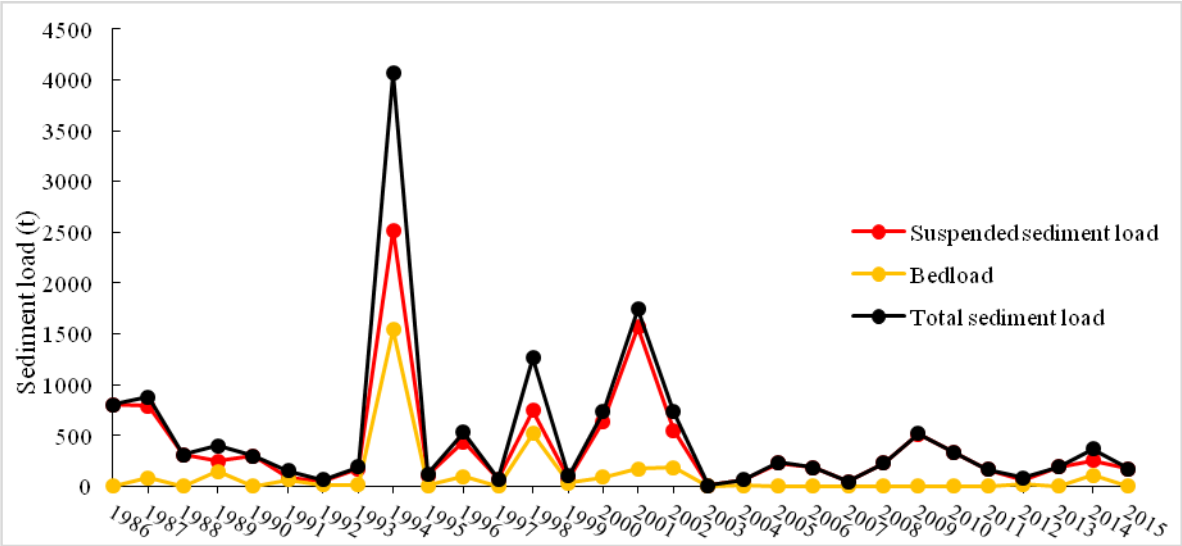

Figure 26: Annual sediment yield of the 1986-2015 period.

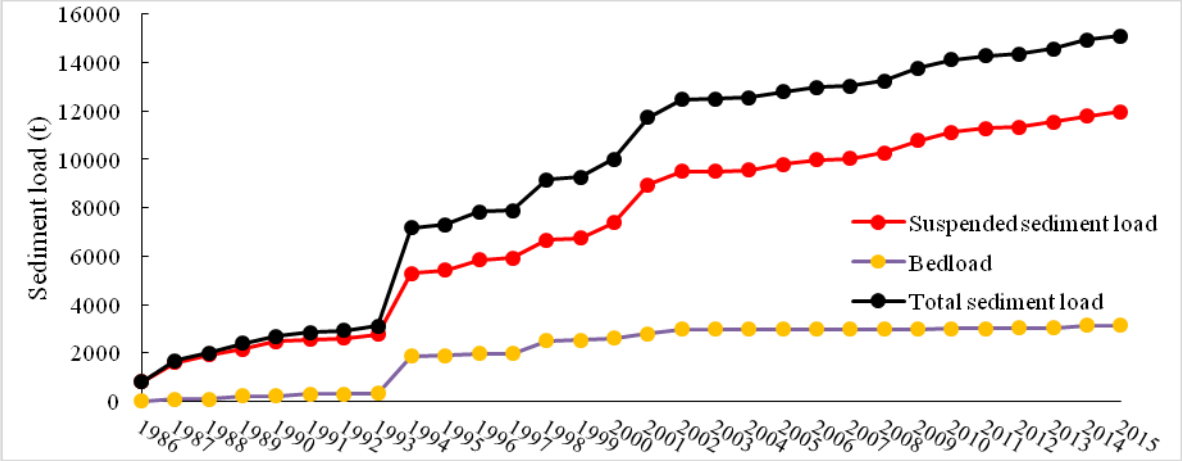

Figure 27: Annual cumulated sediment yield of the 1986-2015 period.

The year 1994 was characterized by the highest contribution from a single event to total sediment load (4067.2 t), due to the September 14th event, in which 98% of the annual amount was mobilized. In addition to 1994, there were relevant contributions to the sediment yield in 1998 (1261.5 t) and 2001 (1742.6 t).

Figure 28 shows that the annual bedload fraction was usually lower than the suspended load. In fact, the long term partitioning lead into a bedload fraction of 0.21. This prevalence of suspended sediment loads is more clear in the third period (2002-2015), in which barely 7% of the total annual yield had its origin in bedload transport. If applied to the Rio Cordon, the formula proposed by Schlunegger and Hinderer (2003) predicts a suspended load fraction of 0.56 and the formula proposed by Turowsky et

al. (2010) predicts a fraction of 0.61. These estimations, showed in the work by Rainato et al, 2016, are clearly lower than the value obtained through the three decades in this catchment (0.79). The highest contributions of suspended sediment load were registered in 1994 (1543.4 t), 1998 (516.8 t), 2002 (183.4 t), 2001 (174.0 t), 1989 (145.6 t) and 2014 (117.6 t). In addition to the already mentioned September 1994 event, the year 1998 registered an important annual contribution to the bedload yield, mainly due to a flood caused by a high intensity autumn rainfall event.

Table 4: Annual specific yield and suspended load fraction of the 1986-2015 period.

YEAR	Ru 10^3 m^3	SSL t	Bedload t	SS fraction %	Mean specific yield t km^{-2}
1986	6084.47	806.9	0	100	161.4
1987	7249.2	792.2	85.6	90	158.4
1988	5828.6	312.8	0	100	62.6
1989	6406.5	251.8	145.6	63	50.4
1990	4525.4	302.2	0	100	60.4
1991	7824.9	87	67.2	56	17.4
1992	6747.7	50.7	15.5	77	10.1
1993	6950.9	175.6	17.2	91	35.1
1994	7264.1	2520.9	1543.4	62	504.2
1995	6693.7	110.9	10.3	91	22.2
1996	7245.6	436.3	94.7	82	87.3
1997	6558	74	0	100	14.8
1998	8279.3	744.8	516.8	59	149
1999	8199.4	73.6	32.7	69	14.7
2000	5966.4	641.7	92.2	87	128.3
2001	5839.9	1568.4	174	90	313.7
2002	7465.7	551.2	183.4	75	110.2
2003	3673.2	13.7	1.7	86	2.7
2004	3443.1	58.7	7.9	88	11.7
2005	2597.7	232.9	1.6	99	46.6
2006	4973.1	184.3	1.2	99	36.9
2007	4342.1	49.8	0	100	10
2008	6350	229.1	0	100	45.8
2009	6275.1	514.9	3.1	99	103
2010	5899.2	336.1	1.4	100	67.2
2011	5854.4	167.1	0.9	99	33.4
2012	4833	62.4	24.5	72	12.5
2013	7477.4	189.4	3.8	98	37.9
2014	7488.3	258.4	113	70	51.7
2015	4197.7	173.5	0	100	34.7

Figure 28: Suspended load and bedload annual fractions for the 1986-2015 period.

Annual runoff volumes, annual specific yield and suspended load fraction of the whole study period are shown in Table 4. It is important to notice that runoff volumes did not change much from one year to another (mean value=6084.47 10^3 m^3, standard deviation=1453.10), whilst total sediment load showed much higher variability within the study period (mean value=503.33 t, standard deviation=777.73 t 10^{-3} m^{-3}).

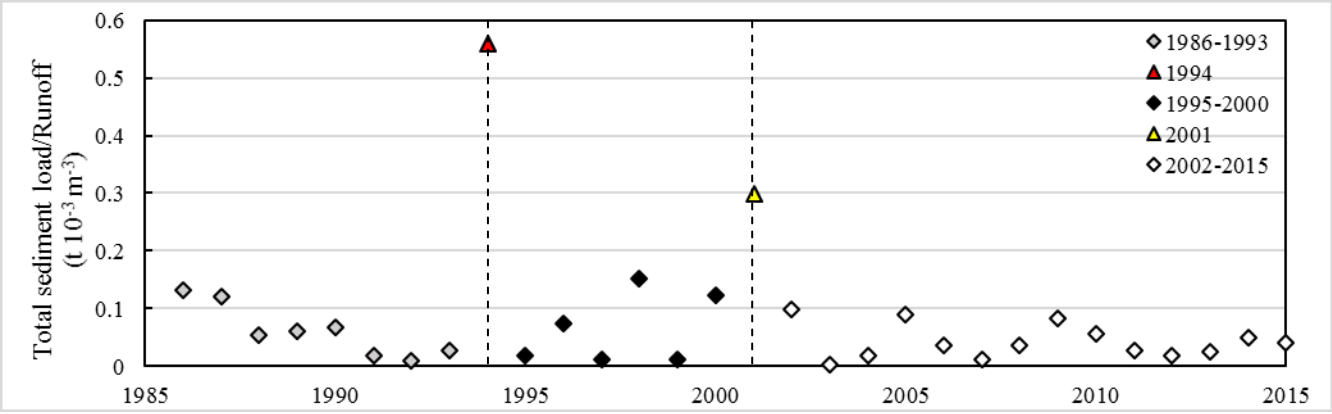

Figure 29: Total sediment load-runoff annual ratios (1986-2015).

Figure 29 shows the annual ratios of the total sediment load against runoff volumes. The period 1986-2001 lacks winter water data. A mean winter runoff was calculated with the winter values registered from 2002 to 2015, and this value was applied to the years lacking winter data. The years 1994 and 2001 are noticeable because of their high TSL/Ru relation, due to the flood events mentioned above. The rest of the years from the study period follow a downward trend, though splitted by these two exceptions. In fact, it is noticeable that before 1994, the TSL/Ru ratios were arriving to very low values, with a mean value of 0.62 t 10^{-3} m^{-3} and values below 0.01 t 10^{-3} m^{-3} in some cases. During 1994, more than 7264 10^3 m^3 of water flowed into the exit channel, and 4064.2 t of solid material were

transported, of which 98% were due to the 14 September extraordinary event, in which 2435 t of suspended material and 1542 t of bed load moved. The intense rainfalls induced into high values of water discharge and the destruction of the bed armor layer, and hence the channel bed became the main source of sediment, creating unlimited supply conditions and causing a considerable alteration in its geometry (Mao, 2004). In addition, many old sediment sources were reactivated and new ones formed (Lenzi et al., 2004). Hence, the ratio reached the highest value of the study period (0.559 t 10^{-3} m^{-3}). Consequently, the sediment availability increased during not only this single event, but also the following years. After the high transport registered during 1994, the 1995-2000 period turns back to a mean value of 0.065 t 10^{-3} m^{-3}, quite similar to the previous period, but some years show considerable higher ratios due to the break of the bed armoring and the subsequent higher availability of sediments during the following years. In fact, a considerable quantity of solid material is transported during some moderate events happening within this period, such as the one registered in October 7, 1998, in which more than 900 t of fine and coarse sediment were transported. The 2001 ratio, though below the 1994 ratio, is still a high value equal to 0.298 t 10^{-3} m^{-3}, with 5839.9 10^3 m^3 of runoff volumes and 1742 t of sediments. After this year there is a clear diminishing trend in the TSL/Ru ratio, with a mean value of 0.04^3 t 10^{-3} m^{-3} and several years showing values around 0.01 t 10^{-3} m^{-3}, such as 2003, 2004, 2007 and 2012.

3.1.2. Interannual study of the suspended sediment fluxes

Results from last chapter have shown that during the three decades, 79% of the total load registered in Rio Cordon was suspended load, demonstrating that the study of the suspended sediment transport dynamics requires a special attention in this catchment. Data of water discharge and suspended sediment concentration were used to calculate the seasonal suspended sediment load and the runoff volumes associated to them in the 1986-2015 period. The seasons are divided in winter, snowmelt, summer and autumn. Winter is considered from 1 December to 31 March. The snowmelt is the period in which the snowpack from the winter months melts. This period is variable, but usually it takes from two to five weeks between 1 April and 15 June. The rising of the daily temperatures and the variations of the water discharge permits to accurately establish the weeks in which snowmelt takes place. We consider that summer goes from 16 June to 31 August in the Rio Cordon. Autumn is the period from 1 September to 30 November. During winter, low values of water level can be registered despite the snow cover in the inlet channel of the monitoring station. Those values permit to calculate the winter

runoff, which is usually lower than the volumes registered during the other seasons. Due to the snow cover, no sediment transport occurs during this season. Still, we applied systematically a value of 0.1 t for the winter, because the water present in the channel transports a small quantity of suspended sediment from the baseflow. Some turbidity values registered occasionally during winter permitted to estimate this representative value.

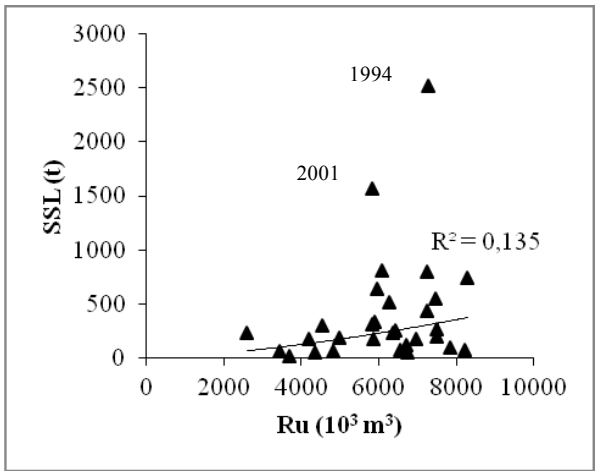

Figure 30: Annual runoff volumes against annual suspended sediment loads.

The low correlation between the annual runoff volumes and the total suspended loads can be appreciated in Figure 30. This result shows that the relationship between these two parameters is weak (R^2=0.135). Changes in the annual suspended loads are not dependant of runoff variations. In particular, the years 1994 and 2001 feature high sediment loads even though they are characterized by ordinary runoff volumes.

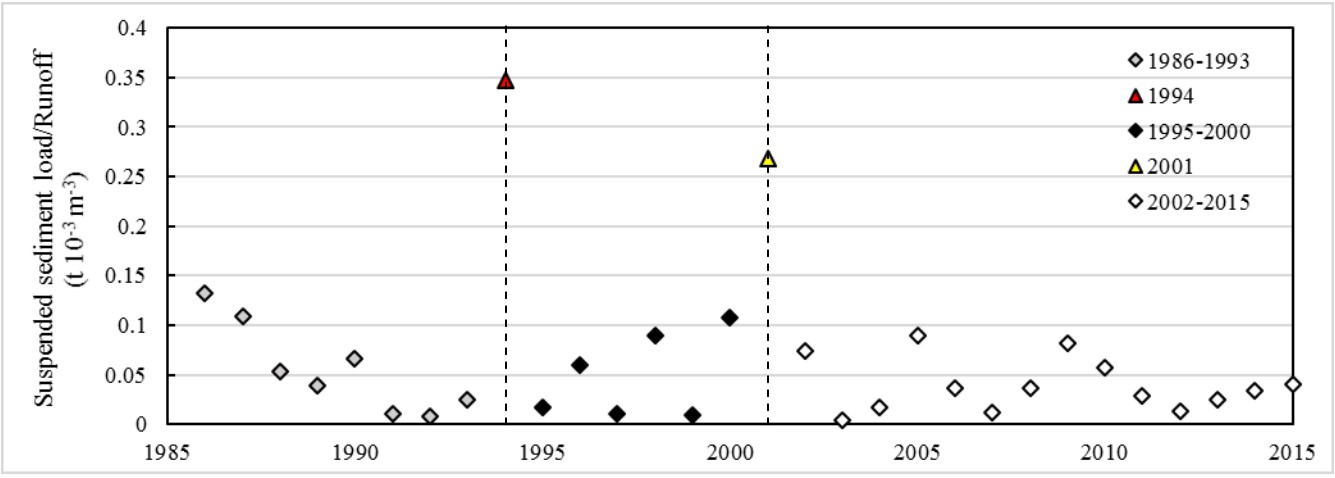

Figure 31: Suspended sediment load-runoff annual ratios (1986-2015).

The ratio between the suspended sediment budget and the annual runoff volumes was assessed for every year of the study period (Figure 31). A falling trend of this ratio can be noted through the three decades of study. In fact, while the annual runoff does not show any important trend through the period, the suspended annual budget shows a diminishing trend. Therefore, the ratio SSL/Ru tends to reduce from year to year, with the interruption of the already mentioned events registered in 1994, 1998 and 2001. September 1994 extraordinary event breaks dramatically the decreasing trend of the suspended sediment annual yield. This event registered a maximum water discharge value of 10.42 m^3 s^{-1}, and moved 2435 t of suspended material, that is to say, the 96.7% of the total annual suspended sediment yield. The SSL/Ru ratio of 1994 is 0.347 t 10^{-3} m^{-3}. Due to this event, the sediment availability increased during the following years, and it is noticeable that some years following 1994 had higher suspended budgets compared to the previous. In fact, the period 1986-1993 shows a mean SSL/Ru ratio of 0.056 t 10^{-3} m^{-3}, while the ratio for the 1995-2000 is 0.049 t 10^{-3} m^{-3}. In May 2001, there were almost-unlimited supply conditions due to a mud flow of the medium-high zone of the catchment. Although it mobilized more than 1500 t of fine material and was the main cause of the high SSL/Ru ratio of that year (0.269 t 10^{-3} m^{-3}), this event did not alter the general diminishing trend of the sediment availability any further than the year after. In fact, the third period presents the lowest SSL-R ratio of the whole study period (0.039 t 10^{-3} m^{-3}).

3.1.3. Suspended sediment seasonal budget and annual hysteresis

The annual suspended budget was divided in seasons in aims of deepening in the analysis of the temporal variations in the suspended sediment dynamics. It is interesting to notice the difference in the annual distribution of the suspended sediment budget within the study period (Figure 32). In fact, a division can be made based on the interruptions of the diminishing trend made by the years 1994 and 2001, therefore having three periods: 1986-1993, 1995-2000 and 2002-2015. Differences are noted between the two first periods (1986-1993 and 1995-2000) and the 2002-2015 period, based on their seasonal budgets. While snowmelt is the season that registers more suspended sediment budget in most part of the years between 2002 and 2015, this situation rarely occurs in the first half of the study period. In fact, from 1986 to 2000, only in the years 1988, 1990, 1992, 1993 and 1997 the higher contribution comes from the snowmelt (Figure 33). That makes 5 cases out of 15. The mean snowmelt budget for these years is 77.6 t. Instead, from 2002 to 2015 the most common situation is to have the higher budget during the snowmelt. In fact, the mean snowmelt budget for this second period is 248.9 t.

During summer, the 1987-2000 period shows a mean SSL of 76.6 t, much higher than the 37.3 t from the mean summer SSL of the 2001-2014 period. The mean autumn suspended budgets are 2435.1 t and 123.0 t, respectively. Hence, rainfall events were the main origin of fine material transport in the first half of the study period, while snowmelt processes had this role in the second. In any case, the mean annual SSL of the second half is lower than its precedent: 309.3 t versus 389.5 t in the first half. This seems to corroborate the possible depletion of the sediment sources within the catchment.

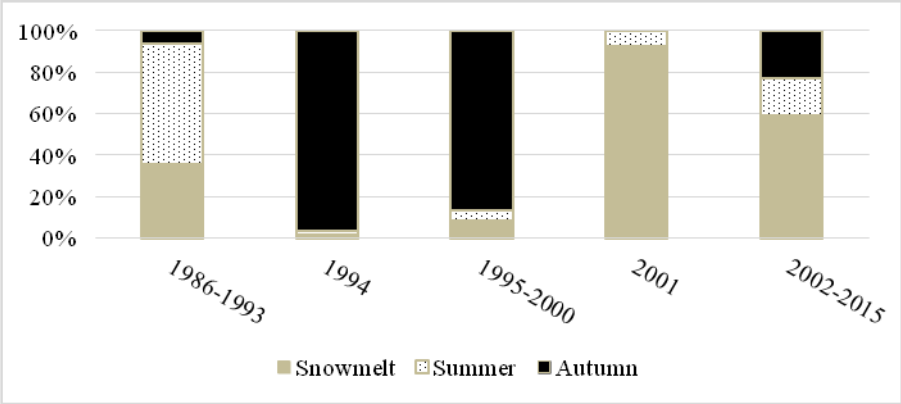

Figure 32: Seasonal distribution of the suspended budget in the different periods of the study.

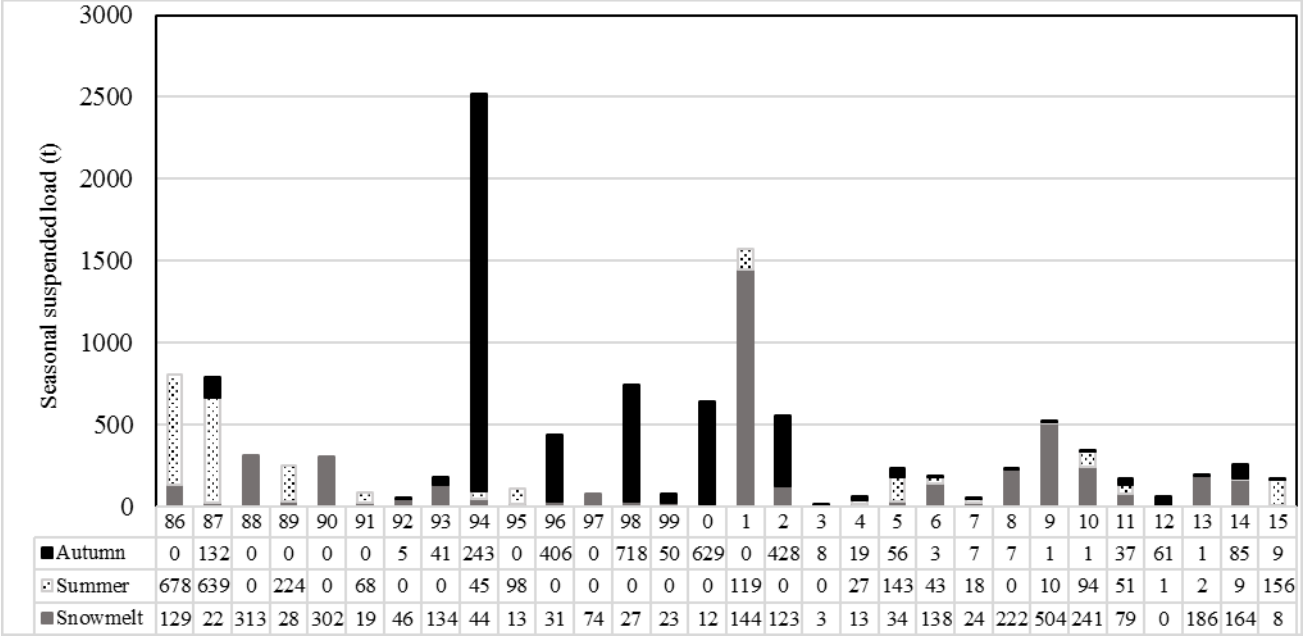

	86	87	88	89	90	91	92	93	94	95	96	97	98	99	0	1	2	3	4	5	6	7	8	9	10	11	12	13	14	15
Autumn	0	132	0	0	0	0	5	41	243	0	406	0	718	50	629	0	428	8	19	56	3	7	7	1	1	37	61	1	85	9
Summer	678	639	0	224	0	68	0	0	45	98	0	0	0	0	0	119	0	0	27	143	43	18	0	10	94	51	1	2	9	156
Snowmelt	129	22	313	28	302	19	46	134	44	13	31	74	27	23	12	144	123	3	13	34	138	24	222	504	241	79	0	186	164	8

Figure 33: Seasonal suspended budget through the three decades of study.

Once the seasonal values of total runoff (Ru) and total suspended sediment load (SSL) were established for every year, they were plotted in a graphic in order to assess a comparison among years.

We considered the consecutive increasing of the values throughout a single year because they described clearer shapes when plotted in a graph than single seasonal values. Because runoff volumes and suspended sediment load do not have a univocal relationship, the four seasonal values of ΔRu and ΔSSL during winter, snowmelt, summer and autumn describe a shape that helps understanding the transport dynamics during the year. The rising branch of the cycle shows the seasonal increasing of both variables from winter loads to snowmelt loads, from snowmelt to summer and from this to autumn. The falling branch links the autumn values with the winter values, that is to say, connects the initial values of the year with the total annual values. The study of the seasonal increasing values respect to this branch permits to establish similarities between years. In order to group the years based in their similar seasonal behavior, the author has classified them in triangle (upward and downward), eight-shaped and linear (Figure 34). When the major SSL contribution occurs during the snowmelt, the slope of the rising branch shows its higher slope from winter values to snowmelt values, and hence the shape described by the seasonal values is an upward triangle. When the major SSL contributor is the summer, the higher slope is drawn from snowmelt to summer, and the cycle can be described as eight-shaped. A downward triangle is described when the major SSL contributor is the autumn, because the rising branch is steeper from summer to autumn. Linear or almost-linear shapes are found in the years in which the seasonal contribution is balanced and there is not a season that mainly contributes to the annual loads.

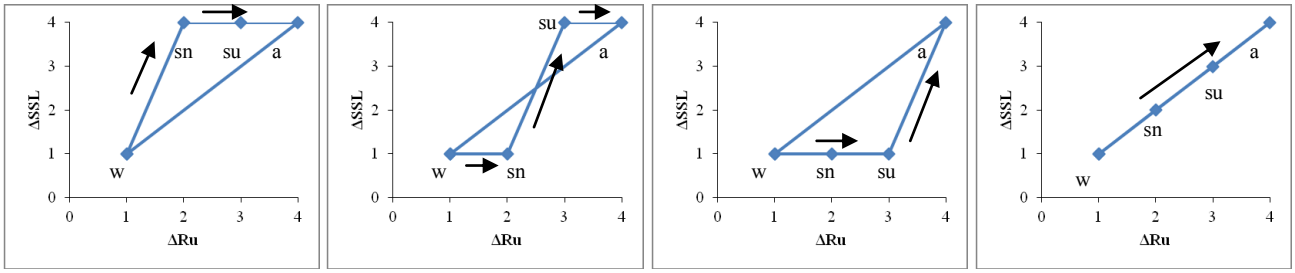

*Figure 34: Theoretical shapes of the annual hysteresis. From the left to the right: upward triangle, eight shape, downward triangle, linear. Winter, snowmelt, summer and autumn values are represented by **w**, **sn**, **su** and **a**, respectively.*

1986-2000 period

From 1986 to 2000, more than 6576 t of suspended sediments were transported towards the measuring station of the Rio Cordon catchment. The mean annual suspended budget is 492 t and the annual runoff

volumes are 6788.3 10^3 m^3. This period is characterized by a considerable contribution from the rainfall events (Figure 35). In fact, 83.5% of the total load was provided by floods from this season. Snowmelt processes contributed only in 16.5% to the total suspended sediment budget of the period. Autumn was the major contributor in 1994, 1996, 1998, 1999 and 2000. Summer contribution prevailed the years 1986, 1987, 1989, 1991 and 1995. Nonetheless, the annual behavior of every single case should be taken into account.

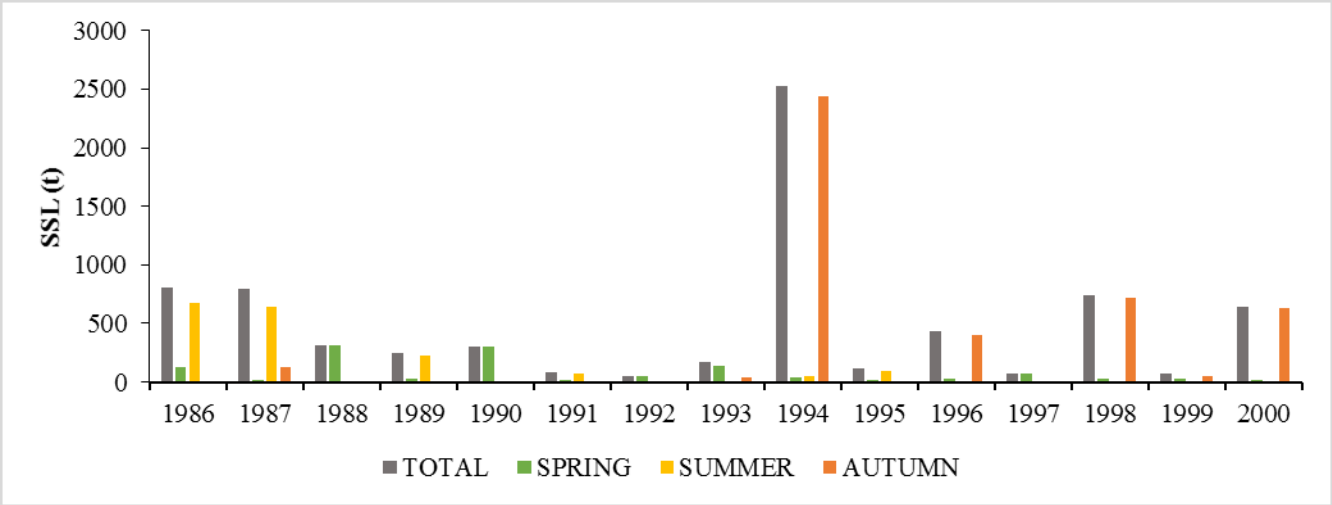

Figure 35: Annual and seasonal suspended budget of the 1986-2000 period.

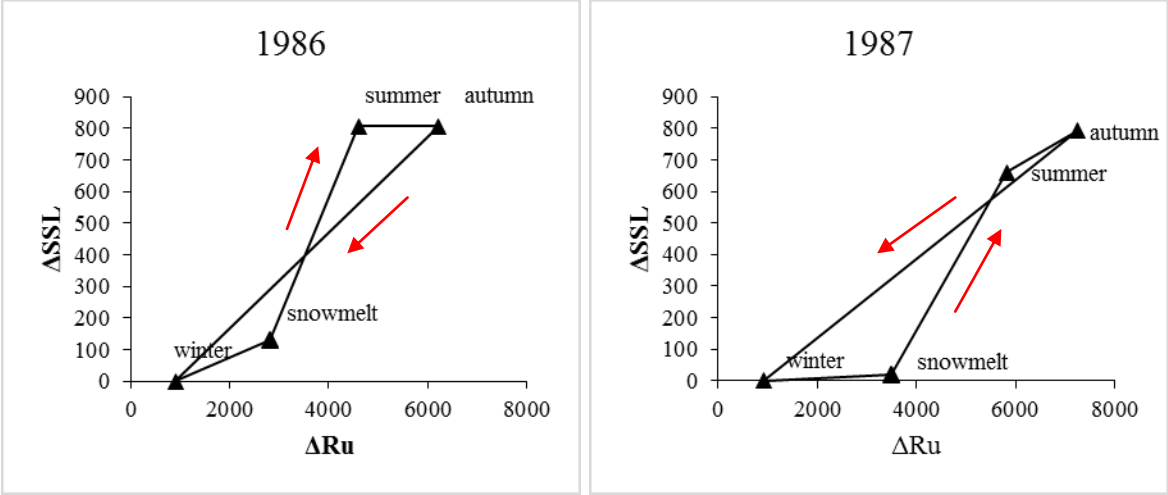

Figure 36: Seasonal runoff volumes (10^3 m^3) increasing versus seasonal suspended sediment load (t) increasing during the years 1986 and 1987.

The year 1986 was characterized by little transport during spring and autumn and high transport rates during the summer. In fact, almost 85% of the annual suspended budget was transported during

summer, though total runoff volumes were quite similar in all the seasons. This makes us think that this year must have been characterized by a slow snowmelt followed by strong rainfalls the first months of the summer. Total annual suspended sediment budget was 807 t, considerably above the main value. The curve described by plotting the ΔRu values against the ΔSSL values is eight-shaped, due to the fact that most of the material was transported during the second half of the year (Figure 36).

During 1987, the snowmelt budget was minimum, but the storms that took place in the catchment during the summer induced considerable suspended transport. From this point of view, 1987 is quite similar to its precedent year. In fact, also the total annual budget (792 t) is close to the one from 1986. The autumn storms moved some t of material. The curve described by plotting the ΔRu values against the ΔSSL values is eight shaped, due to the wide gap among spring and summer SSL (Figure 36).

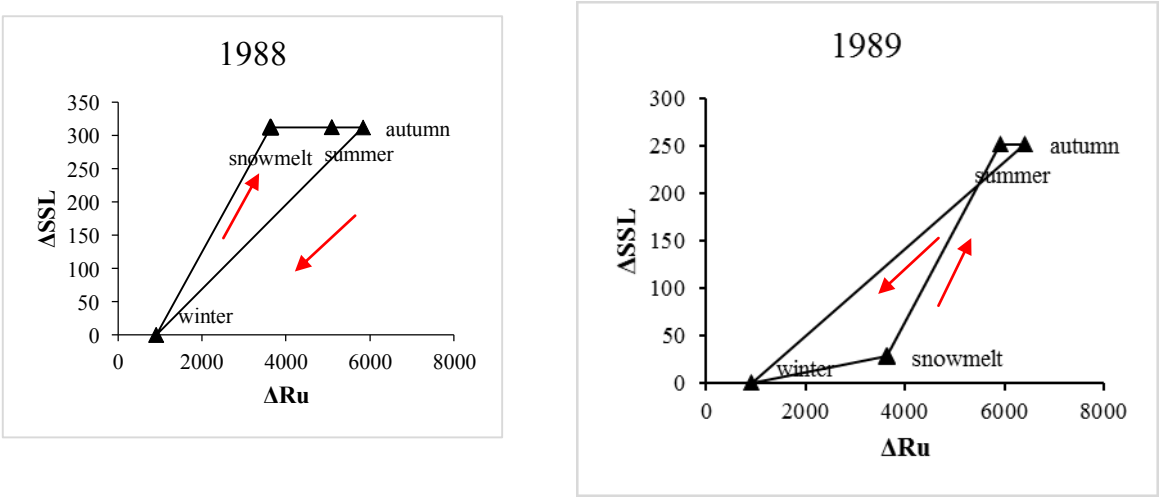

Figure 37: Seasonal runoff volumes (10^3 m^3) increasing versus seasonal suspended sediment load (t) increasing during the years 1988 and 1989.

In 1988, the only significant sediment transport took place during the snowmelt event, and so the hysteresis described between ΔRu and ΔSSL has a upward triangle shape (Figure 37). Though the runoff values from summer are quite high, no transport was registered during this season, nor during autumn. This result leads us to believe that snowmelt runoff induced into the depletion of the sediment supply of the year. The annual budget, of 312.8 t, corresponds almost entirely to this process. It is a value lightly under the average value of the 1986-2000 period.

The 1989 was characterized by a low transport during the snowmelt, nonetheless the high runoff volumes registered in spring, and some interesting events during the summer. This case is similar to 1986 and 1987, though showing a total budget below the media: in total, 251.8 t were mobilized. The eight shape of the curve supports the fact that 1989 is similar to 1986 and 1987 (Figure 37).

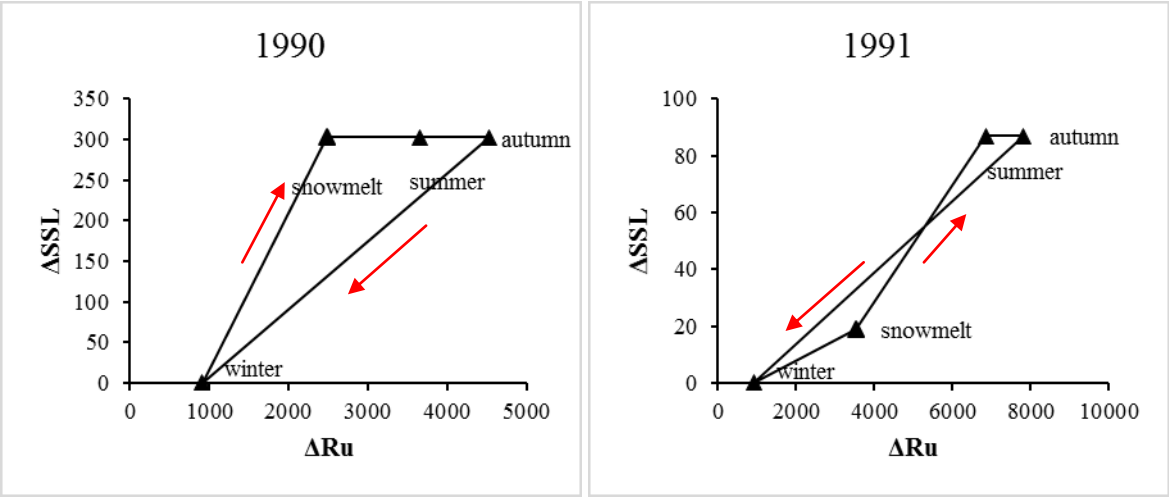

Figure 38: Seasonal runoff volumes (10^3 m^3) increasing versus seasonal suspended sediment load (t) increasing during the years 1990 and 1991, consecutively.

The transport characterizing 1990 is quite close to the 1988 behavior, with almost all the material transported during the snowmelt and a total suspended load narrowly below the mean value (302.2 t). The curve, as in 1988, describes an upward triangle (Fig. 38). As in the 1988 case, the results lead us to think that a high transport activity during the snowmelt depleted the active sediment sources and left low sediment available for the following rainfall events.

Even if their runoff volumes indicate there were potential conditions for the transport in the catchment, during 1991 low amount of material was transported. In fact, the total annual budget was 87 t, a value considerably below the mean annual SSL. Almost the totality of the fine material was registered during a flood event in June in 1991, therefore describing an eight-shaped curve (Figure 38).

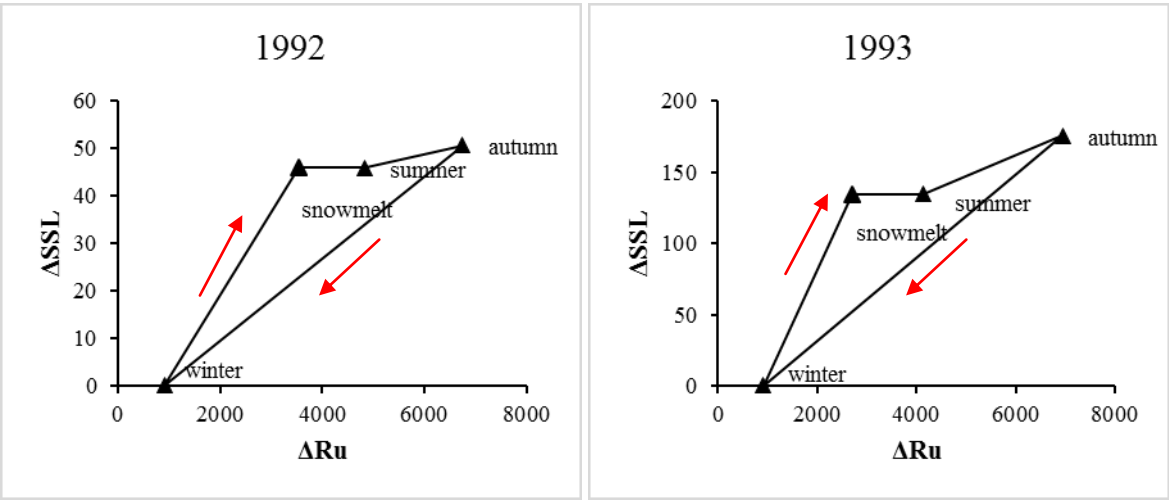

Figure 39: Seasonal runoff volumes (10^3 m^3) increasing versus seasonal suspended sediment load (t) increasing during the years 1992 and 1993, consecutively.

As in the precedent year, during 1992 a low quantity of suspended sediments was transported. Most of the material moved slowly during the snowmelt, and 4.8 t moved during a rainfall event in October. The curve described by plotting the ΔRu values against the ΔSSL values shows a shape that is close to the theoretical upward triangle (Fig. 39). Nonetheless the runoff volumes indicate there were potential conditions for the transport in the catchment, the annual budget was only 50.7 t. This consecution of years registering low transport rates suggests a general depletion of the sediment sources in the catchment.

During the snowmelt of 1993, more than 130 t of fine sediment moved downstream. It was a snowmelt characterized by high values of runoff. An important rainfall event taking place during October was the responsible of the 41 t of suspended material mobilized during autumn. In all, 175 t of suspended sediments were transported during this year, and because of the major contribution during snowmelt, the annual hysteresis between ΔRu and ΔSSL presents an upward triangle shape, even though there is some autumn load (Fig. 39).

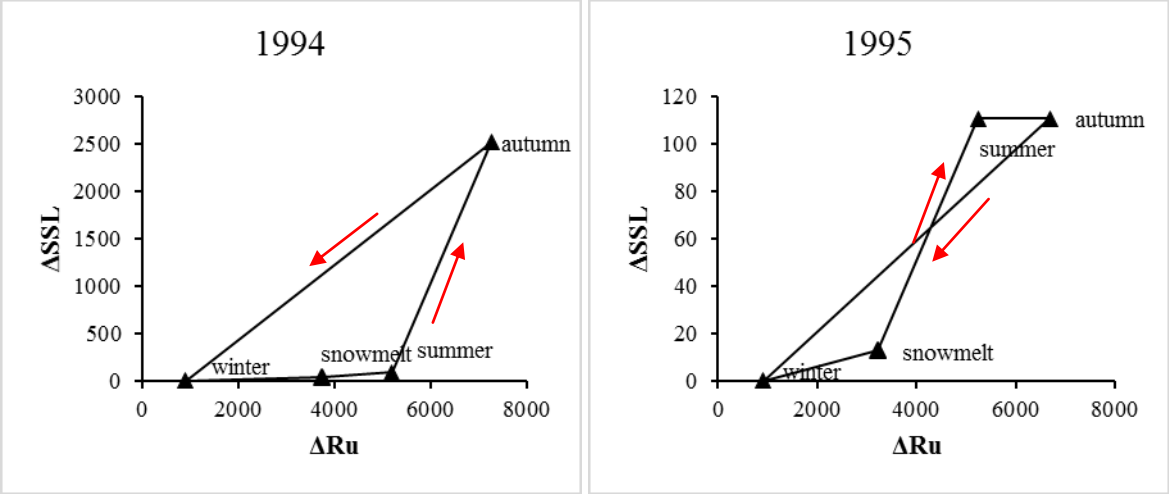

Figure 40: Seasonal runoff volumes (10^3 m^3) increasing versus seasonal suspended sediment load (t) increasing during the years 1994 and 1995, consecutively.

The year 1994 was a significant year in the history of the Rio Cordon catchment. It was characterized by low amount of material transported during the snowmelt process, nonetheless the significant runoff volumes registered, and low transport during summer. What makes this year interesting is the event taking place the 14th of September. This extraordinary flood registered a water discharge peak equal to 10.42 m^3 s^{-1}, which is considered to have a recurrence interval >100 years. The high intensity of the event created unlimited supply conditions, due to which 2435 t of suspended material and 1542 t of bed load were transported. As a consequence, this year registered the higher suspended budget of the whole

study period (2524 t), and created new availability conditions in the catchment area, thus modifying the diminishing trend that had characterized the Rio Cordon until that moment. More details about this event will be discussed in chapter 3.2. The seasonal values clearly describe a downward triangle, because of the great contribution of the autumn (Fig. 40).

During 1995, snowmelt process was slow and moved less than 13 t of suspended solid material. The sediment budget registered during this year was mainly transported during a summer storm occurring in August. Still, it was a year characterized by low sediment transport, despite of the increase of sediment supply released during the September 1994 event. In total, 110.9 t of fine material were mobilized, significantly below the main value. Because most of the material arrived during the summer, this year describes a eight-shaped curve (Fig. 40).

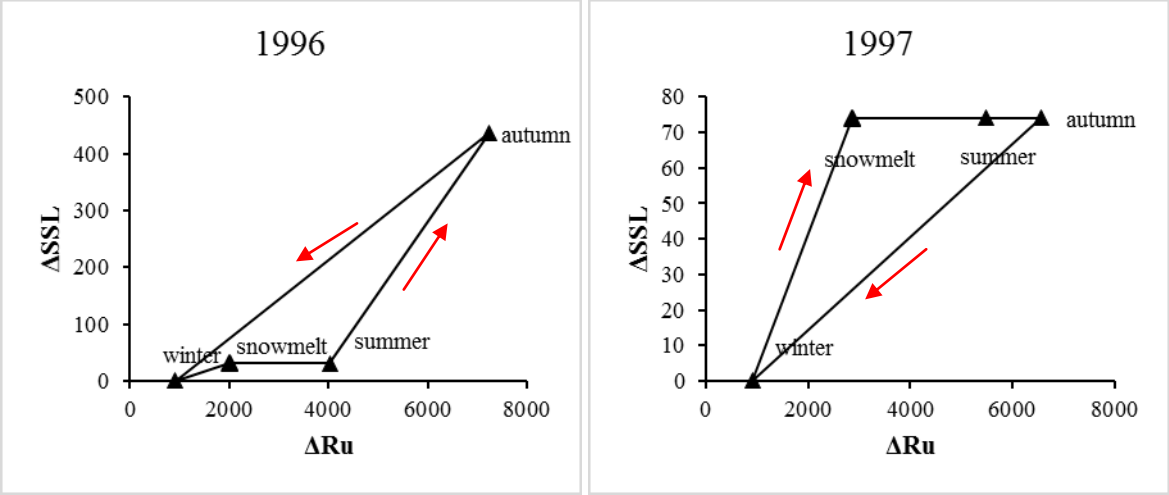

Figure 41: Seasonal runoff volumes (10^3 m^3) increasing versus seasonal suspended sediment load (t) increasing during the years 1996 and 1997, consecutively.

The year 1996 shows similarities with 1994, yet the sediment loads are markedly lower. During this year, a low quantity of suspended sediments moved during the snowmelt, and the summer lacked transport processes. Instead, autumn was characterized by a considerable quantity of fine material transported during some flood events that took place in October. The high intensity rainfalls registered during this month suggest that some of the sediment sources activated during the 1994 flood got reactivated, releasing more than 400 t of suspended solids. The total annual suspended budget is 436.3 t, considerably above the mean value. The curve obtained when plotting the ΔRu values against the ΔSSL values is a downward triangle (Figure 41), due to the fact that most of the material was transported towards the end of the hydrologic year.

The 1997 is characterized by low transport activity even if the runoff volumes were above the average. Fine sediments moved only during the snowmelt and no rainfall event was registered, so the curve described is similar to the curves of 1988 and 1990. The total annual fine budget was 74 t. The hypothesis is that runoff from snowmelt washed away the solid material that the events from October 1996 had released and, after that, the catchment area was characterized by low sediment supply. The curve described by plotting ΔRu against ΔSSL shows an upward triangle (Fig. 41), due to the fact that the fine material was transported during snowmelt.

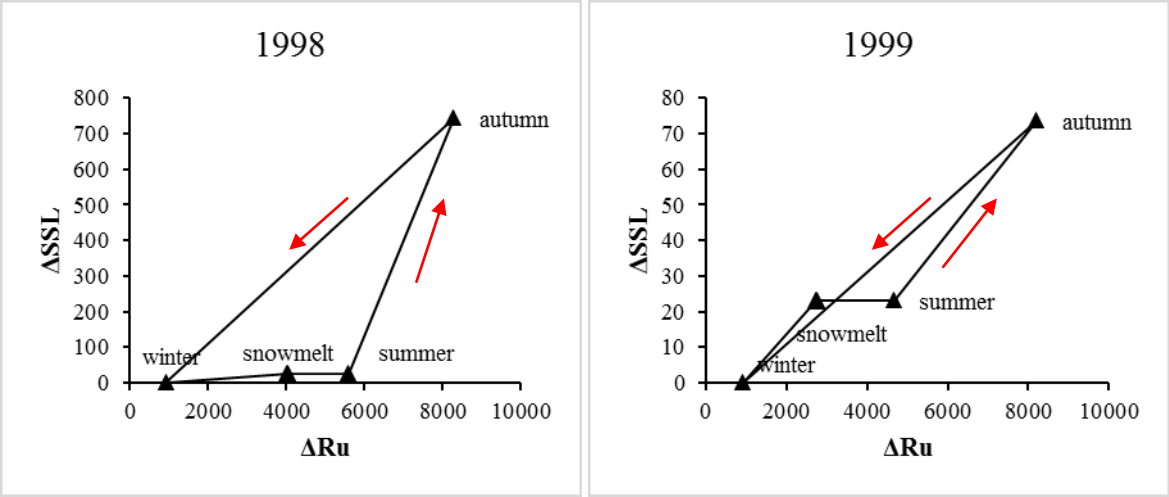

Figure 42 : Seasonal runoff volumes (10^3 m^3) increasing versus seasonal suspended sediment load (t) increasing during the years 1998 and 1999, consecutively.

During 1998, the main sediment contribution occurred in autumn. Though its annual sediment budget is lower than 1994 or 2001, this year is essential in the long-term study of the Rio Cordon catchment. Whilst 26.5 t of fine material were transported due to the snowmelt process and no transport was registered during the summer, more than 700 t were mobilized due to rainfall events occurring in September and October. Concretely, a non ordinary event on October 5th reached 4.73 m^3 s^{-1} of water discharge and moved almost 208 t of fine material. The annual suspended sediment budget was 744.8 t, and, because of the high transport registered during autumn, the curve describes downward triangle (Fig. 42).

The following year shows a quite different situation. A low amount of suspended sediments was transported during 1999. The annual sediment budget was divided between the snowmelt and the autumn storms, whilst summer lacked sediment transport. Autumn was the season that mostly contributed to the annual suspended budget. The total suspended load was only 73.9 t, and the curve

describes a mix between a linear and a downward triangle (Fig. 42), because of the higher fraction of autumn sediments.

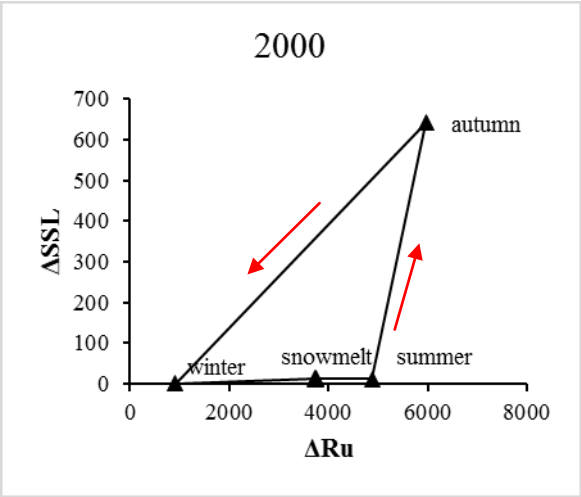

Figure 43: Seasonal runoff volumes (10^3 m^3) increasing versus seasonal suspended sediment load (t) increasing during the year 2000.

The last year of this period, 2000, is a particular case because snowmelt did not release any important amount of sediments, and nor did the summer season. During autumn, water discharge did not reach any extraordinary value, but still, consecutive rainfall event released more than 600 t of fine material. The total suspended budget was 641.7 t, and, because autumn was the main contributor, the shape was a downward triangle (Fig. 43), as in most of the cases of the 1986-2000 period.

The 1986-2000 is characterized by higher seasonal suspended loads from the rainy seasons than from the snowmelt. In fact, the years showing higher loads from snowmelt events than from rainfall events are just 5 years of 15, while 66.7% of the years show higher transport during one of the two rainfall seasons. For this reason, this period shows a higher frequency of years in which the seasonal values of ΔRu and ΔSSL describe an eight shape or a downward triangle.

2001-2015 period

From 2001 to 2015, up to 4500 t of fine sediment transport were transported in the Rio Cordon catchment. The mean annual suspended budget for this period was 305.5 t, while the mean annual runoff volume was 5381 10^3 m^3.

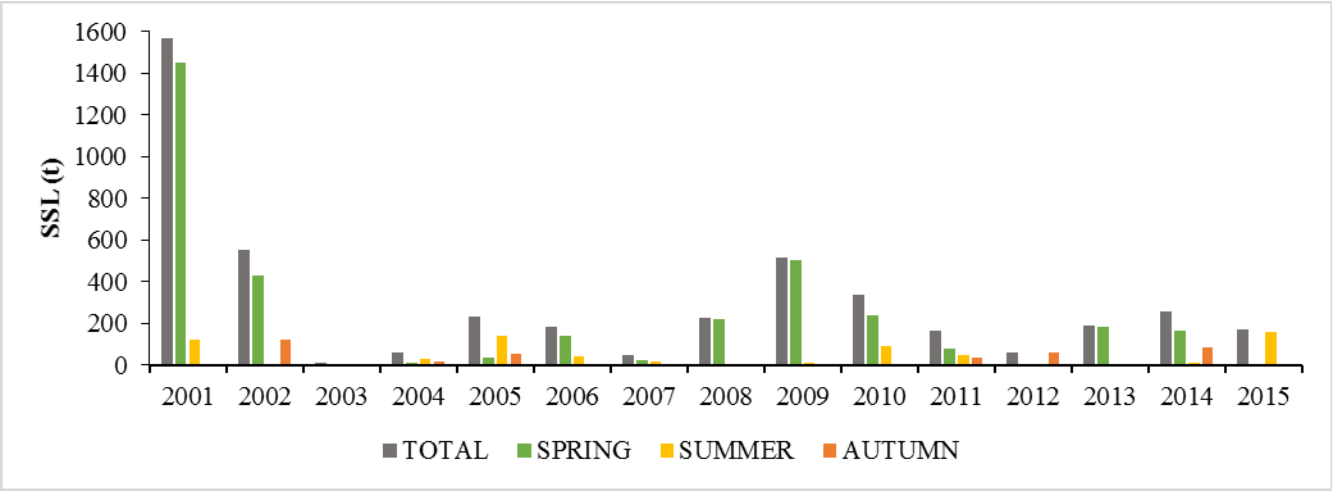

Figure 44: Annual and seasonal suspended budget of the 2001-2015 period.

This period differs from its precedent in the principal seasonal contribution (Figure 44). The snowmelt process replaces autumn rainfall as the mean fine material source. In fact, during the 2001-2015 period, 80.46% of the total suspended sediment budget was transported during the weeks in which the catchment featured snowmelt processes. Only in 2004, 2005 and 2015 summer contribution prevailed. There are no cases in this period in which autumn is the major contributor (2012 cannot be taken into account because sensors did not work until July).

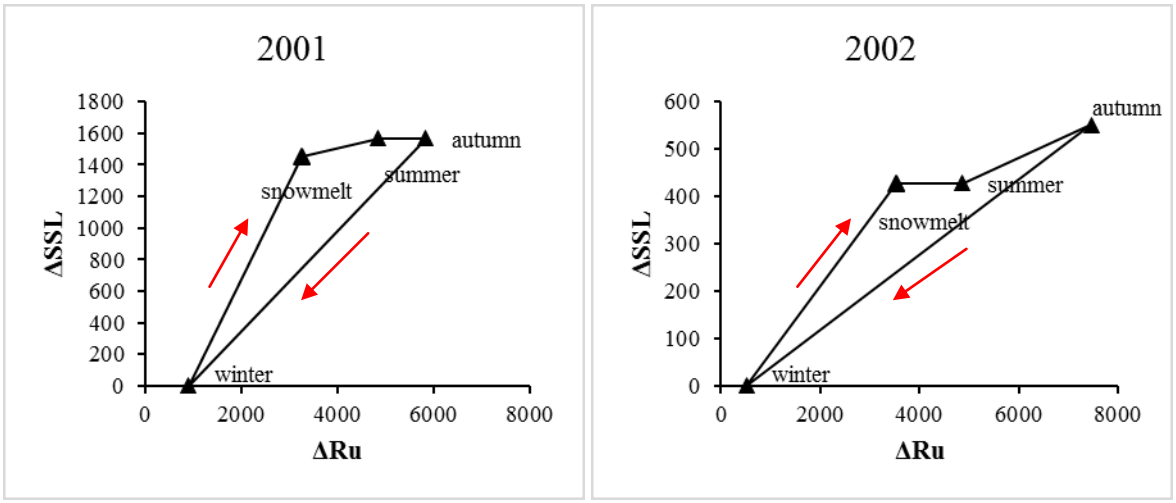

Figure 45: Seasonal runoff volumes (10^3 m^3) increasing versus seasonal suspended sediment load (t) increasing during the years 2001 and 2002, consecutively.

The 2001 is characterized by high rates of suspended sediment transport during the snowmelt. The high solar radiation during the last days of the snowmelt induced a mud flood in the medium part of the basin. This mud flood mobilized and transported almost 1020 t of fine material, and released an

important amount of fine sediments that moved during the following summer events (almost 120 t). The total annual suspended budget was 1568.4 t, and the shape of the curve plotting ΔRu values against ΔSSL values was an upward triangle (Fig. 45). There is a noticeable the steep slope in the first part of the year due to the average snowmelt runoff volumes in contrast with the extremely high snowmelt sediment load. More details about this event are discussed in the analysis of the single events.

The following year, 2002, is characterized by a great quantity of suspended sediments moving during the snowmelt (more than 400 t, noticeably over the mean values), a summer almost lacking transport and several small autumn events that moved more than 100 t in total. The annual suspended load is 551.2 t a value greater than the mean annual budget. This year features an upward triangle shape, even if there is also a considerable fraction of autumn load (Fig. 45).

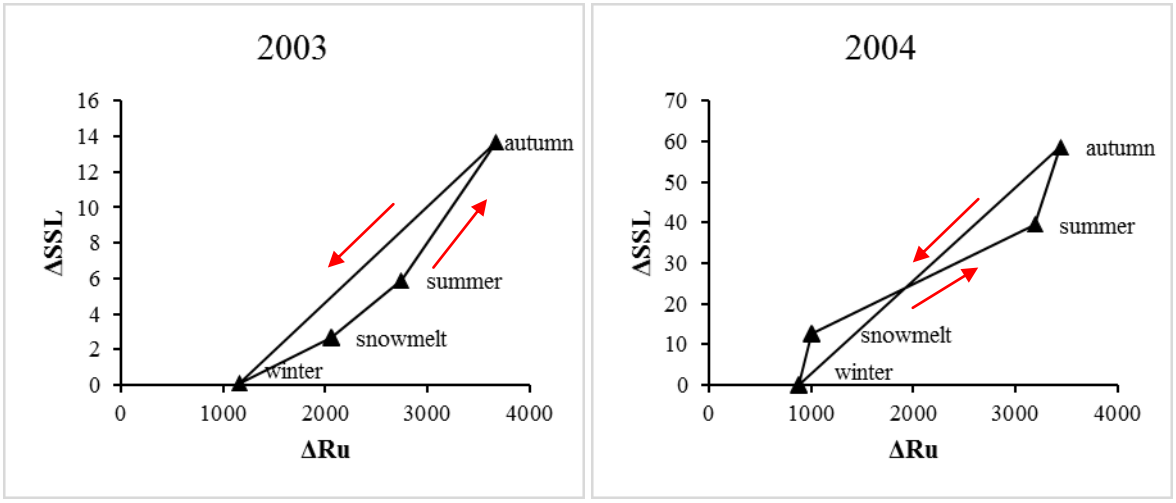

Figure 46: Seasonal runoff volumes (10^3 m^3) increasing versus seasonal suspended sediment load (t) increasing during the years 2003 and 2004, consecutively.

The 2003 is characterized by noticeable low sediment loads. In fact, in three decades it is the only year featuring less than 40 t of annual budget. The main reason is that the water discharge did not show any particular peak. In fact, the maximum water discharge value registered was 1.02 m^3 s^{-1}, taking place in May, and the suspended sediment transport associated to that peak was only 0.2 t. The annual runoff volume (3673 10^3 m^3) was considerably below the mean value. The total suspended sediment transport, of just 13.7 t, was distributed throughout the year. The curve described by ΔRu values against ΔSSL tends to the linear shape (Figure 46).

2004 is also characterized by low transport rates, probably due to the low runoff volumes registered during this year. Still, the annual budget was higher than 2003. Almost 59 t of fine material were transported during this year, of which 12.5 during the snowmelt, and the rest during summer and

autumn storms. The major contributor was the summer, but still, the load distribution through the year was quite balanced. This is why the curve described this year is an eight shape but it tends to a linear shape (Fig. 46).

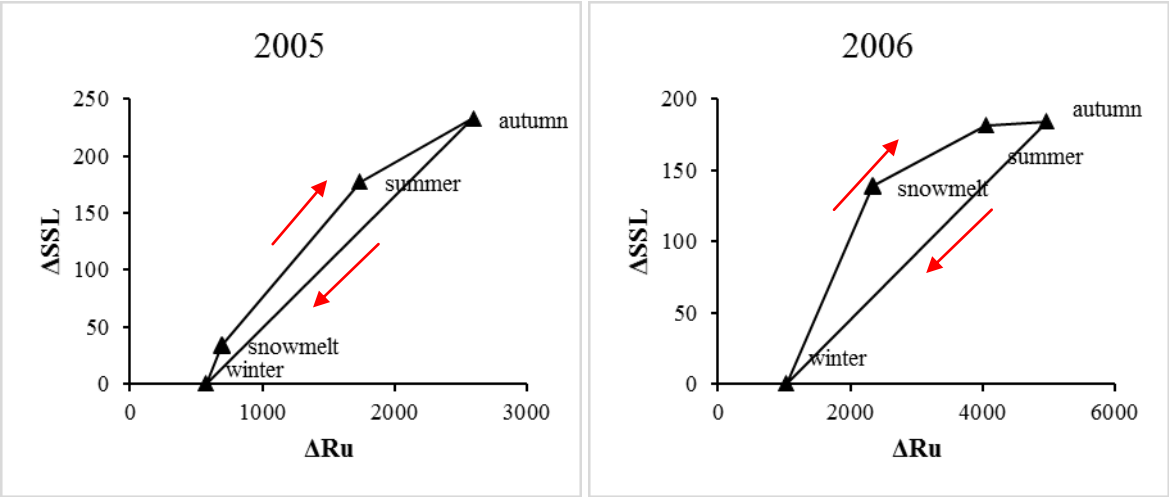

Figure 47: Seasonal runoff volumes (10^3 m^3) increasing versus seasonal suspended sediment load (t) increasing during the years 2005 and 2006, consecutively.

The 2005 is characterized by low transport during the snowmelt, due to low volumes of runoff. During the summer and the autumn, though, some rainfall events transported a considerable amount of suspended material. Even if also in this case the runoff volumes are lower than the average, the total suspended budget is greater than the previous two years. In total, 232.9 t were transported, a value below the average. The shape described by the ΔRu -ΔSSL values is .almost linear (Fig. 47).

The snowmelt of 2006 moved almost 140 t of suspended sediments, due to high volumes of runoff. A summer storm moved more than 40 t. In total, 184.3 t of suspended sediment transport were registered during this year in the monitoring station. The shape of this year tends to be an upward triangle, due to the fact that most of the suspended load moved during the snowmelt but still summer and autumn contributed considerably to the total load (Fig. 47).

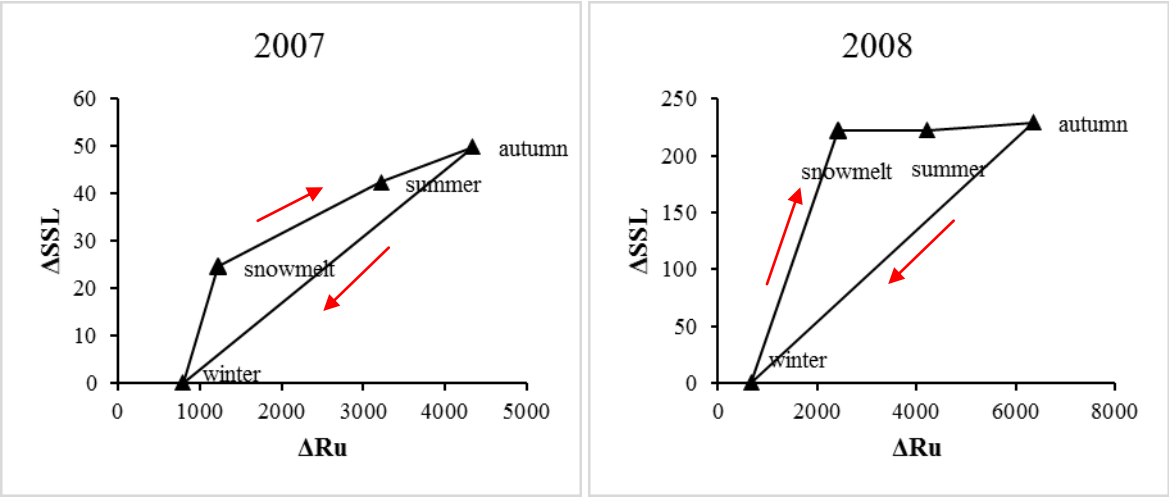

Figure 48: Seasonal runoff volumes (10^3 m^3) increasing versus seasonal suspended sediment load (t) increasing during the years 2007 and 2008, consecutively.

The year 2007 is another good example of low transport activity. The snowmelt registered average levels of runoff, but moved only 24.4 t of fine material. Some rainfall events were registered, but the suspended concentration values were too low for the water discharge values registered. The annual suspended sediment budget was 49.8 t. As the snowmelt contribution is close to the 50% of the total load, and because of that the year 2007 features an upward triangle shape, though it is close to a linear shape (Fig. 48). This year is similar to 2006.

2008 repeats the behavior observed in many previous years, such as 1988 or 1997, among others. The snowmelt of 2008 moved an important quantity of suspended sediment, whilst the summer lacked flood events and autumn registered two rainfall events of small entity and low values of sediment load. The total annual budget was 229.10 t, of which 96.9% correspond to the melting processes. It is hence easy to infer an upward triangle from the ΔRu-ΔSSL curve (Fig. 48).

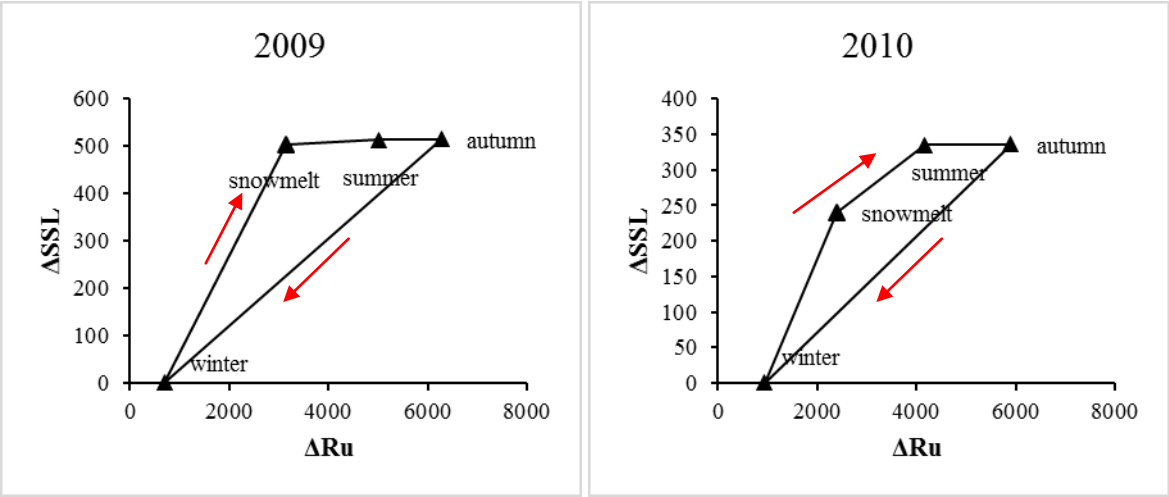

Figure 49: Seasonal runoff volumes (10^3 m^3) increasing versus seasonal suspended sediment load (t) increasing during the years 2009 and 2010, consecutively.

The year 2009 looks much as its precedent, with the typical upward triangle shape. High values of snowmelt runoff that induced into high rates of suspended transport during the spring left low sediment availability for the summer and autumn rainfalls. In fact, 514.9 t constituted the annual fine sediment budget, of which 503.6 correspond to the snowmelt period, and less than 12 t correspond to the following rainfall events. For this reason, this year has a marked upward triangle shape (Fig. 49).

The year 2010 registered 240.6 t of suspended sediment transported during the snowmelt and almost 95 t during summer brief storms. Some autumn rainfall events took place in the catchment this year, but they released low quantity of fine material. In total, 336.1 t were registered in the 2010, a value slightly above the 2001-2015 period average. Because of its high fraction of snowmelt contribution to the total budget, this year presents an upward triangle shape (Fig. 49). Still, this shape is not very marked because of the contribution from the summer storms.

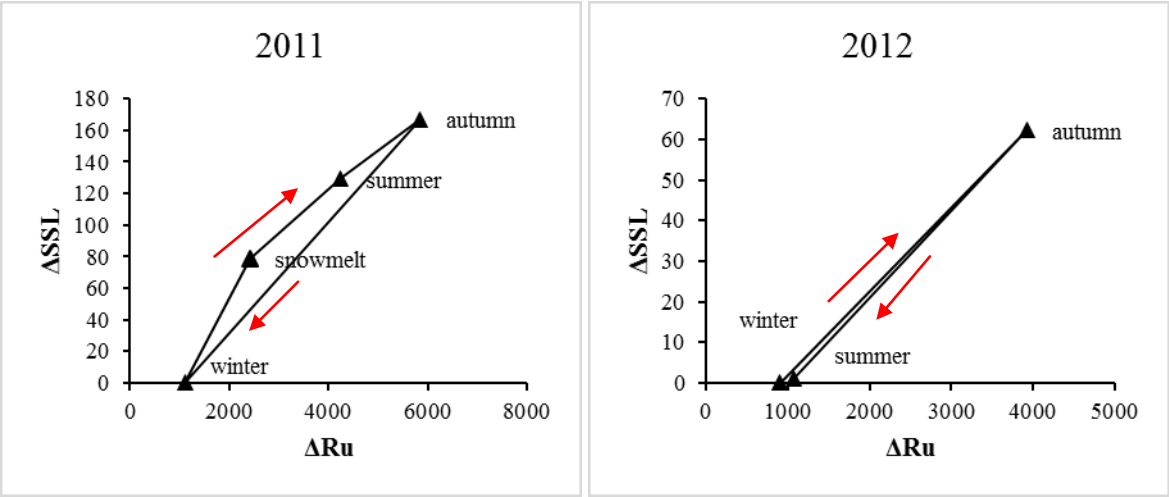

Figure 50: Seasonal runoff volumes (10^3 m^3) increasing versus seasonal suspended sediment load (t) increasing during the years 2011 and 2012, consecutively.

The year 2011 is a particular case because the seasons contributed almost homogeneously to the annual budget, and in correspondence with the seasonal runoff volumes. This situation is not very common in the Rio Cordon catchment, as noted when observing the previous years. Only the 2003 shows an annual hysteresis that looks a little like this one, with the three seasons contributing in almost equal proportional quantities. The annual budget was 167.1 t of fine material. The annual hysteresis tends to the upward triangle shape, though very close to the linear shape due to the almost homogeneous seasonal contribution (Fig. 50).

In 2012, some technical problems occurred in the monitoring station of the Rio Cordon and sensors of water levels and turbidity did not work during the first part of the year. Therefore, no data is available until the second week of July, and it is not possible to estimate the snowmelt and summer budget. An intense rainfall event in November was the responsible of the autumn suspended load. From July to December 2012, 62.35 t of suspended material were transported.

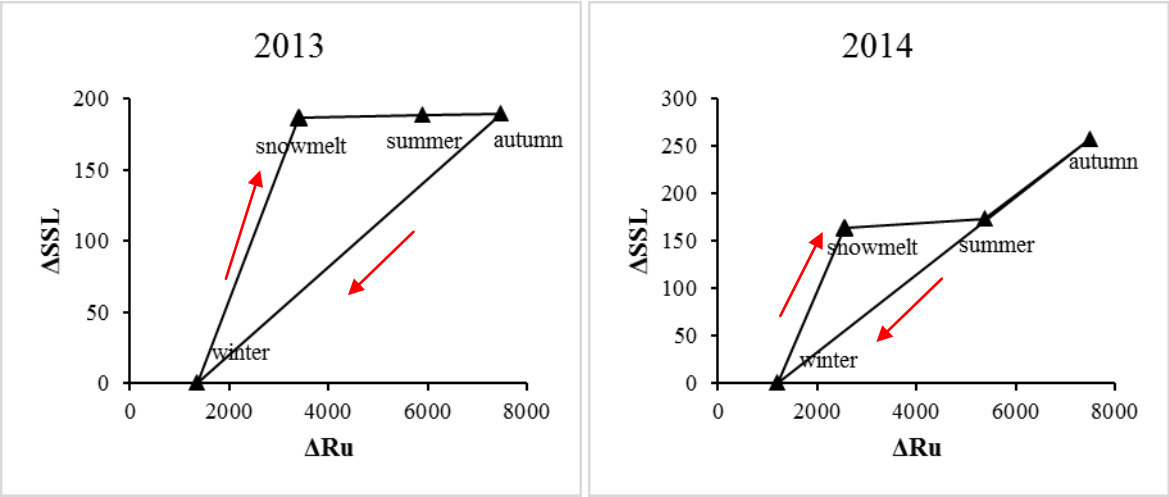

Figure 51: Seasonal runoff volumes (10^3 m^3) increasing versus seasonal suspended sediment load (t) increasing during the years 2013 and 2014, consecutively.

The year 2013 follows the upward triangle pattern (Figure 51) widely diffused in the catchment, already observed in several previous years, with almost the totality of the annual sediment budget transported during the snowmelt. The runoff snowmelt had enough energy to mobilize 186 t of suspended sediments, and then the transport of the summer and autumn storms was almost inexistent, apart from a small rainfall event in July that transported 2 t of suspended material. In the complex, 2013 registered 189.4 t of suspended budget, a value significantly below the average despite of its high volumes of annual runoff (7477.4 10^3 m^3).

The 2014 presents a different situation. During the snowmelt, 164.2 t of fine sediments were mobilized, but this was not the only contributor of the year, because the summer storms moved some material and during November a rainfall event moved 84 t. The annual budget of suspended sediment was 258.4 t. In this particular case, the annual hysteresis shows a particular shape, as can be appreciated in Fig 51. Snowmelt, though, registered the highest seasonal suspended load and lower runoff volumes than the summer and autumn ones.

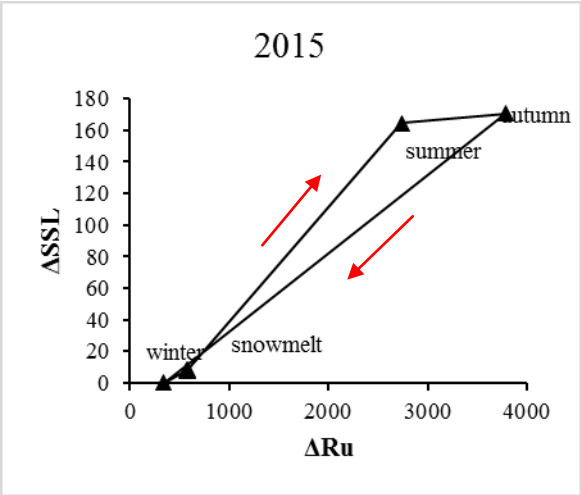

Figure 52: Seasonal runoff volumes (10^3 m^3) increasing versus seasonal suspended sediment load (t) increasing during the year 2015.

Very low runoff volumes characterized the year 2015 during snowmelt. Hence, this process almost lacked suspended sediment load. The main sediment contribution took place during summer (156 t were mobilized due to summer storm), and very low loads were registered during the autumn. The total annual load is 170.5 t, and, because the higher seasonal suspended load arrived during the summer, the year presents an eight-shaped curve, though it is not very marked (Figure 52).

The upward triangle shape is the most common one during the 2001-2015 period (10 of 15 cases). Therefore, it is characterized by higher snowmelt sediment loads compared to the loads from the rainy seasons. Variations of the mean daily values through the whole 2001-2015 period help understanding the seasonal dynamics (Figure 53). It is noticeable that no substantial change among years is registered in the distribution of the annual precipitations, or in their quantity. A similar deduction can be made with the mean daily water discharge. Instead, the mean suspended sediment concentration values show a parked diminishing trend in accordance with the passing of time. Results suggest that this falling trend through the years is not linked to lower values of water discharge or rainfall volumes.

Figure 53: Daily precipitations and mean daily values of water discharge and suspended sediment from the monitoring station between 2001 and 2015.

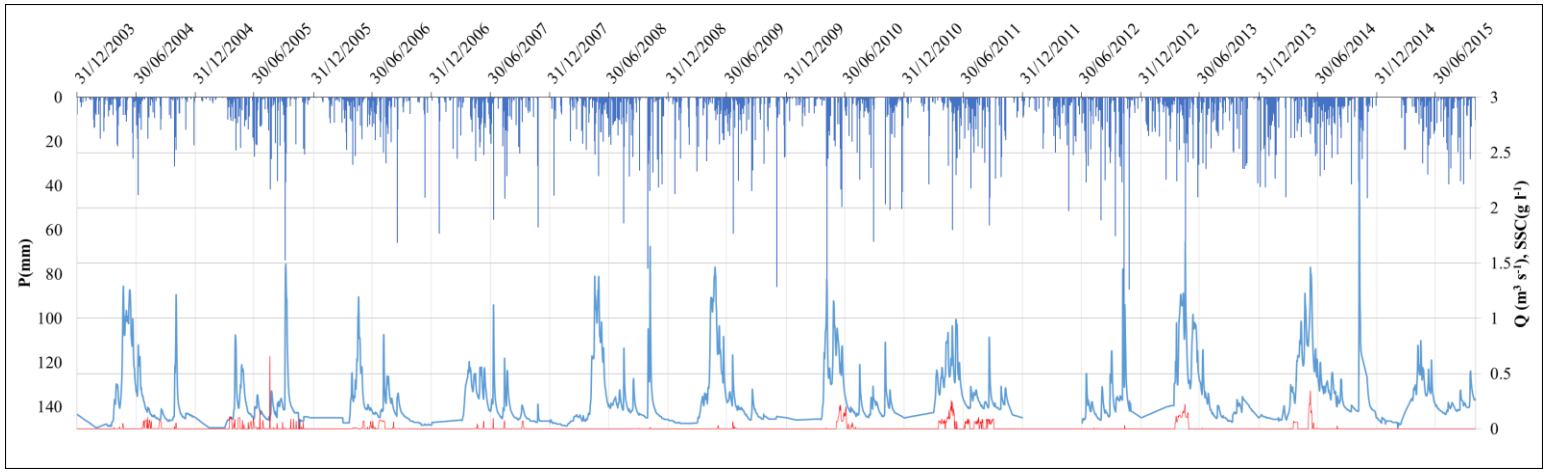

Regarding the whole study period, it is noticeable that in Rio Cordon years showing homogeneous seasonal sediment contribution are rare (only 3 cases of 30 showed linear shape). Instead, years with a marked prevalence of one season over the others are quite common. Concretely, years showing upward triangle shape are the most common (15 years, 50% of the cases), highlighting that in the Rio Cordon it is more likely to have years with major sediment contribution from the snowmelt rather than years with major sediment contribution coming from autumn or summer. These years are 1988, 1990, 1992, 1993, 1997, 2001, 2002, 2006, 2007, 2008, 2009, 2010, 2011, 2013 and 2014. It is important to bear in mind that 10 of the 15 years showing this behavior belong to the 2001-2015 period. The other twelve years of the study period show downward triangle or eight shaped curves. The years showing a downward triangle shape are 1994, 1996, 1998, 1999 and 2000. In these years, autumn is the major contributor. The years showing a marked higher summer contribution, characterized by an eight-shaped curve, are 1986, 1987, 1989, 1991, 1995, 2004 and 2015.

3.2. Suspended sediment transport recorded single events, 1986-2015.

3.2.1. Single events characteristics

Once identified the water discharge peaks registered during the study period, 34 flood events were isolated in the Rio Cordon catchment (period 1986-2014). Events from 2015 could not be analyzed because turbidity meters did not work during this year due to maintenance problems. Only the events showing a response in suspended sediment concentration are analyzed in this work. Some of the registered events could not be used for this work because of unreliable turbidity data or data gaps within the event. Table 5 reports the variables studied for every event, divided in flow event conditions and previous conditions.

The events were isolated identifying their initial moment as the time with a significant increase of water discharge or suspended concentration, while the end of the event was identified by the time in which both variables show constant values in their respective recession limbs. In the case of rainfall events, using rain diagrams permitted to better isolate and understand single or multiple rainfall events. In the case of continuous rainfall causing a multi peak flood event, it was divided into individual events only when it was possible to clearly identify the rising limb and the exhaustion limb for both for water discharge and suspended sediment concentration. Otherwise the event was considered multiple. In this case, Δt was calculated considering the absolute Q and SSC maximum values. Further and more detailed information about this classification can be found in the work from García-Rama et al. (2016).

The hysteresis relationship between water discharge (Q) and suspended sediment concentration (SSC) at the event scale was described by analyzing the SSC/Q ratios of the rising and descending limbs of hydrograph and sedigraph and events were subsequently classified in circular (clockwise or counter-clockwise) or eight-shaped loops. In this work, the eight-shaped loops were classified as prevalently clockwise or counter-clockwise according to the arrival order of the absolute flow peak and concentration peak. Together with the maximum values of P, SSC and Q, the barycenters of the pluviograph, sedigraph and hydrograph were calculated in aims to add information about the way P, SSC and Q change within the event. In fact, barycenters are rarely contemporaneous to the peak of their respective curve. Varignon's theorem of moments has been used for their calculation, assuming the initial moment of the event as the origin. Rainfall, water discharge and sediment concentration diagrams have been subdivided in accordance to the monitoring time interval (1 hour or 5 mins). Subsequently, the elementary volumes have been calculated. More information about this technique can be found in previous works (García-Rama et al., 2016; Pagano et al., 2016; Pagano et al. under review). The main characteristics of the events described below are reported in Table 6.

Only the temporal evolution and the hysteresis of the events occurred from 2004 to date are exposed in this work. Although the characteristics of those flood events, as well as the previous conditions registered, were used for the analysis, this work reports the shape of the graphs and the hysteresis loops that were performed by this author. The main characteristics of the events occurred between 1986 and 2003 can be consulted in previous works (Lenzi et al., 2003; Mao, 2004).

Table 5: Variables used for the single events analysis and their units.

Flow event conditions	
Q_p (m^3 s^{-1})	Water discharge peak
Q_m (m^3 s^{-1})	Mean water discharge
Q_i (m^3 s^{-1})	Initial discharge value
Q_{SSC} (m^3 s^{-1})	Water discharge value when SSC_p takes place
Q_{a1d} (m^3 s^{-1})	Average water discharge during the day previous to the event
R (m^3 10^3)	Total runoff
SSC_p (g l^{-1})	Suspended sediment concentration peak
SSC_m (g l^{-1})	Mean suspended sediment concentration
SSC_Q (g l^{-1})	Suspended concentration value when Q_p takes place
TSS (ton)	Total sediment yield
P_{tot} (mm)	Total rainfall causing the event
I_{max} (mm h^{-1})	Maximum hourly rainfall intensity in one hour range
I_{av} (mm h^{-1})	Average hourly rainfall intensity
t event (hours)	Duration of the event

$tQ_p(0)$ (hours)	Time lapse between Q_p and the event initial moment
$tSSC_p(0)$ (hours)	Time lapse between SSC_p and the event initial moment
Δt (hours)	Time lapse between Q_p and SSC_p
t rainfall (hours)	Duration of the rainfall that causes the event
tBQ(0) (hours)	Time lapse between hydrograph barycenter and the event initial
tBSSC(0) (hours)	Time lapse between sedigraph barycenter and the event initial
$\Delta t(tQ-tP_{max})$ (hours)	Time lapse between discharge peak and rainfall peak
Δt(tBSSC-tBQ) (hours)	Time lapse between sedigraph barycenter and hydrograph barycenter
Previous conditions	
Q_{a1d} ($m^3 s^{-1}$)	Mean water discharge during the 24 hours previous to the event
P_3 (mm)	Total rainfall during the 3 hours previous to the event
P_6 (mm)	Total rainfall during the 6 hours previous to the event
P_{12} (mm)	Total rainfall during the 12 hours previous to the event
P_{24} (mm)	Total rainfall during the 24 hours previous to the event
P_{48} (mm)	Total rainfall during the 48 hours previous to the event

Table 6: Principal characteristics of the 1986-2015 analyzed events.

event ID	Date	Qp	Qm	Qi	R	SSCp	SSCm	TSS	P_{TOT}	Imax	Iav	Δt	Δt(BSSC-BQ)	P_3	P_6	P_{12}	P_{24}	P_{48}	Hysteresis direction	Hysteresis shape
1	17/06/1991	4.00	2.49	1.40	138.98	3.74	0.62	35.63	72.4	16.8	7.2	-1.00	-9.60	1.8	4.6	5.0	6.8	8.4	Clockwise	Circular
2	05/10/1992	2.91	1.71	0.55	283.68	1.18	0.17	6.17	122.1	14.0	2.2	-1.00	-12.09	1.8	5.6	86.0	78.0	90.2	Clockwise	Circular
3	02/10/1993	4.28	1.92	0.34	379.86	0.47	0.23	52.13	97.2	12.0	2.9	-4.25	-10.36	0.2	0.2	2.8	10.0	18.8	Clockwise	Circular
4	18/07/1994	1.86	0.44	0.23	10.63	7.84	2.61	32.35	15.0	8.6	0.8	0.00	0.99	0.2	0.2	1.4	2.4	22.7	Counter-Clockwise	Circular
5	14/09/1994	10.42	2.60	0.94	97.50	57.89	6.49	1059.90	56.0	32.6	16.0	0.08	-1.63	14.4	16.8	16.8	59.4	61.0	Counter-Clockwise	Eight-shaped
6	31/05/1995	1.66	1.46	0.67	94.60	1.33	0.39	15.40	34.8	6.8	3.9	0.50	5.53	0.0	0.0	1.0	23.3	24.3	Counter-Clockwise	Eight-shaped
7	13/08/1995	2.72	0.97	0.23	11.65	6.57	1.51	42.59	34.8	28.6	3.5	-0.33	0.12	0.2	0.2	0.2	0.2	0.4	Clockwise	Eight-shaped
8	16/10/1996	2.96	1.79	0.72	308.38	15.44	0.49	170.27	121.0	11.8	2.5	0.00	-14.07	15.2	31.4	34.4	36.0	36.8	Clockwise	Eight-shaped
9	05/09/1998	1.30	0.72	0.16	45.09	0.50	0.15	1.60	62.6	10.0	2.7	-0.17	-4.18	0.0	0.0	3.0	3.2	6.2	Clockwise	Circular
10	05/10/1998	4.73	1.47	0.60	538.67	4.94	0.51	207.75	13.6	1.7	0.4	-4.17	-19.83	7.4	14.8	16.8	32.8	50.0	Clockwise	Eight-shaped
11(*)	11/05/2001	1.47	1.27	1.19	137.03	13.82	1.27	233.92	0.0	0.0	0.0	-1.23	1.52	-	-	-	-	-	Clockwise	Eight-shaped
12	04/05/2002	2.30	1.30	0.72	317.10	9.90	0.34	131.40	126.2	7.7	1.8	-11.17	-7.69	1.0	4.0	9.4	9.4	9.4	Clockwise	Eight-shaped
13	15/11/2002	2.34	2.31	0.72	523.79	9.29	8.46	184.90	198.5	9.1	2.0	0.08	-30.41	13.2	21.8	53.7	71.6	76.1	Counter-Clockwise	Eight-shaped
14	01/11/2004	2.05	1.40	1.02	30.66	1.22	0.15	5.82	15.8	7.9	2.6	-0.08	0.28	4.5	5.0	5.0	25.1	28.1	Clockwise	Circular
15(*)	01/05/2005	0.72	0.67	0.34	13.88	0.99	0.13	1.15	0.0	0.0	0.0	-0.75	-1.94	-	-	-	-	-	Clockwise	Circular
16	03/10/2005	1.09	0.90	0.51	9.56	0.23	0.13	1.41	54.3	10.0	3.1	-0.17	-4.90	12.3	13.0	32.5	43.8	67.1	Clockwise	Circular
17	04/10/2005	1.45	1.24	0.80	52.82	0.13	0.02	1.10	71.5	8.0	2.4	-5.08	-0.64	2.2	2.2	39.1	76.5	106.2	Clockwise	Circular
18	03/08/2006	0.83	0.79	0.34	10.99	2.19	0.90	9.24	40.6	9.1	1.8	-17.00	0.14	1.4	7.4	12.2	14.4	20.6	Clockwise	Circular
19	09/07/2007	1.19	0.90	0.72	6.26	0.50	0.11	1.77	5.0	2.0	1.0	0.08	-0.78	12.4	15.6	26.0	47.8	47.8	Counter-Clockwise	Eight-shaped
20	10/07/2007	1.20	1.07	0.89	45.80	0.09	0.01	0.88	16.2	5.8	1.1	-12.25	-0.81	1.2	13.0	19.6	48.0	51.8	Clockwise	Eight-shaped
21	13/08/2007	1.17	0.81	0.74	27.41	0.38	0.09	1.37	32.9	21.2	6.6	0.00	-0.34	5.5	5.5	5.8	5.9	5.9	Clockwise	Circular
22	13/08/2007	1.20	0.64	0.48	1.76	0.58	0.12	1.00	7.5	4.8	1.5	0.50	-1.01	0.0	0.0	11.7	38.7	38.8	Counter-Clockwise	Circular
23	30/10/2008	1.17	0.96	0.71	16.42	0.01	0.00	0.04	86.0	10.3	2.6	0.08	-0.52	6.2	14.4	43.4	77.5	97.5	Counter-Clockwise	Eight-shaped
24	04/11/2008	2.16	1.68	0.72	55.72	0.20	0.03	3.45	62.4	8.1	3.6	-3.33	0.00	10.7	12.5	12.6	16.8	23.4	Clockwise	Eight-shaped
25	19/06/2009	1.16	0.94	0.72	1.42	0.05	0.01	0.08	13.0	13.0	6.5	0.42	0.12	5.2	5.2	5.2	5.2	5.3	Counter-Clockwise	Circular
26	18/07/2009	1.08	0.87	0.70	2.02	0.13	0.05	0.25	46.4	13.1	5.8	0.08	-0.12	12.3	30.7	32.0	32.1	32.2	Counter-Clockwise	Circular
27	14/08/2010	0.93	0.72	0.54	7.41	0.13	0.02	0.36	36.9	9.0	5.2	-0.83	-1.91	15.7	15.9	15.9	16.0	38.0	Clockwise	Circular
28(*)	15/05/2011	0.93	0.84	0.76	111.52	0.18	0.11	19.49	0.0	0.0	0.0	-2.67	-0.09	-	-	-	-	-	Clockwise	Eight-shaped
29	04/11/2012	1.85	1.16	0.72	93.42	0.09	0.01	0.93	55.0	9.2	3.2	-7.17	-20.98	17.2	20.4	22.0	24.4	24.8	Clockwise	Circular
30	11/11/2012	2.09	1.02	0.72	197.06	9.90	1.24	60.52	135.6	15.6	2.9	-0.17	-27.70	24.6	39.2	52.6	55.2	56.0	Clockwise	Eight-shaped
31(*)	16/05/2013	1.97	1.22	0.89	223.36	1.53	0.13	69.80	0.0	0.0	0.0	-18.83	-6.97	-	-	-	-	-	Clockwise	Circular
32	09/07/2013	2.32	1.12	0.96	5.25	0.59	0.16	2.07	17.6	17.4	5.9	-0.08	-0.87	11.8	11.8	11.8	17.6	18.2	Clockwise	Eight-shaped
33	09/06/2014	2.06	1.55	1.14	79.97	3.41	0.33	45.75	16.6	12.0	1.8	0.17	-2.11	0.0	0.0	0.0	0.0	0.0	Counter-Clockwise	Circular
34	13/06/2014	1.76	1.50	1.26	5.73	0.32	0.16	1.72	9.0	9.0	4.5	0.08	-0.02	0.00	0.00	0.00	7.80	10.20	Counter-Clockwise	Eight-shaped

01/11/2004 rainfall event

The increasing of the water discharge was induced by 15.8 millimeters of rainfall, with a maximum intensity of 7.9 mm h^{-1} that fell after two days of low but continuous precipitations. It was a short event that took 7 hours in which the maximum water discharge, equal to 2.05 m^3 s^{-1}, arrived 5 min after the suspended sediment concentration peak (equal to 1.22 g l^{-1}). The loop described by the Q and the SSC values was circular, as no multiple peak was registered, and with clockwise hysteresis, because of the anticipated arrival of the SSCp respect to the Qp. In total, 5.82 t of suspended sediment material were moved. Some bedload transport characterized this event: the sensors registered 7.9 t of coarse material. Figure 54 shows that SSCp preceded the arrival of Qp (Δt=5 min). Nonetheless, the center of mass of the hydrograph preceded the sedigraph's center of mass (Fig. 54).

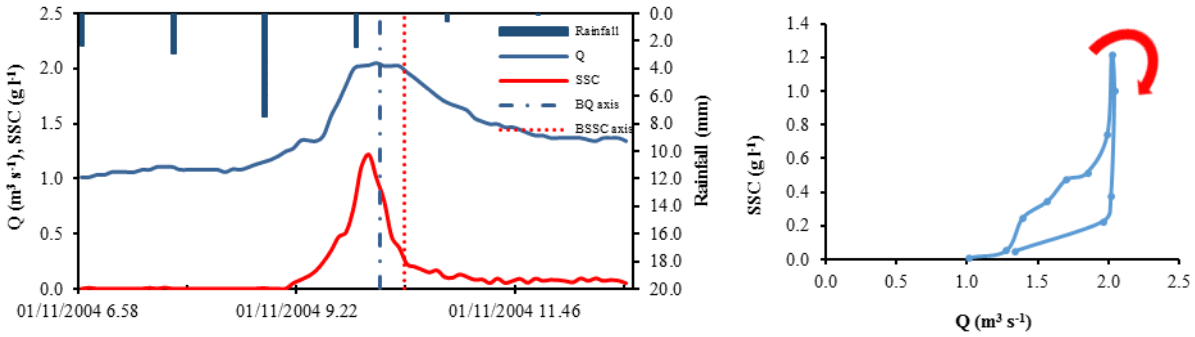

Figure 54: Left: Hydrograph, sedigraph and pluviograph of the 04/11/2004 event, and graphic representation of their barycenters; Right: Hysteresis cycle of the event.

The daily values of 2004 shown in Figure 50 lead us to think that this flood event happened after some weeks registering low water levels and no sediment transport. Hence, several t of solid material could be expected, maybe even more than the amount registered. The center of mass of the hydrograph anticipated the sedigraph center of mass, indicating that the runoff volumes moved mainly before the solids. That is to say, the liquid mass had on the whole a quicker response than the solid mass, even if not so distant. This, together with the parallel shapes of hydrograph and sedigraph, suggests that the sediment sources were spread all over the catchment. The brief time lag between peaks (5 mins) corroborates this hypotesis.

01/05/2005 snowmelt event

The snowmelt from 2005 was characterized by temperatures that increased gradually. Hence, no steep increase of water discharge was registered. The event here reported is the main peak of the water level

values, during which the turbidity meters registered a speedy increase and decrease in the suspended sediment concentration values. The Qp is not high (0.72 m^3 s^{-1}) , and arrives 45 min after the suspended sediment concentration peak (0.99 g l^{-1}), describing a clockwise, circular loop (Fig. 55). In total, 1.15 t of suspended sediment material were moved. No bedload transport characterized this event. The barycenter of the sedigraph precedes the barycenter of the hydrograph. This, together with the hysteresis loop, suggest that the sediment source was local and close to the main channel.

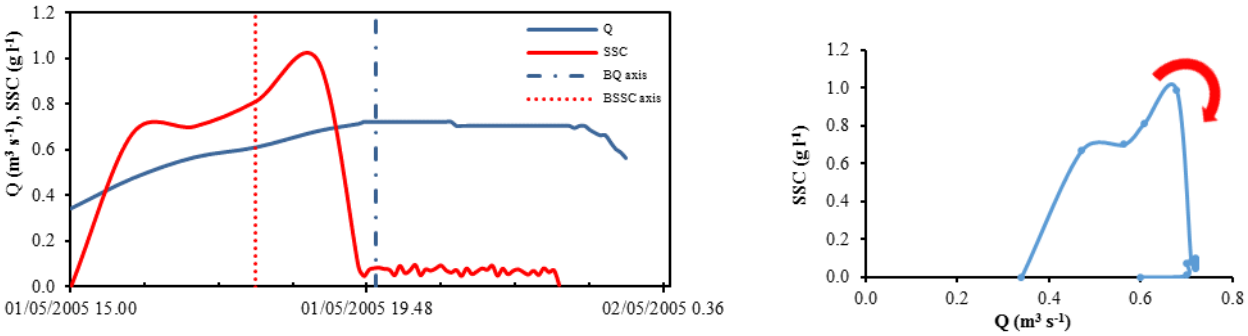

Figure 55: Left: Hydrograph, sedigraph and pluviograph of the 01/05/2005 event, and graphic representation of their barycenters; Right: hysteresis cycle of the event.

Snowmelt events usually show higher intensities in this catchment. The low values of water discharge and the gentle slope of the rising limb of the hydrograph are the main reasons for the low transport rates during this snowmelt event. The barycenter of the sedigraph precedes the barycenter of the hydrograph. This, together with the hysteresis loop, suggest that the sediment source was local and close to the main channel.

03/10/2005 rainfall event

During this event, 58.6 mm fell within 18 hours, with a maximum intensity of 10 mm h^{-1}.. This induced into a quick rising of the hydrograph, followed by an increasing in the concentration of suspended solids. The solid transport took few hours, and the total budget was 1.41 t, composed only by fine material. The peak of the water discharge (0.233 g l^{-1}) arrived 1 h before Qp (equal to 1.089 m^3 s^{-1}). Also the barycenter of the sedigraph preceded that of the hydrograph. The loop described by Q and SSC values is circular, clock-wised (Figure 56). Also this event lacked bedload transport.

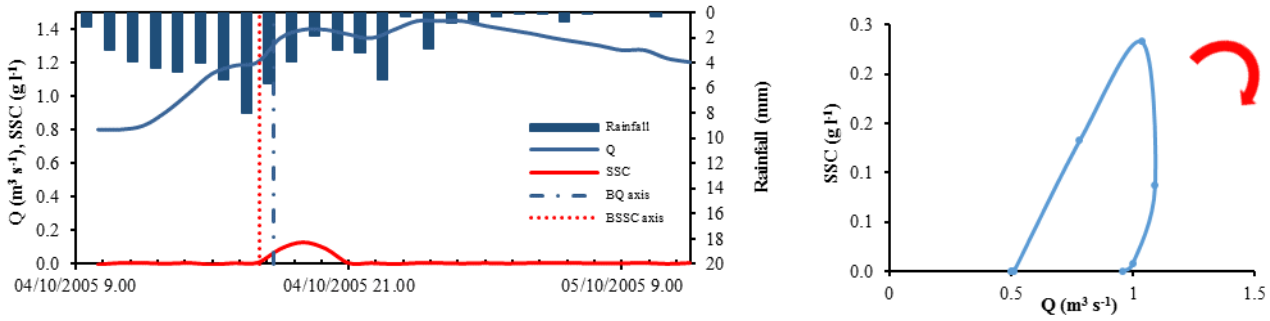

Figure 56: Left: Hydrograph, sedigraph and pluviograph of the 04/10/2005 event, and graphic representation of their barycenters; Right: Hysteresis cycle of the event.

It is noticeable that the suspended sediment concentration started increasing while the maximum rainfall intensity was taking place, suggesting that the solid transport during this event is a direct outcome of the precipitations. The hysteresis described by Q and SSC values, together with the time lag between barycenters, lead us to believe that the sediment source activated during this event was located somewhere close to the monitoring station. This would explain why, even if Q continues on rising and shows high values for an extended period, the sediment transport occurs within few hours. The low amount of total suspended load supports this hypothesis.

03/08/2006 rainfall event

This rainfall event was the only one properly registered during the 2006 year. The event occurred during the 3rd and the 4th of Agust 2006 was a storm of discrete dimensions. The maximum rainfall intensity was 9.1 mm h-1, and precipitations lasted for almost a whole day. Even so, water discharge showed a slow rising, with a Qp= 0.83 m^3 s^{-1}, while suspended sediment concentration showed an abrupt rising during the first hour of precipitations. After this peak, SSC values decreased brusquely, but still remained quite high. Due to this first SSC peak (equal to 2.19 g l^{-1}), that arrived several hours before the Qp, the hysteresis that characterizes this event is a counter-clockwise loop. This loop is eight-shaped, due to the presence of two small peaks of water discharge (Figure 57). The barycenter of the sedigraph preceded some minutes the barycenter of the hydrograph. The falling limb of the hydrograph diminished gently, probably due to underground contributions. The total sediment budget of this event, composed entirely by suspended material, was 9.24 t.

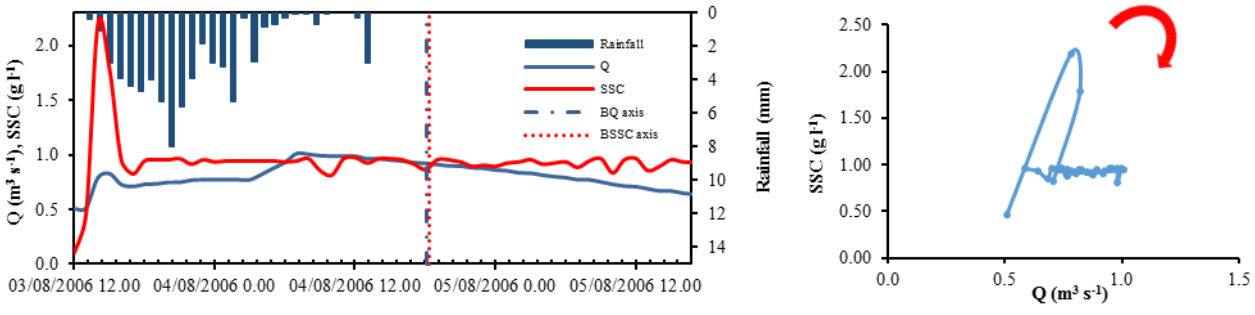

Figure 57: Left: Hydrograph, sedigraph and pluviograph of the 03/08/2006 event, and graphic representation of their barycenters; Right: Hysteresis cycle of the event.

This event arrived after a quite dry summer, as can be noticed from the low initial water discharge value. Rainfall volumes probably infiltrated into the underground, and a low quantity of it actually reached the channel network. For this reason, water discharge shows lower values than expected if considering the total amount of precipitation. The peak showed by SSC during the first hour of the event is presumably from resuspension processes. The fact that SSC values diminish immediately validates this idea. Still, SSC values remained quite high after this peak, suggesting that some material arrived from the hillslopes and hence channel bed was not the only sediment source of the event. The fuzzy shape of the hysteresis loop has its origin in the first SSC peak of the event. Barycenters do not give any additional information during this event.

09/07/2007 first rainfall event

In aims of simplifying the analyses, event occurred between 9th and 10th July 2007 was split in two small events, regarding the criteria explained above. The first of them registered a small Q peak due to 8.2 mm that fell in less than one hour. This hydrograph peak was accompanied by a noticeable rising of the suspended sediment concentration. Rainfall was not enough to maintain high levels of water discharge, and hence the hydrograph diminished suddenly almost to its initial value (Fig. 58). Qp and SSCp registered values of 1.19 m^3 s^{-1} and 0.9 g l^{-1}, respectively, and Qp was preceded by SSCp. Also the barycenter of the sedigraph preceded that of the hydrograph. Because of the low values of water discharge and the gentle rising of the Q values, no bedload transport characterized this event. The total suspended load during this event was 1.77 t.

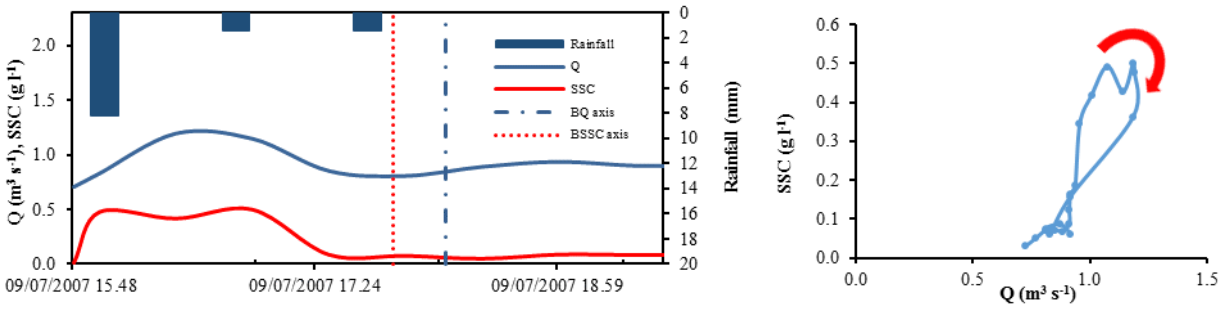

Figure 58: Left: Hydrograph, sedigraph and pluviograph of the 09/07/2007 event, and graphic representation of their barycenters; Right: hysteresis cycle of the event.

This event shows a quick response to rainfall from both hydrograph and sedigraph. The quick rising of the suspended sediment concentration values, together with the clockwise direction of the hysteresis cycle, lead us to think about the hypothesis of a close location of the sediment source.

09/07/2007 second rainfall event

The second part of this small event registered a water discharge peak of 1.19 m^3 s^{-1}. Q values raised from the values that preceded the 9 July event, which origin can be considered the old water, and took several days to reach the original water level. Suspended sediment concentration values remained lower than the previous event, and there was not a proper SSC peak (Fig. 59). Still, the maximum value was equal to 0.09 g l^{-1} and arrived contemporaneously to the Qp. Sedigraph barycenter arrived before the hydrograph barycenter. As its precedent, this event registered any bedload transport, and the total suspended budget was 0.88 t.

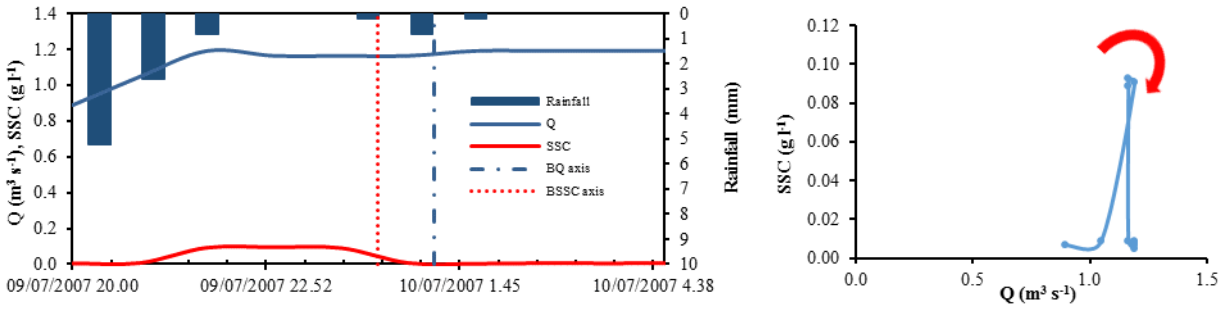

Figure 59: Left: Hydrograph, sedigraph and pluviograph of the 10/07/2007 event, and graphic representation of their barycenters; Right: Hysteresis cycle of the event.

This event started at a high Q value, because it is a continuation of the previous rainfall event. Both hydrograph and sedigraph is more extended than the previous case. Still, the sediment transport if this event is quite low, with very low values of concentration and a small amount of total sediment load. The hypothesis is that all sediment load arrived from the depletion of the sediment source area of the previous event and there was no new active sediment source.

13/08/2007 first rainfall event

During 13th of august of 2007, some rainfall generated a flood event that showed two different water discharge peak. Because every peak could be associated with a different peak in the pluviograph, the author considered it as two different events rather than a multi-peak event. The first of them was a typical summer storm, with a high rainfall intensity that generated a speedy increasing of the water discharge. It took just 5 hours long and, in total, 32.9 mm of water contributed to this event, with a maximum hourly intensity of 21.2 mm h^{-1}. Water discharge maximum value was 1.19 m^3 s^{-1}.The SSC and Q values described a clockwise loop (Figure 60), even if SSCp arrived almost simultaneously to Qp, showing a value of SSCp=0.38 g l^{-1}. No bedload characterized this event. The total suspended load was 1.37 t.

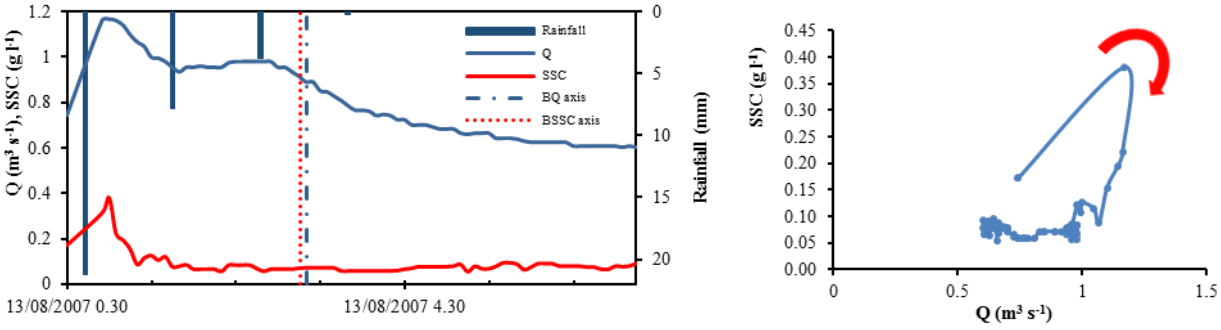

Figure 60: Left: Hydrograph, sedigraph and pluviograph of the first 13/08/2007 event, and graphic representation of their barycenters; Right: Hysteresis cycle of the event.

It is interesting to notice that despite the clockwise sense of the event, the barycenter of the SSC curve anticipated the Q barycenter in this event. Even though, the time lapse between peaks is reduced, and so is the time lapse between centers of mass. Both liquid volumes and solid mass showed a quick response to the high intensity rainfall. In fact, curves show a similar behavior during the first hour.

Probably, the high intensity of the rainfall induced to a contribution of sediments from different points of the catchment area.

13/08/2007 second rainfall event

The second event of this day showed a similar intensity than its precedent. In fact, Qp was 1.20 m^3 s^{-1}, generated by a maximum rainfall intensity of 4.8 mm h^{-1}. SSC reached higher values than the previous event. It is noticeable that the suspended sediment concentration showed high values (SSCp=0.58 g l^{-1}). This peak was probably due to resuspension processes affecting material that arrived to the main stream during the previous event. A circular, counter-clockwise loop is obtained when plotting Q values against SSC values (Fig. 61). Also in this case, the barycenter of the sedigraph showed an anticipation respect to the hydrograph barycenter. No bedload transport was registered during this event. The suspended sediment load was 1 ton.

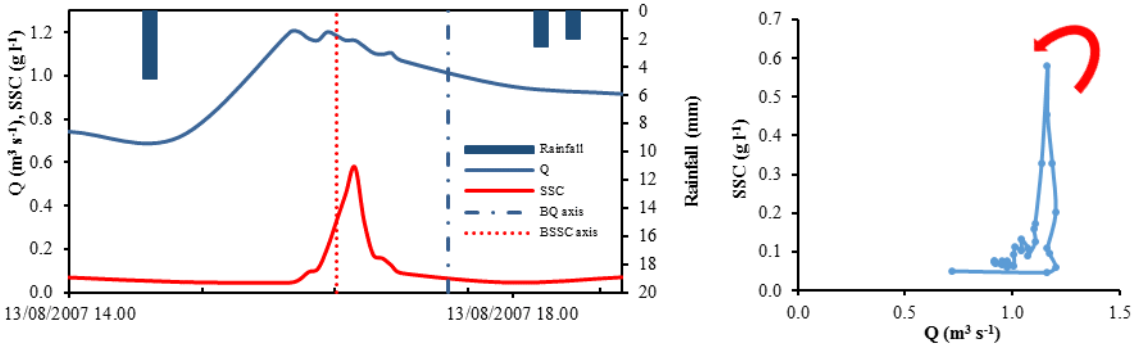

Figure 61: Left: Hydrograph, sedigraph and pluviograph of the second 13/08/2007 event, and graphic representation of their barycenters; Right: Hysteresis cycle of the event.

This short event is a consequence of its precedent. In fact, only because the moisture content of the soil was high due to the previous rainfall, it was possible for the 4.8 mm of rainfall registered during the first hour to induce such a steep rising of the hydrograph. The brief time of the development of the event should be taken into account in the analysis of the hysteresis pattern. Even if this event has a counter-clockwise loop, the quick arrival of the SSC peak and the sedigraph barycenter suggest that sediment sources might not be far away from the main channel.

30/10/2008 rainfall event

This event was characterized by considerably low values of suspended sediment concentration. In fact, it is difficult to figure out the shape of the sedigraph from the graphic because all the SSC values were too close to the X axis. Anyway, this flood started due to a rainfall event that registered a maximum intensity of 10.3 mm h^{-1}. Qp was 1.17 m^3 s^{-1}, whilst SSCp was 0.002 g l^{-1}. The loop described by these two variables was counter-clockwised. The total suspended load was 0.04 t, and no bedload transport was registered. The center of mass of the sedigraph anticipated the barycenter of the hydrograph (Fig. 62).

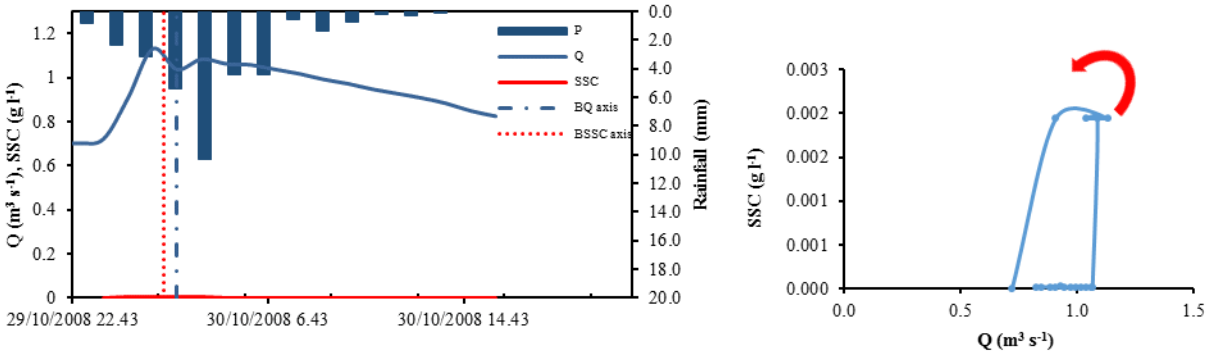

Figure 62: Left: Hydrograph, sedigraph and pluviograph of the 30/10/2008 event, and graphic representation of their barycenters; Right: Hysteresis cycle of the event.

This flood event showed an atypical response to rainfall. The continuous low values of suspended sediment concentration indicate that no sediment source activated through the duration of the event. Moreover, no second peak of water discharge accompanied the maximum rainfall intensity. This suggests that the soil was quite dry and the rate of infiltration was high, leading into a poor immediate runoff contribution to the main channel. In fact, no rainfall had been registered in the previous 20 days in the catchment. This situation is not common in this area, where autumn is usually the more humid season.

04/11/2008 rainfall event

This event registered 62.4 mm of rainfall, with a maximum intensity of 8.1 mm h^{-1}. The maximum suspended sediment concentration was 0.2 g l^{-1}, lower than expected if considering that water discharge showed a mean value of 1.68 m^3 s^{-1} and a peak of 2.16 m^3 s^{-1}. The SSC-Q relationship during the event described a eight-shaped, clock wised loop, as shown by Fig. 63. The total suspended sediment load

was 3.45 t. There was no bedload registered. Also in this case the center of mass of the sedigraph anticipated the barycenter of the hydrograph.

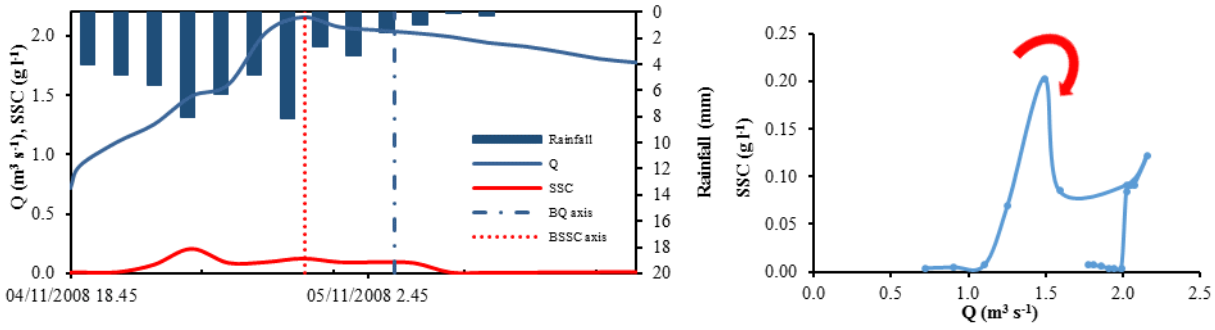

Figure 63: Left: Hydrograph, sedigraph and pluviograph of the 30/10/2008 event, and graphic representation of their barycenters; Right: Hysteresis cycle of the event.

During this rainfall event, high moisture values characterized the soil because of the previous event, occurred 5 days before. Compared to the previous flood, runoff volumes registered during this event induced greater transport rates. Still, 3.42 t are a small quantity if considering that the water discharge reached 2.16 m^3 s^{-1}, and that the runoff volumes were high. This suggests that the catchment was under low availability conditions. The distance between barycenters and the hysteresis loop indicate that the sediment sources were quite close to the main channel.

19/06/2009 rainfall event

This event is characterized by a mixed runoff, induced by both rainfall and snowmelt. Still, the author classifies it as "rainfall event", because the main snowmelt process of the year was already finished, but some remaining of snow were still present in the catchment. The few mm of rain that fell on 19 June helped in the thawing process. The water discharge showed a quick rising, starting at 0.72 m^3 s^{-1} and arriving up to 1.16 m^3 s^{-1} in less than 30 min. The suspended sediment concentration values remained low, showing a maximum value of 0.05 g l^{-1}. The total suspended transport during this event was 0.08 t. The SSC-Q values described a counter-clockwise, circular loop (Fig. 64). In concordance with the direction of the hysteresis, the barycenter of the hydrograph preceded the center of mass of the sedigraph.

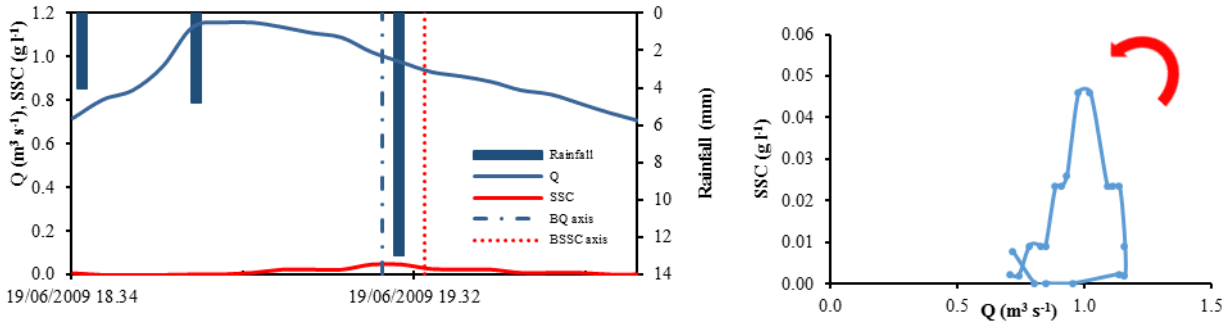

Figure 64: Left: Hydrograph, sedigraph and pluviograph of the 19/06/2009 event, and graphic representation of their barycenters; Right: Hysteresis cycle of the event.

The speedy increase of the water discharge during the first half hour of the event despite the low amount of rainfall suggests that during the rising limb of the graph, the in-channel water was composed by both snowmelt and rainfall runoff water. After the peak, the water level decreased slowly, nonetheless rainfall was more intense than during the previous hour while the falling limb of the graph has its origin only in rainfall water. The sedigraph shows that the sediment source was active only during the rising limb of the hydrograph, thus indicating that rainfall was the key factor in its activation or that the sediment source was located far away from the main channel. Still, the sediment source did not release an important quantity of sediments. The barycenter of the hydrograph anticipated the barycenter of the sedigraph due to the contribution of the snowmelt to the total runoff volumes during the first half of the event.

18/07/2009 rainfall event

This short event was induced by a brief summer storm that registered a maximum rainfall intensity of 13.1 mm h-1. The maximum water discharge value was 1.08 m^3 s^{-1}. Fine sediments were weakly transported during this event; in fact, the peak of suspended sediment concentration reached 0.13 g l^{-1}, and the total suspended load was 0.25 t. The peak of water discharge arrived before the two peaks of SSC, describing a circular, counter-clockwise loop. The barycenter of the sedigraph took place before that of the hydrograph, as shown by Figure 65.

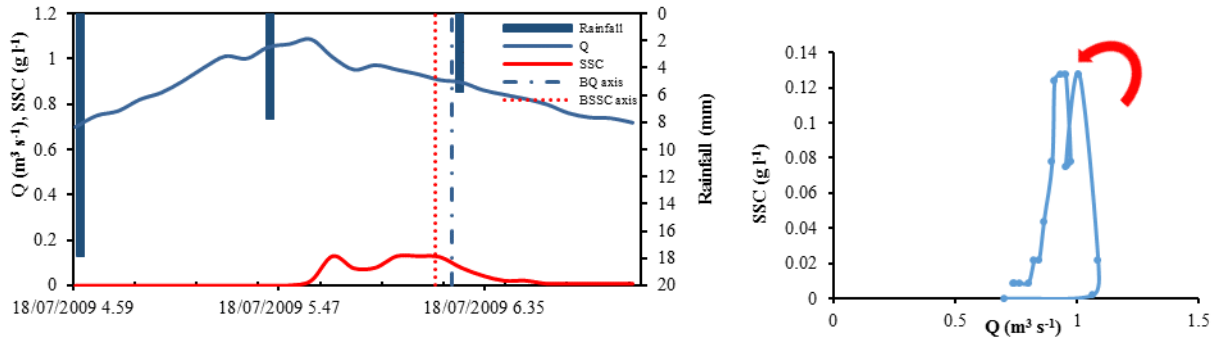

Figure 65: Left: Hydrograph, sedigraph and pluviograph of the 18/07/2009 event, and graphic representation of their barycenters; Right: Hysteresis cycle of the event.

The rainfall during the previous hours contributed to the rising of the hydrograph during the event considered. The shape of the hysteresis cycle during this event suggests that the sediment source was not in the nearby of the monitoring station. Still, the source area did not release much material. As its precedents, this event transported a low amount of suspended sediments. This consecution of events showing low transport rates highlights the depletion that was taking place in the catchment.

14/08/2010 rainfall event

This summer event was characterized by a maximum intensity rainfall of 9 mm h^{-1}, that induced into a speedy increase in the water discharge values. The Q peak was 0.93 m^3 s^{-1}, and the suspended sediment concentration remained in low values through the whole event (SSCp=0.13 g l^{-1}). Moreover, those two variables did not describe a clean loop, as shown by Figure 66. The center of mass of the concentration curve arrived earlier than the barycenter of the hydrograph. The total suspended load was 0.36 t.

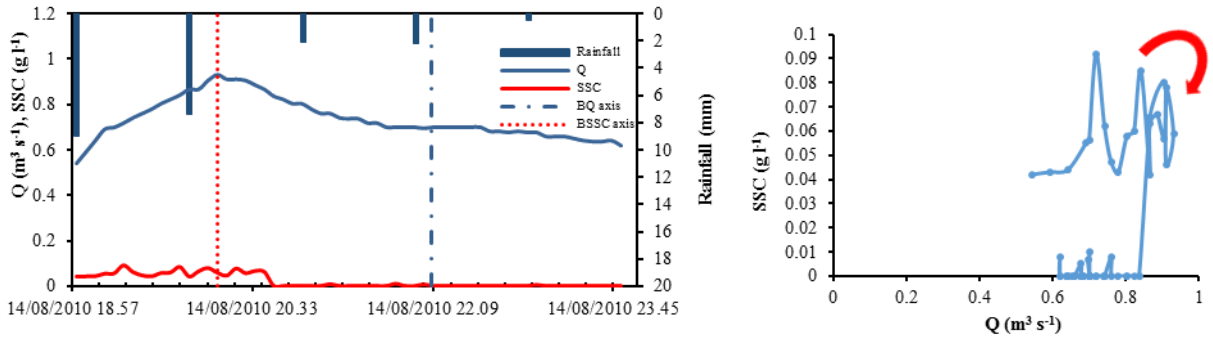

Figure 66: Left: Hydrograph, sedigraph and pluviograph of the 14/08/2010 event, and graphic representation of their barycenters; Right: hysteresis cycle of the event.

Because transport occurred only during the first half of the event, the barycenter of the sedigraph preceded in many hours the barycenter of the hydrograph. The sediment source seems to be more active during the hours in which rainfall shows higher intensity. The shape of the hysteresis loop suggests that the sediment source area was close to the main channel, but they released low amount of suspended solids. In fact, SSC values remained low and did not describe a proper sedigraph.

13/05/2011 snowmelt event

The snowmelt event of this year was quite low, characterized by a thin snow pack, and took place in almost a week. Here we report the 3 days in which water discharge reached higher values and some suspended sediment concentration was registered. Still, it was a snowmelt characterized by low intensity. In fact, Qp was 0.93 m^3 s^{-1}, and SSCp reached only 0.18 g l^{-1}. Due to the continuous risings and fallings showed by the sedigraph, he hysteresis loop described by water discharge values and suspended sediment concentration values was too complicated ad did not report useful information (Fig. 67). The barycenters were almost synchronized, separated only by few minutes. The total suspended load from the whole snowmelt event was 19.49 t.

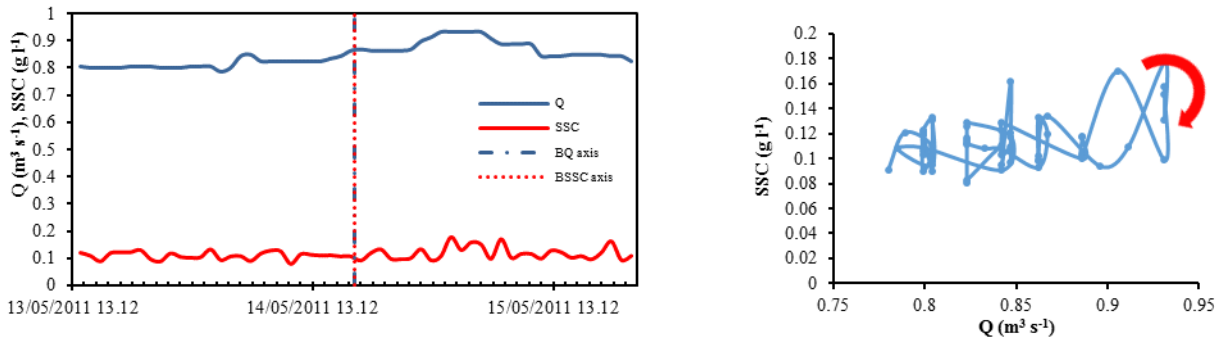

Figure 67: Left: Hydrograph, sedigraph of the 13/05/2011 event, and graphic representation of their barycenters; Right: Hysteresis cycle of the event.

The fuzzy shape of the hysteresis loop, together with the evolution of the sedigraph, suggests that sediment sources were spread all over the catchment area. Snowmelt affected the whole basin, and the runoff volumes washed away a small but continuous amount of solids in their way towards the channel network.

04/11/2012 rainfall event

This event was characterized by 55 mm of rainfall distributed through few hours (Imax= 9.2 mm). This induced into a quick rising of the hydrograph, and a noticeable low diminishing velocity of the falling branch of it. In fact, what we report here is only the rising limb and the first hours of the falling limb, because it actually takes several days. In fact, the barycenter of the hydrograph took place the 6th of November, and due to this reason it is not possible to visualize it in Figure 68. Maximum water discharge reached 1.85 m^3 s^{-1}. The suspended sediment transport did not reflect the high intensity of the event, with the concentrations remaining below 0.1 g l^{-1} (maximum value equal to 0.09 g l^{-1}) and the total load equal to 0.93 t. There was no bedload transport. The event can be considered clock-wised and eight-shaped, though the hysteresis between Q and SSC was not very clear due to the low values of SSC (Fig. 68).

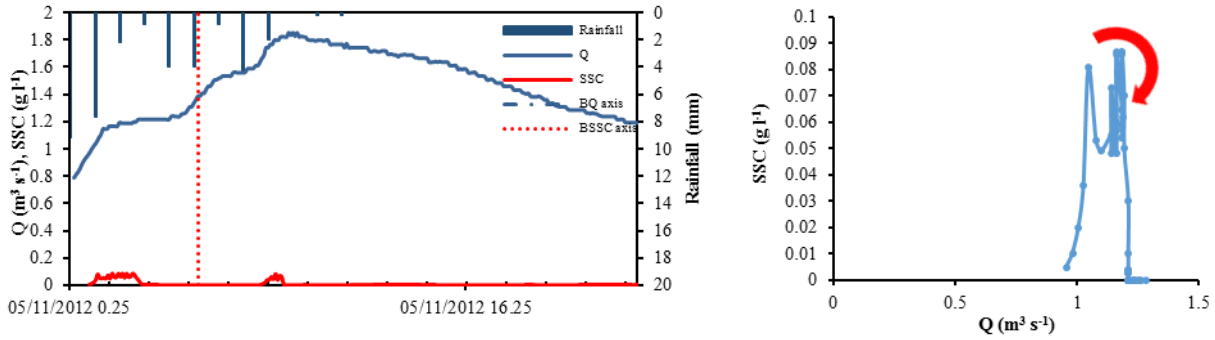

Figure 68: Left: Hydrograph, sedigraph and pluviograph of the 04/11/2012 event, and graphic representation of their barycenters; Right: Hysteresis cycle of the event.

Also in this case an event showing high values of water discharge and very low values of suspended concentration can be observed. The sediment source was active since the first hour of rainfall. The quick arrival of the sediments to the channel network suggests that the source area was nearby the main channel.

11/11/2012 rainfall event

During the 11 November, the water discharge raised quickly (Qp= 2.10 m^3 s^{-1}) due to a high intensity rainfall event. In total, 135.6 mm of rainfall were registered in few hours, with a maximum rainfall intensity of 15.6 mm. The principal characteristic of this event is the high concentration of suspended solids. In fact, this parameter registered two high peaks, of 9.89 g l^{-1} and 9.86 g l^{-1} respectively, much

higher values than the SSCp of the previous events analyzed in this work. A considerable amount of sediments was transported during this event: 60.52 t of fine material and 24.4 t of bedload. The loop described by the SSC and the Q values was fuzzy, but still it was possible to identify an eight-shaped, clockwise loop (Figure 69). Because suspended sediment transport took place mainly during the first hours of the event whilst the hydrograph took more than one day to go down to its initial value of Q, the barycenter of the sedigraph preceded the center of the mass of the hydrograph.

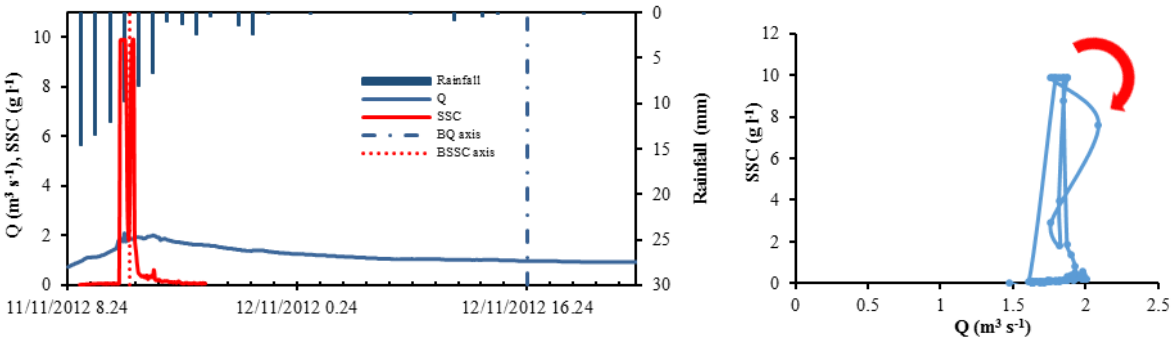

Figure 69: Left: Hydrograph, sedigraph and pluviograph of the 11/11/2012 event, and graphic representation of their barycenters; Right: Hysteresis cycle of the event.

This was the major event in ten years. In fact, the return interval of its water discharge peak (Qp=2.10 m^3 s^{-1}, RI=1.7) is the largest since the flood from November 2002. This value is close to the bankfull discharge, estimated in 2.3 m^3 s^{-1} (Lenzi et al., 2006a). In addition, the suspended sediment concentration reached the highest value of the decade. The high transport rates of the flood can be explained by the high amount of rainfall registered, but also by the antecedent conditions originated by the previous event. The clockwise shape of the hysteresis suggests that the sediment source should have been located close to the main channel. In fact, a debris flow channel located near the monitoring station was identified as the main source in the field observations developed after the event (Figure 70). The low amount of sediment transported during the 5th November event suggests that the debris flow occurred between this event and the 11th November flood event. No geomorphic changes on the main channel of the Rio Cordon were identified during the field surveys (Rainato, 2016). Therefore, despite some fine material remained available for the subsequent floods, in general this event did not induce into higher sediment availability, as the analysis of the subsequent events will reveal. Suspended sediment transport took place mainly during the first hours of the event whilst it took more than one day for the hydrograph to reach its initial value of Q. Therefore, the barycenter of the sedigraph preceded the center of the mass of the hydrograph.

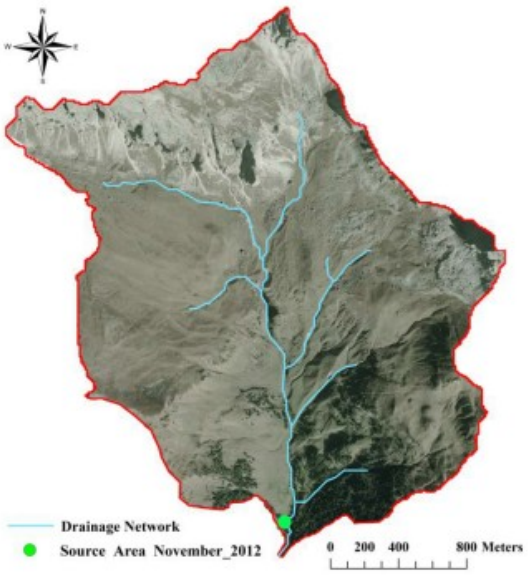

Figure 70: Sediment source area of the 11/11/2012 flood event (after Rainato, 2016).

16/05/2013 snowmelt event

Both snowmelt and rainfall contributed to the runoff volumes of this event, so it can be considered a mixed event. The year 2013 was characterized by a thick snowpack that originated high volumes of runoff when the thaw started. This, combined with strong rainfalls (up to 71.8 mm during the 17th), induced into a considerable rising of the water discharge. In fact, Q reached 1.98 m^3 s^{-1}. Suspended sediment concentration registered a peak equal to 1.53 g l^{-1} 18 hours before the Qp, but apart from this instantaneous value, remained in low values during the whole snowmelt. The total suspended budget from the whole snowmelt was 69.80 t and the hysteresis loop described when plotting Q values against SSC values is clockwised and circular (Fig. 71). Also in this case the barycenter of the sedigraph arrived earlier than the barycenter of the hydrograph. The intensity of the event was enough to create bedload transport: 3.8 t of coarse material were moved during this flood event.

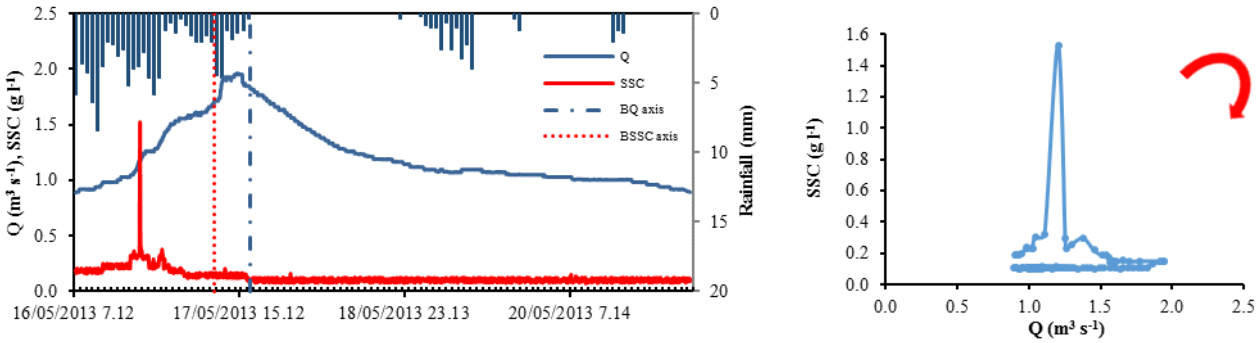

Figure71: Left: Hydrograph, sedigraph and pluviograph of the 16/05/2013 event, and graphic representation of their barycenters; Right: Hysteresis cycle of the event.

The narrow peak of the suspended sediment concentration arrived at the beginning of the event, generating an anticipation of the sedigraph barycenter in respect to the hydrograph barycenter. The hysteresis loop shows a marked clockwise shape. The SSC peak, occurring the 16th at 20:20, arrived 8 hours after the maximum rainfall intensity This suggests that the sediment source was probably activated by a thawing process accelerated by the rainfall in an area close to the monitoring station, perhaps the debris flow channel that generated the sediment transport during the 11th November 2012 event.

09/07/2013 rainfall event

A high intensity summer storm originated this event. In total, 17.6 mm were registered, of which 17.4 arrived during the first hour of the event. The maximum water discharge registered was 2.32 m^3 s^{-1}, whilst the suspended sediment peak reached 0.59 g l^{-1}. The total suspended load was 2.07 t, and there was no bedload transport. The water discharge and suspended sediment concentration values described a clockwise, eight-shaped loop (Fig. 72). Still, SSC peak arrived only few minutes earlier than the maximum value of water discharge. As usual, the barycenter of the suspended concentration curve preceded the center of mass of the hydrograph.

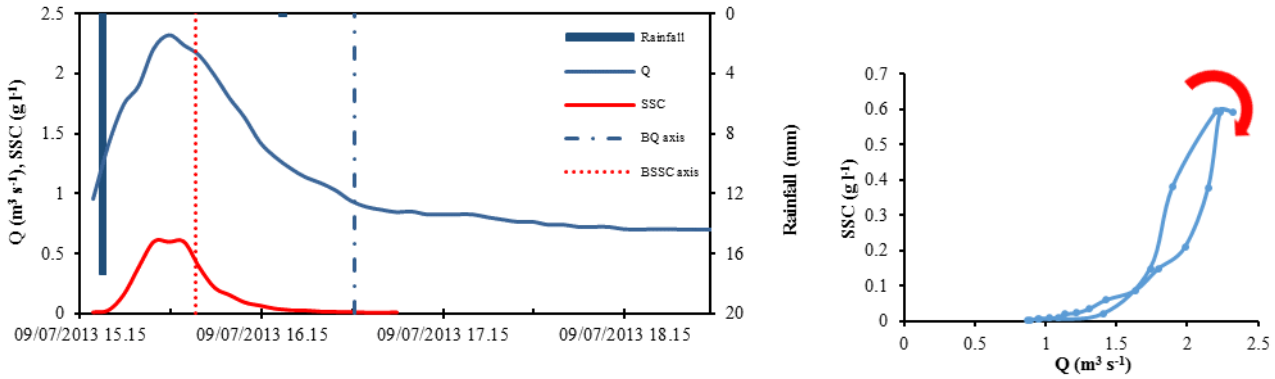

Figure 72: Left: Hydrograph, sedigraph and pluviograph of the 09/07/2013 event, and graphic representation of their barycenters; Right: Hysteresis cycle of the event.

The clockwise shape of the hysteresis loop indicates the rapid response of the sedigraph to the rainfall. Still, the time lag between peaks is less than 10 min, and the curves show a noticeable parallelism. This suggests that the sediment sources were not located in a concrete area, but spread throughout the basin area. Still, transport loads are low if considering the intensity of the rainfall and the high values reached by the water discharge (Qp=2.32 m^3 s^{-1}, higher than bankfull discharge). In the falling limb, the sedigraph takes less time than the Q curve to reach its initial value, thus creating the eight shape hysteresis. This is also the reason why the center of mass of the sedigraph anticipates the barycenter of the hydrograph.

09/06/2014 rainfall event

This event was characterized by a water discharge peak of 2.06 m^3 s^{-1}, due to 16.6 mm of rainfall. Field works taken some days before permitted to assess the absence of snowpack in the catchment, so this event can be considered entirely induced by rainfall, despite it occurred during spring. The most important feature of this event was the bedload budget. In total, 113 t of coarse material were transported due to this flood event. The suspended sediment transport was considerable: 45.75 t were moved during this flood event, and a maximum suspended sediment transport of 3.41 g l^{-1}. The water discharge peak arrived 10 mins before the suspended sediment concentration peak, and these two variables described a circular, counter-clockwise hysteresis. Nonetheless, the rapid decrease in the falling limb of the sedigraph induced into an anticipation of the sedigraph barycenter respect to the hydrograph barycenter (Fig. 73).

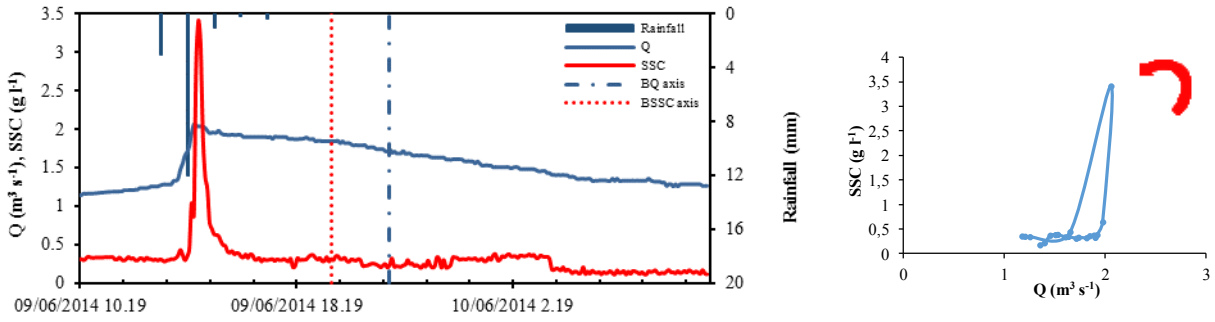

Figure 73: Left: Hydrograph, sedigraph and pluviograph of the 09/06/2014 event, and graphic representation of their barycenters; Right: Hysteresis cycle of the event.

The counter-clockwise shape of the hysteresis cycle suggests that the source area is located far away from the monitoring station. Field activities developed in aims to assess the sediment sources validated this hypotesis: A debris flow channel was located in the medium part of the basin (Fig. 74). Field evidences such as traces of moved soil permitted to identify this debris flow as the main sediment source during this event.

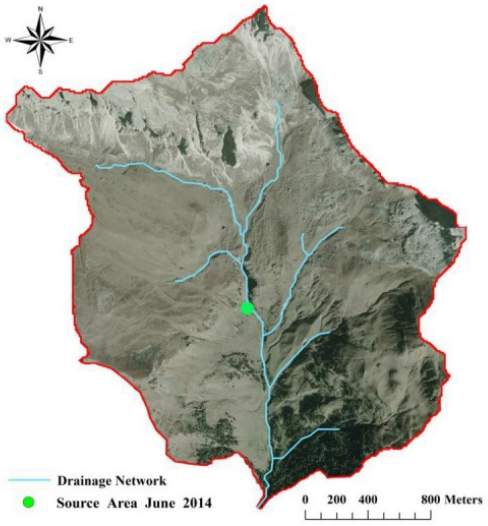

Figure 74: Sediment source area of the 09/06/2014 flood event (after Rainato, 2016).

13/06/2014 snowmelt event

This event and its previous can be considered a multiple event, but the criteria described before determined to split them in two different events. A rainfall of 9 mm that fell in less than 1 hour originated a rising of the water discharge when the hydrograph of the previous event was still in its

falling limb. As a result, a quick rising of the water level was registered (Qp=1.76 m^3 s^{-1}) and the suspended sediments increased its concentration in the water up to 0.32 g l^{-1}. The barycenter of the hydrograph was preceded by the barycenter of the sedigraph, but the peak of water discharge preceded the peak of the suspended sediment concentration, describing a counter-clockwise, eight-shaped loop (Fig. 75). The total suspended load was 1.72 t, a smaller amount than the previous event, probably because the high intensity of the discharge during the previous days washed away most part of the available solids.

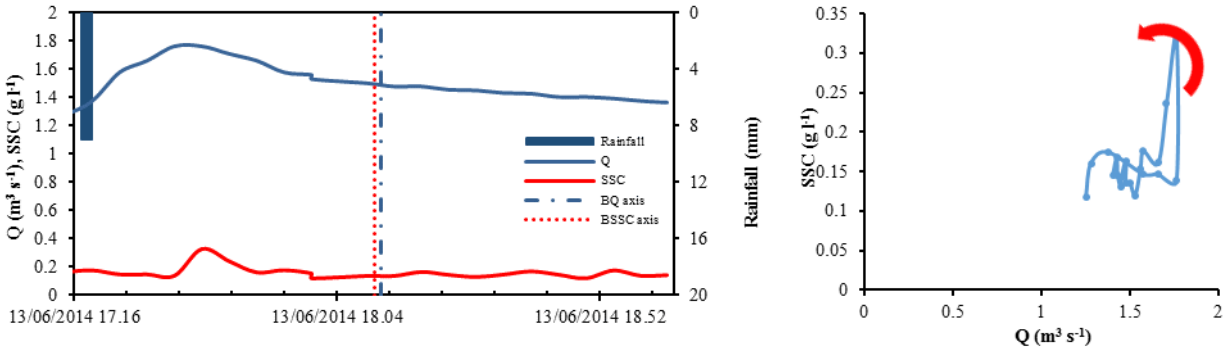

Figure 75: Left: Hydrograph, sedigraph and pluviograph of the 14/09/2014 event, and graphic representation of their barycenters; Right: Hysteresis cycle of the event.

The hysteresis cycle of this event, together with the low values of SSC registered, suggests that no hillslope sediment source was active during the event. It is more likely that solids arrived from the source activated during 9 June 2014 and from channel resuspension processes. Therefore, the transported sediments were just residuals from the precedent event.

Analysis of the registered events

This first study of the single events leads into remarkable outcomes. When considering not only the events described here in detail, but also the events from the previous years observed by previous authors (Lenzi and Marchi, 2000; Mao, 2004), the first thing to notice is that the clockwise behavior is the most common in this catchment. In fact, 67.6% of the events analyzed presented a clockwise behavior (23 events), showing that in the events registered in this catchment suspended sediment peak usually takes place during the rising limb of the hydrograph. It is important to bear in mind that the distance between peaks in case of counter-clockwise loops is usually small (counter-clockwise mean

Δt=0.2 hours, clockwise mean Δt=-3.3 hours), thus indicating that, even if the peak of SSC is preceded by Qp, it arrives immediately after it. The 4 snowmelt events had clockwise hysteresis. A quick reduction of the SSC values after the peak accompanied by a especially slow diminution of the Q values along the falling limb characterized some clockwise events (1, 16, 23, and 31). The very low values of SSC measured at high water level values on the falling limb of the discharge wave may be due to the dilution of the suspended sediment concentrations caused by an increased proportion of the baseflow on the falling limb of the hydrograph. These events are often characterized by an inflexion point that represents the end of the direct (quick) runoff. After this point, SSC shows low values independently from the high values of Q, because only the baseflow contributes to the total runoff. Division between circular and eight-shaped loops is quite balanced: 18 events showed a circular loop (around 53% of the events), and 16 presented an eight-shaped loop, explained by the presence of more than one peak in the hydrograph, in the sedigraph or in both. Negligible or no clear hysteresis loops were registered in the events of May 2002, 10th July 2007, May 2011. In this case, the sedigraph did not show a clear peak or succession of peaks, but featured quite constant values, with low variation of suspended sediment concentration through the event. Regarding the centers of mass, it is noticeable that the barycenter of the sedigraph preceded the center of mass of the hydrograph in most of the cases. In total, 26 events (76.5%) showed an anticipation of the BSSC respect to the BQ.

Furthermore, it has been noted a lower sediment load in the recent years. When plotting SST/Ru ratio of every event (Fig. 76), it can be observed a diminishing trend of this parameter through the years. The events from the recent years show lower suspended sediment concentration and total suspended budget than the previous years. Some high-intensity events occurred through the years (i. e. the events of September 1994, October 1998, May 2001). In those events, the suspended loads are directly proportional to the high values of water discharge. As observed in Figure 76, the years before the 1994 extraordinary event showed ratios that were close to 0, and the period after 1994 presents higher values of SST/Ru due to the higher availability released by the extraordinary events. From 2004, the catchment shows a slow diminishing trend of the sediment loads through the years, thus proving the reduction of the sediment supply in the catchment (events from November 2012 and June 2013 are particular cases due to the debris flows occurred on a small sub-basin located near the outlet or in a small tributary located close to the measuring station contributed with debris-flow input into the main channel).

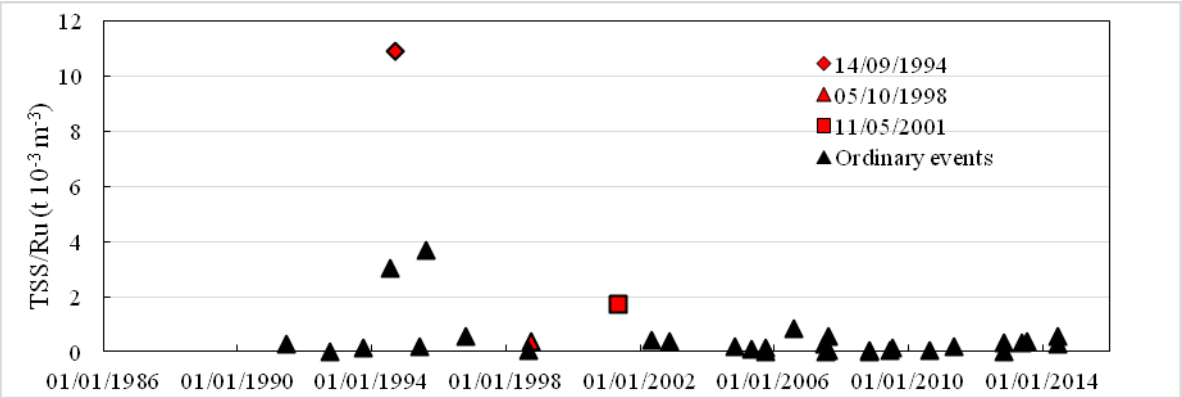

Figure 76: SST-Ru relation for every recorded event since 1986

The analysis of the single events would not be complete without a statistical analysis taking into account the main variables playing any role during flood events. For this reason, the correlation between variables was analyzed, as shown in Table 7. After evaluating the descriptive statistics, a principal component analysis (PCA) was performed with the SPSS program package.

A first analysis was carried out considering all the events showing suspended sediment transport, independently of their runoff origin. As exposed in the previous pages, 4 of the 34 events can be considered as snowmelt events, and the rest are rainfall events. For this analysis, precipitation variables were not considered in aims of taking into account only those parameters that are common to all the events. Hence, rainfall and rainfall intensity during the event as well as the antecedent precipitations and all the time lapses linked to the barycenter of P were eliminated for the analysis here reported.

Table 7: Correlation matrix of the significant variables of the 34 events.

Variables	Qp	Qm	Qi	QSSC	Ru	SSCp	SSCm	SSCQ	TSS	Δt	Δt(tBSSC-tBQ)
Qp	**1**										
Qm	**0.729**	**1**									
Qi	0.183	**0.503**	**1**								
QSSC	**0.915**	**0.707**	0.264	**1**							
Ru	0.379	**0.557**	0.009	0.145	**1**						
SSCp	**0.833**	**0.514**	0.161	**0.889**	0.182	**1**					
SSCm	**0.532**	**0.505**	0.020	**0.605**	0.377	**0.671**	**1**				
SSCQ	**0.798**	**0.482**	0.122	**0.889**	0.110	**0.983**	**0.688**	**1**			
TSS	**0.873**	**0.558**	0.189	**0.869**	0.248	**0.973**	**0.665**	**0.946**	**1**		
Δt	0.079	0.055	0.018	0.192	-0.173	0.106	0.146	0.155	0.060	**1**	
Δt(tBSSC-tBQ)	-0.219	-0.377	0.019	-0.078	**-0.750**	-0.102	-0.378	-0.079	-0.104	0.059	**1**

The correlation matrix shows good relationships between water discharge peak and the concentration variables. The correlation values between Qp and SSCp, SSCm and SSC_Q are: R=0.83, R=0.53, R=0.80 respectively. Lower results are observed between these transport variables and Qm. This variable shows correlations of R=0.51, R=0.50 and R=0.48 when plotted against SSCp, SSCm and SSC_Q respectively. This is probably due to the fact that we are considering snowmelt and rainfall events altogether. During the extended duration of the snowmelt events, the water discharge increases and decreases with quite slow rates, and often shows several peaks. Consequently, its mean value is less significant and its influence in the sedigraph peak and the mean value of suspended sediment concentration less direct than in the rainfall event. The initial water discharge Qi does not show any close relation with any transport variable.

As the suspended concentration variables, the total suspended sediment load shows a quite good relationship with the water discharge peak Qp and lower but still close correlation with the mean water discharge Qm (R=0.87 and R=0.56, respectively), suggesting that the sediment loads are influenced by the intensity of the event. Higher values of water discharge are linked to higher participation of the local sediment sources. On the other hand, the correlation between the suspended load and the runoff volumes is considerably poor (R=0.25), indicating that there is not a univocal relationship between those variables, probably due to the fact that the sediment sources are located in areas spread within the catchment and do not show an homogeneous response to the volumes of water from runoff. In other words, the activation of the sediment sources seems to be mainly linked to the intensity of the event rather than its magnitude. In fact, Ru shows low correlations also when linked to SSCp, SSCm and SSC_Q.

No good correlation is shown between Δt (time lapse between Qp and SSCp) and any other variable. A possible explanation for this result is the small size of the basin area. In this catchment, time between peaks is usually reduced and does not show significant responses according to the variations of the hydrological parameters. In fact, 68% of the events show a time interval between peaks lower than 1 hour, independently from the magnitude of the liquid volumes or the solid masses.

Despite it is not well related to any transport variable, runoff volume shows an interesting correlation (R=-0.75) with the time lapse between BSSC and BQ. Higher volumes of runoff lead into a greater lapse between the barycenter of the sedigraph and the hydrograph barycenter. That is to say, the higher is the magnitude of the runoff, the more the sedigraph barycenter anticipates the hydrograph barycenter. This result suggests that a greater event will present its hydrograph shifted to the right,

whilst the sedigraph does not show such a direct displacement behavior respect to the runoff magnitude. In other words, if we study two events that show the same sedigraph and hence the same BSSC, the event with a higher runoff will have a hydrograph with a BQ placed towards the right. Therefore, the anticipation of the BSSC will be greater respect to the BQ. Nevertheless, another interpretation could be that the volumes of runoff are a key factor for the sediment masses to move faster or slower, and consequently a great value of R could make us expect a rapid mobilization of the sediment loads and hence an anticipation of the sedigraph barycenter respect to the hydrograph barycenter.

A Principal Component Analysis was performed to highlight the main drivers controlling the sediment transport in the events registered during the study period. This analysis explains the 69.79% of the variance (Fig. 77).

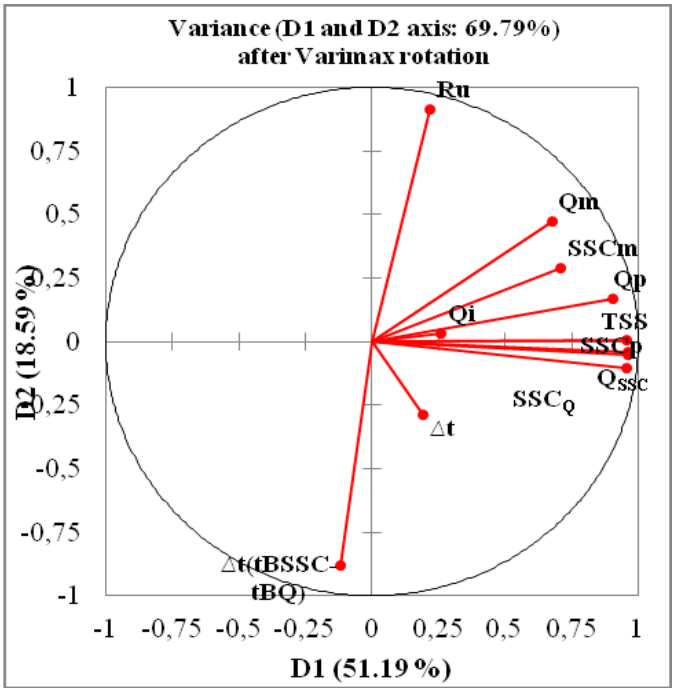

Figure 77: PCA from the 34 registered events. Component plot in rotated space.

The first factor D1explains the 51.19% of the variance and is mainly influenced by Qp, Qm, Qssc, SSCp, SSCm, SSC_Q and TSS. The second factor D2 explains only the 18.59% of the variance and is influenced positively by Ru and negatively by Δt(tBSSC-tBQ). This result is in accordance with the correlation matrix, in which these two variables had a strong negative correlation.

3.2.2. Rainfall events analysis and comparison with a Mediterranean Catchment

A second similar analysis was performed excluding the 4 events that present snowmelt, in order to consider only the variables that play a role in the rainfall events. The same analysis was done considering 34 rainfall events occurred in the Carapelle basin. The aim was to compare the rainfall events occurred in the Rio Cordon with those occurred in a catchment showing quite different characteristics. Due to the different geographic location, these catchments feature noticeable differences concerning their size, climate, lithology, morphology and land use. These differences can be useful to assess the factors that play a different role when the hydrogeologic conditions change. This comparison can also help to analyze the factors affecting sediment dynamics under general conditions. Turbidity and water discharge were monitored during the floods occurring in 2010 and 2011. As with the events taken place in the Rio Cordon, hysteresis between SSC and Q was assessed, as well as the runoff volumes, the suspended sediment load, the barycenters of the hydrograph and the sedigraph and the characteristics of the precipitation (during the event and during the previous hours).

As a first result, 88% of the events in the Carapelle had a counter-clockwise hysteresis, whilst the analysis resulted in 68% of the events showing a clockwise behavior in the Rio Cordon. In the Carapelle torrent, the rainfall causing the flow event usually started several hours before the beginning of the flood. Besides, the clockwise events registered in this catchment are always characterized by eight-shaped loops.

Table 8: Characteristics of the single events recorded in the Carapelle Catchment.

event ID	Date	Qp	Qm	Qi	QSSC	R	SSCp	SSCm	SSCQ	TSS	PTOT	Imax	Iav	Δt	Δt(BSSC-BQ)	Qa1d	P3	P6	P12	P24	P48	Hysteresis direction	Hysteresis shape
1	02/01/2010	16.05	9.05	4.89	12.09	1874	4.72	1.27	3.40	2870	15.0	2.2	0.6	5.0	-4.12	4.53	0.0	0.0	0.0	0.0	0.6	Counter-Clockwise	Circular
2	31/01/2010	13.34	8.81	6.65	0.64	1982	4.12	0.78	0.64	1721	4.7	1.4	0.3	7.0	-4.19	7.15	0.0	0.1	0.5	0.5	1.6	Counter-Clockwise	Eight-shaped
3	20/02/2010	11.20	9.48	8.50	9.27	751	0.93	0.52	0.47	388	1.8	1.0	0.2	10.5	1.34	11.79	0.0	0.0	0.1	6.1	6.9	Counter-Clockwise	Circular
4	24/02/2010	12.71	8.37	5.25	8.75	799	3.02	1.19	0.18	974	7.6	3.2	1.3	8.5	-0.38	5.55	0.0	0.0	0.0	0.5	1.6	Counter-Clockwise	Circular
5	14/03/2010	14.66	10.44	9.01	11.49	1052	2.76	1.10	0.58	1189	4.6	1.8	0.6	6.0	-0.46	9.70	0.0	0.0	0.0	0.0	2.9	Counter-Clockwise	Circular
6	14/04/2010	9.27	6.69	4.72	5.25	313	1.11	0.71	0.51	215	13.5	2.6	1.2	6.5	1.52	3.87	0.0	0.1	0.3	1.9	7.8	Counter-Clockwise	Circular
7	20/05/2010	8.01	4.16	2.32	3.09	487	8.73	2.92	0.50	1251	17.2	8.9	2.9	12.5	0.48	2.08	0.0	0.0	0.0	0.1	6.9	Counter-Clockwise	Eight-shaped
8	11/09/2010	20.62	7.49	3.35	16.77	1349	15.24	3.30	1.23	5957	58.8	7.7	1.7	2.5	-2.25	2.99	0.2	0.4	1.3	7.8	12.3	Counter-Clockwise	Circular
9	22/11/2010	58.84	28.93	1.41	56.76	1510	27.81	10.84	26.44	22118	20.2	6.1	1.8	-0.5	0.57	1.22	0.0	0.0	0.0	0.4	0.5	Clockwise	Eight-shaped
10	23/11/2010	55.39	30.42	15.00	55.39	1917	11.14	7.28	11.14	15514	10.2	3.0	0.8	0.0	0.72	17.68	0.0	0.2	16.5	20.2	20.7	Counter-Clockwise	Eight-shaped
11	24/11/2010	17.51	11.85	8.50	12.09	640	5.40	3.31	2.14	2135	3.1	1.3	0.4	4.5	1.05	15.34	0.0	0.2	0.9	4.1	32.2	Counter-Clockwise	Circular
12	26/11/2010	12.71	5.73	2.97	7.09	516	5.82	4.72	5.06	2509	3.6	1.2	0.7	6.5	2.08	3.48	0.1	0.2	0.4	0.8	1.5	Counter-Clockwise	Eight-shaped
13	29/11/2010	3.92	2.49	1.98	2.32	170	1.83	1.19	0.58	195	2.0	0.6	0.2	7.0	2.02	2.26	0.0	0.1	0.1	0.5	0.6	Counter-Clockwise	Circular
14	30/11/2010	20.22	8.21	2.32	18.64	1123	8.65	5.24	5.89	6373	11.3	2.8	0.7	1.5	2.02	2.40	0.0	0.0	0.1	1.3	2.5	Counter-Clockwise	Eight-shaped
15	02/12/2010	33.68	16.16	3.77	28.15	785	18.85	8.46	6.52	7823	5.9	3.2	0.5	1.0	0.14	6.36	0.0	0.0	0.0	5.3	11.4	Clockwise	Circular
16	02/12/2010	11.79	8.49	8.50	7.78	428	2.57	1.76	1.53	750	1.7	1.0	0.2	5.5	0.73	10.70	0.0	0.0	5.0	5.9	15.2	Counter-Clockwise	Eight-shaped
17	03/12/2010	72.16	23.52	5.44	65.33	3345	16.92	3.81	11.95	22719	16.1	4.8	1.1	-2.0	-0.93	7.79	0.1	0.1	0.1	1.8	7.7	Clockwise	Eight-shaped
18	18/12/2010	18.64	4.99	2.14	10.35	772	16.74	3.80	1.11	4508	10.9	3.2	0.6	3.5	-2.19	1.57	0.0	0.0	0.0	0.0	0.1	Counter-Clockwise	Circular
19	24/12/2010	12.10	5.67	1.64	3.77	286	21.32	10.25	0.82	2325	6.4	2.9	1.2	8.5	3.19	1.58	0.0	0.0	0.2	0.3	0.3	Counter-Clockwise	Circular
20	24/12/2010	20.62	8.37	3.48	12.40	528	14.81	7.32	4.99	4327	4.0	3.3	0.9	3.0	0.60	3.93	0.0	0.1	4.5	6.4	6.7	Counter-Clockwise	Circular
21	28/01/2011	25.81	10.12	2.32	22.28	1312	14.20	5.80	6.38	8969	11.1	1.3	0.5	3.0	5.23	2.25	0.0	0.0	0.0	0.0	0.1	Counter-Clockwise	Circular
22	17/02/2011	2.32	1.66	1.45	1.54	218	1.41	0.72	0.18	149	6.3	2.1	0.5	14.5	5.36	1.37	0.0	0.0	0.0	0.0	0.0	Counter-Clockwise	Eight-shaped
23	19/02/2011	159.50	32.28	1.59	111.50	5114	37.36	7.83	35.13	111226	37.7	6.9	2.6	-2.0	0.17	1.55	0.0	0.0	0.0	0.0	6.4	Clockwise	Eight-shaped
24	22/02/2011	4.07	3.03	2.52	2.52	420	0.88	0.66	0.88	283	4.0	0.9	0.2	14.5	0.76	3.16	0.0	0.0	0.0	0.0	0.0	Counter-Clockwise	Eight-shaped
25	28/02/2011	2.74	2.04	1.76	1.83	239	0.70	0.41	0.24	96	1.8	1.0	0.3	21.5	3.62	1.83	0.0	0.2	1.1	2.4	2.4	Counter-Clockwise	Eight-shaped
26	01/03/2011	59.55	11.26	1.90	47.54	2169	23.48	3.23	5.06	15286	21.1	4.2	1.0	1.5	-0.85	1.89	0.2	0.3	0.4	0.4	2.7	Counter-Clockwise	Circular
27	03/03/2011	4.22	3.33	2.14	3.09	264	0.99	0.61	0.53	162	2.3	1.2	0.5	9.0	1.54	3.80	0.1	0.1	0.1	0.1	15.7	Counter-Clockwise	Circular
28	17/03/2011	13.99	3.63	1.35	2.97	366	10.66	4.34	0.99	1516	5.8	2.6	0.9	8.5	2.94	1.50	0.6	0.9	1.0	4.9	4.9	Counter-Clockwise	Circular
29	19/03/2011	12.40	4.02	1.64	11.49	724	8.73	2.50	8.28	2465	8.2	1.8	0.3	-0.5	2.11	3.56	0.0	0.0	0.2	6.0	10.9	Clockwise	Eight-shaped
30	06/04/2011	19.82	3.12	1.20	7.78	506	47.83	7.03	12.69	7461	13.7	4.2	1.6	3.5	-1.75	0.81	0.0	0.0	0.0	0.0	0.0	Counter-Clockwise	Circular
31	01/05/2011	42.65	11.74	0.73	35.28	1987	21.12	4.89	6.88	18453	31.4	3.2	1.3	2.5	0.77	0.78	0.0	0.1	0.2	0.3	2.5	Counter-Clockwise	Eight-shaped
32	03/05/2011	34.21	13.15	1.59	22.71	757	20.26	8.29	16.83	8549	10.5	2.8	0.8	1.5	1.07	1.94	0.0	0.0	0.0	0.1	19.6	Counter-Clockwise	Circular
33	03/05/2011	24.45	10.42	5.25	19.03	1126	15.72	4.02	4.69	5759	11.2	1.1	0.9	1.5	-0.87	9.24	0.0	0.0	8.8	10.5	10.6	Counter-Clockwise	Circular
34	05/05/2011	8.75	3.10	3.48	3.22	329	1.71	1.20	1.53	437	3.3	1.4	0.7	8.0	2.26	8.85	0.0	0.0	1.8	8.1	21.7	Counter-Clockwise	Circular

Table 9: Correlation matrixes for the variables of the rainfall events in Rio Cordon (left) and Carapelle (right).

Variables	Qp	Qm	Qi	Q_{SSC}	Ru	SSCp	SSCm	SSC_Q	TSS	Ptot	Imax	Iav	Δt	Δt(BSSC-BQ)	P3	P6	P12	P24	P48
Qp	**1**																		
Qm	**0,718**	**1**																	
Qi	0,197	**0,518**	**1**																
Q_{SSC}	**0,913**	**0,698**	0,288	**1**															
Ru	**0,381**	**0,560**	-0,042	0,146	**1**														
SSCp	**0,859**	**0,515**	0,122	**0,911**	0,184	**1**													
SSCm	**0,530**	**0,499**	0,002	**0,602**	**0,385**	**0,669**	**1**												
SSC_Q	**0,817**	**0,480**	0,090	**0,905**	0,111	**0,983**	**0,685**	**1**											
TSS	**0,902**	**0,564**	0,145	**0,894**	0,244	**0,973**	**0,666**	**0,947**	**1**										
Ptot	0,153	**0,460**	-0,077	0,184	**0,649**	0,201	**0,449**	0,181	0,153	**1**									
Imax	**0,555**	0,298	0,077	**0,701**	-0,142	**0,595**	0,357	**0,614**	**0,535**	0,109	**1**								
Iav	**0,637**	**0,412**	0,343	**0,752**	-0,220	**0,672**	0,342	**0,682**	**0,689**	-0,063	**0,753**	**1**							
Δt	0,105	0,085	0,123	0,205	-0,110	0,096	0,140	0,150	0,076	-0,045	0,261	0,283	**1**						
Δt(BSSC-BQ)	-0,194	**-0,366**	-0,006	-0,055	**-0,767**	-0,117	**-0,384**	-0,090	-0,120	**-0,697**	0,064	0,193	0,034	**1**					
P3	0,139	0,076	0,101	0,148	0,120	0,284	0,238	0,324	0,258	0,312	0,132	0,254	0,195	**-0,511**	**1**				
P6	0,082	0,087	0,096	0,082	0,236	0,243	0,212	0,278	0,203	**0,411**	0,049	0,105	0,051	**-0,557**	**0,895**	**1**			
P12	-0,019	0,144	-0,046	0,007	0,344	0,038	0,193	0,061	0,025	**0,631**	-0,049	-0,152	0,052	**-0,519**	**0,437**	**0,546**	**1**		
P24	0,141	0,216	0,065	0,166	0,246	0,215	0,306	0,240	0,245	**0,454**	-0,086	-0,036	0,044	-0,328	0,352	**0,438**	**0,849**	**1**	
P48	0,090	0,129	-0,025	0,083	0,218	0,138	0,241	0,163	0,176	**0,401**	-0,154	-0,099	0,023	-0,267	0,291	0,347	**0,812**	**0,961**	**1**

Variables	Qp	Qm	Qi	Q_{SSC}	Ru	SSCp	SSCm	SSC_Q	TSS	Ptot	Imax	Iav	Δt	Δt(BSSC-BQ)	Qa1d	P3	P6	P12	P24	P48
Qp	**1**																			
Qm	**0,841**	**1**																		
Qi	-0,013	**0,353**	**1**																	
Q_{SSC}	**0,977**	**0,902**	0,059	**1**																
Ru	**0,907**	**0,768**	0,093	**0,892**	**1**															
SSCp	**0,634**	**0,449**	**-0,340**	**0,587**	**0,472**	**1**														
SSCm	**0,500**	**0,557**	-0,179	**0,506**	0,265	**0,758**	**1**													
SSC_Q	**0,858**	**0,784**	-0,157	**0,848**	**0,688**	**0,714**	**0,661**	**1**												
TSS	**0,948**	**0,701**	-0,122	**0,881**	**0,847**	**0,574**	**0,404**	**0,826**	**1**											
Ptot	**0,530**	**0,362**	-0,221	**0,524**	**0,569**	**0,500**	0,252	**0,413**	**0,514**	**1**										
Imax	**0,506**	**0,401**	-0,225	**0,495**	**0,442**	**0,557**	**0,413**	**0,456**	**0,466**	**0,748**	**1**									
Iav	**0,529**	**0,370**	-0,266	**0,482**	**0,429**	**0,590**	**0,422**	**0,507**	**0,551**	**0,670**	**0,906**	**1**								
Δt	**-0,612**	**-0,646**	-0,112	**-0,648**	**-0,575**	**-0,579**	**-0,572**	**-0,612**	**-0,452**	**-0,423**	-0,316	-0,244	**1**							
Δt(BSSC-BQ)	-0,186	-0,213	-0,248	-0,159	**-0,386**	-0,240	0,052	-0,088	-0,103	-0,338	-0,298	-0,189	**0,357**	**1**						
Qa1d	-0,031	0,306	**0,934**	0,037	0,036	**-0,349**	-0,182	-0,158	-0,136	-0,299	-0,312	-0,335	-0,123	-0,155	**1**					
P3	0,004	-0,128	-0,186	-0,026	-0,029	0,023	-0,034	-0,137	-0,053	0,119	0,104	0,051	0,030	0,088	-0,196	**1**				
P6	-0,042	-0,097	-0,037	-0,061	-0,059	-0,055	-0,052	-0,173	-0,085	0,146	0,063	0,008	0,093	0,102	-0,055	**0,940**	**1**			
P12	0,101	**0,355**	**0,652**	0,175	0,060	-0,035	0,158	0,041	-0,005	-0,064	-0,098	-0,079	-0,205	-0,047	**0,617**	-0,035	0,091	**1**		
P24	0,026	0,276	**0,629**	0,104	-0,019	-0,111	0,092	-0,035	-0,077	-0,005	-0,080	-0,139	-0,221	0,000	**0,679**	0,070	0,218	**0,872**	**1**	
P48	0,042	0,201	**0,456**	0,067	-0,056	-0,148	0,014	0,032	-0,021	-0,054	-0,072	-0,096	-0,217	0,029	**0,649**	-0,029	0,075	**0,406**	**0,569**	**1**

The second correlation matrix of the Rio Cordon (Table 9) also shows good relations between water discharge peak and the concentration variables. The correlation values between Qp and SSCp, SSCm and SSC_Q are R=0.859, R=0.530 and R=0.817, respectively. These values are noticeably higher than in the previous matrix. Because only rainfall events are taken into account now, a higher homogeneity can be expected. Moreover, the water discharge peak and the total suspended load show a strong correlation (R=0.902). As in the previous case, Qm shows lower correlations than Qp with this variables, of R=0.515, R=0.499 and R=0.480 when plotted against SSCp, SSCm and SSC_Q respectively.

No good correlation is noticed between Δt and any other variable. As noticed in the previous analysis, time between peaks is usually short in this catchment and does not show any significant response to the variations of the hydrological parameters.

Regarding the precipitation variables, Qp shows a good correlation with Imax and Iav (R=0.555 and R=0.637, respectively), but no good correlation with the total precipitations or the antecedent rainfall conditions. Good correlations between SSCp and TSS with the maximum rainfall intensity Imax are found (R=0.595 and R=0.672). The correlations of those two transport variables with the average intensity during the events are a bit higher (R=0.672 and R=0.689 respectively). On the other hand, the total precipitation did not present any good correlation with the water discharge variables (with the exception of Qm, R=0.460), or the transport variables. Instead, a good correlation is found between the runoff volumes and the total precipitation (R=0.649). Once again, runoff volume shows a close correlation (R=-0.767) with the time lapse between BSSC and BQ. The antecedent rainfall conditions are not related to any discharge or concentration variable, nor to the runoff or the total transport. the antecedent rainfall does not show a clear correlation with the initial conditions of the flood either. Instead, 3, 6 and 12 hours previous to the event are inversely related to the time lag between the barycenter of the sedigraph and the barycenter of the hydrograph Δt(BSSC-BQ) (R=0.511, R=0.557 and R=0.519, respectively). This linkage is due to the rapid response of the catchment induced by its small size Also the runoff volume shows a close correlation (R=-0.767) with the time lapse between BSSC and BQ, for the reasons stated above.

The correlation matrix of the Carapelle showed that in this catchment only at the beginning of the event the water discharge is affected by antecedent rainfall. In particular, there is a good correlation between the initial water discharge and the precipitation from the previous 12 and 24 hours (R = 0.652 and R = 0.629, respectively), and a moderate correlation (R = 0.456) with the precipitation from the

previous 48 hours. Besides, mean water discharge during the 24 hours before the flow event Qa1d showed good correlations with the previous 12, 24 and 48 hours precipitation (R = 0.617, 0.679 and 0.649 respectively). It is noticeable that Qa1d shows its better correlation with P24, while the initial discharge Qi are better correlated to P12. The water discharge values Qa1d and Qi are also strongly correlated between them (R= 0.934).

Regarding the transport variables, in the Carapelle catchment the correlations between Qp and the transport variables SSCp and SSCm are good (R=0.634 and R=0.500, respectively), while it shows a stronger relationship when linked to SSCq and TSS (R=0.858 and R=0.948, respectively). On the other hand, the correlations between the transport variables and the average water discharge during the event Qm are quite moderate (R=0.449, R=0.557 and R=0.784, respectively). TSS and the runoff volumes Ru show a strong correlation (R=0.847). The main transport variables are well correlated to the rainfall that generates the flood event. SSCp shows R=0.5, R=0.577 and R=0.590 when correlated to Ptot, Imax and Iav, respectively, while those values for the TSS are 0.514, 0.466 and 0.551, respectively.

The time lapse Δt between the flow and the concentration peak shows an inverse relationship (R=-0612) with the flow peak value Qp. The inverse correlation between Δt and SSCp is also good (R=-0.58). Lower correlations are shown between Δt and total runoff Ru (R= -0575) and between Δt and the total suspended sediment TSS (R=-0452). Time lag between peaks is not directly related to the rainfall conditions, as shown in the correlation matrix, but depends on the runoff and the sediment transport generated by them. As happened in the Rio Cordon catchment, the correlation matrix shows that the variables Δt and Δt(BSSC-BQ) are not well correlated in the Carapelle either. However, these two parameters are often both positive or negative in both catchments, as shown in Figure 78.

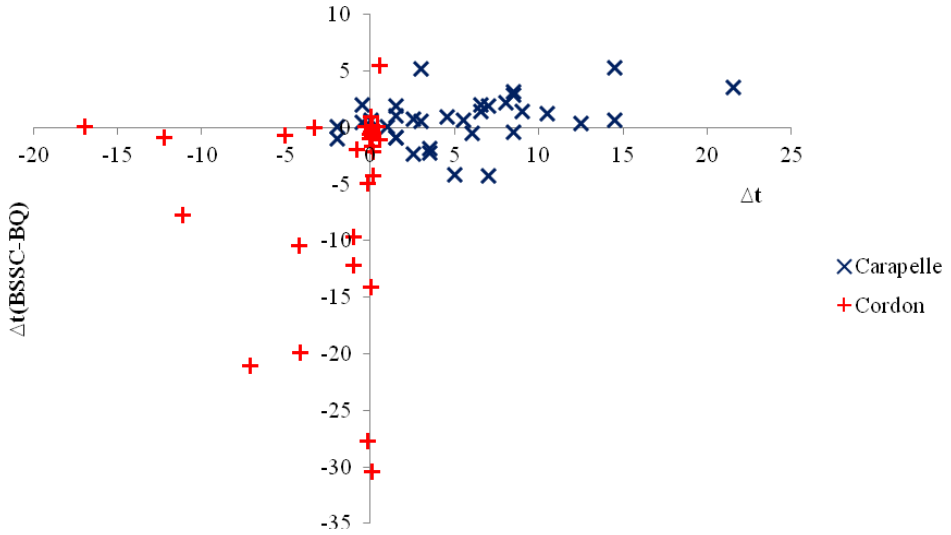

Figure 78: Time delays of both catchments (after Pagano et al., under review).

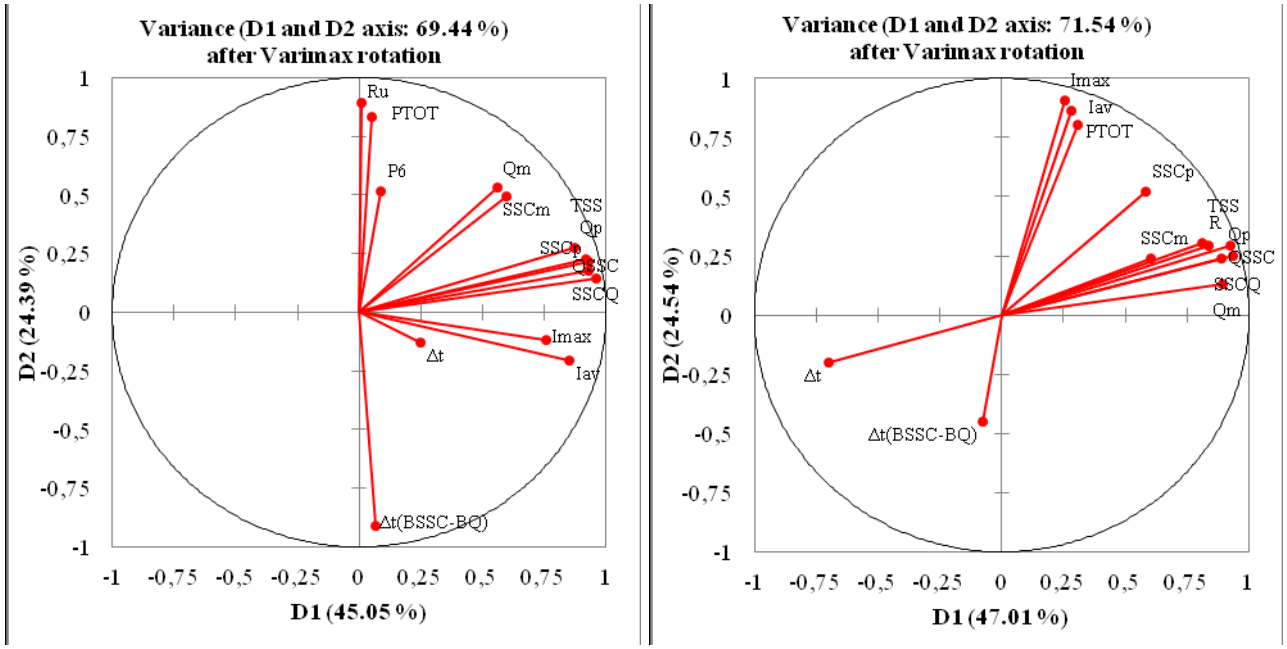

Figure 79: PCA from the rainfall events occurred in Cordon (left) and Carapelle (right). Component plot in rotated space (after Pagano et al., under review).

A Principal Component Analysis was performed to highlight the main drivers controlling the sediment transport in the rainfall events from each catchment (Fig. 79). In the case of the Rio Cordon, the main factors of the PCA analysis explain the 69.44% of the variance. The first factor is influenced by Qp, Qssc, SSCp, TSS, Imax and Iav. Keeping in mind that results from the correlation matrix demonstrate

that the rainfall intensity plays a key role in the flood entity, and considering that the intensity of the flood can be defined by the Qp, and SSCp values and the total load generated by it, the principal component D1 can be related to the flood intensity. The second factor D2 is affected by Ru, Ptot and Δt(BSSC-BQ). Δt(BSSC-BQ) can be considered a mere consequence of the Ru and Ptot magnitudes in this catchment. Hence, we can consider D2 to be related to the liquid volumes. Plotting the 30 rainfall events in the factorial planes, neither the loop direction nor the loop shape are explained by the main two components. Extraordinary event number 5 affects sharply the first component D1 (Figure 80). The PCA carried out on the 30 rainfall events from the Cordon catchment evidences that the loops corresponding to the events do not seem to be explained by the main components D1 and D2. No behavior of the direction of the loops in correspondence with D1 and D2 is shown. The components do not seem to explain the hysteresis shape either (Figure 80). It is noticeable, though, how all the rainfall events are closely linked to D2, with the only exception of event number 5, which is the extraordinary flood of September 1994, when high dynamics on sediment sources spread all over the catchment. Furthermore, all the events except number 13 fit D1. The peculiarity of this long autumn rainfall event is that due to the high sediment released during the 2001 snowmelt year on the channel network, the fine material availability conditions were almost un-limited. Therefore, suspended sediments were easily mobilized during the extended rainfall that characterized event number 13 (15/11/2002).

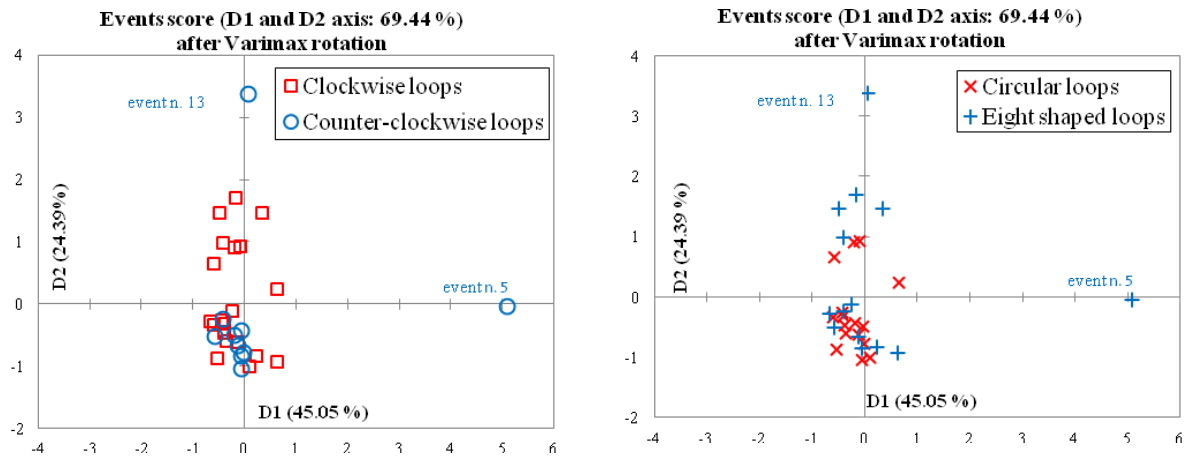

Figure 80: Event distributions in the factorial planes according to the hysteresis directions (left) and shape (right) in the Rio Cordon (after Pagano et al., under review).

The principal component analysis performed for the Carapelle events explains 71.54% of the variance. The first factor D1, which explains 47.01% of the variance, is influenced by Qp, Qm, Qssc, Ru, TSS and Δt. these variables characterize the flood and the loads transported by it. The second factor D2

explains 24.54% of the variance and is dependent on the variables that define the rainfall conditions that generate the event, that is to say, Ptot, Imax and Iav. The PCA carried out on the 34 events from the Carapelle catchment shows that 3 of the 4 clockwise loops are influenced by the first component D1 (explaining the 47.01% of the variance). On the other hand, the event n. 29 is the only event that shows a lower discharge respect to the high peaks that characterize the clockwise behavior in the Carapelle catchment and is influenced by D2. Moreover, hysteresis shape fits both the principal components D1 and D2 in this catchment.

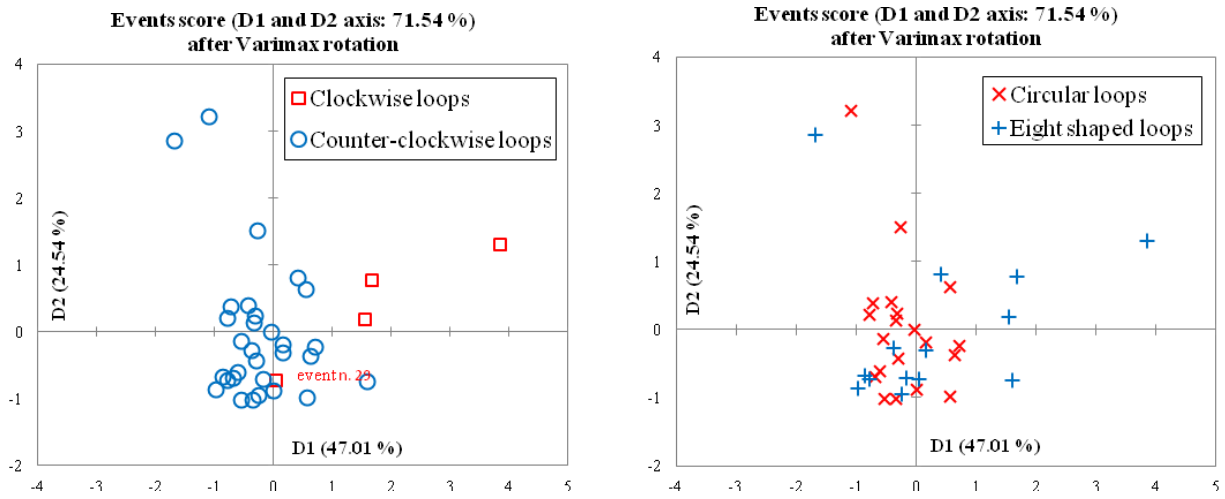

Figure 81: Event distributions in the factorial planes according to the hysteresis directions (left) and shape (right) in the Carapelle (after Pagano et al., under review).

Once assessed the characteristics of the sediment transport and the factors that influence it in both catchments, a PCA considering the 64 rainfall events was performed in aims of assessing the role of the studied variables in the suspended sediment transport dynamics taking into account both basins. This common PCA explains the 67.95% of the variance. Results suggest that Qp, Qm, Ru, SSCp, SSCm and TSS are the parameters that mainly influence D1, which explains 44.51% of the variance. These variables characterize the transport during the flood. D2, explaining 23.44% of the variance, is defined by the rainfall variables that originate the event: Ptot, Imax and Iav (Fig. 82).

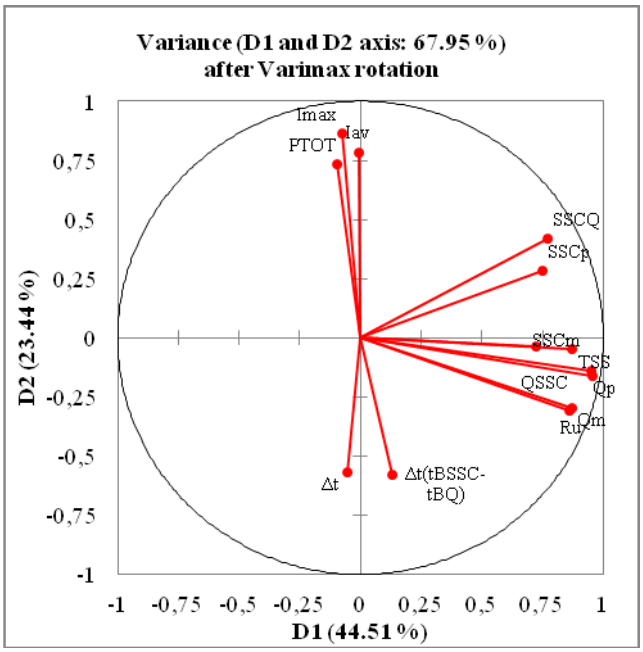

Figure 82: PCA considering the rainfall events from both catchments (after Pagano et al., under review).

.

3.3. Field monitoring events, period 2014-2015.

In aims of studying the spatial variations featured by the suspended sediment transport within single flow events, field campaigns were performed between 2014 and 2015 in the catchment area of the Rio Cordon. The electrical conductivity and suspended sediment content of the in-channel water were monitored hourly in two different sections of the main channel (SST1 and SST3). Furthermore, water level was registered automatically every 15 min and subsequently converted into water discharge values.

Snowmelt 2014. 8-9, 26-29 May

Two sampling campaigns were developed during the snowmelt of 2014 (Figure 83). The snowmelt started the last days of April, and finished the 30th of May. The main factor inducing the snowmelt was the temperature. The mean daily temperature presented high values since 23rd April, minimum values were above zero and the weather was sunny. The consecution of 2-3 days showing these conditions brought the beginning of the melting and hence the rising of the water discharge and the mobilization of the fine sediments. Some rainfall events took place during the snowmelt, generating a mixed event.

The first sampling campaign was developed during 8th and 9th May, in the first days of the snowmelt. The second sampling campaign took place from 26th to 29th of that month.

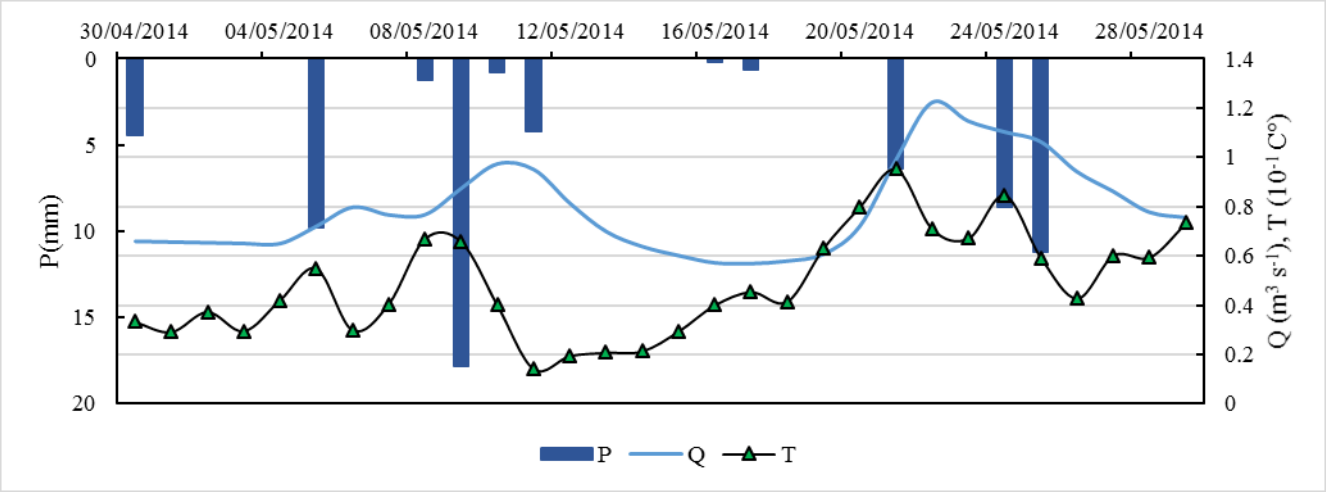

Figure 83: Daily values of rainfall, mean water discharge and mean temperature from 2014 snowmelt.

Development of the snowmelt during 8-9th May

The sampling campaign took 24 hours, from 8th May at noon until the consecutive noon. Weather was sunny during those days and therefore water discharge values raised during the light hours and showed a slight diminution during the night due to the low temperatures. Superficial runoff had its origin only in the snowmelt process, because no rainfall was verified during the field works. No precipitation was registered during the previous days either. Hence, two components were taken into account when assessing the hydrograph separation: water from the underground and water from the thawing. Conductivity of the water was used as a tracer.

Figure 84: Snowmelt at the medium part of the catchment the 9th of May 2014.

Thawing processes had likely started some days before this sampling campaign; nonetheless, snowmelt was at its presumable beginnings (Figure 84), with freezing and thawing cycles due to the temperature changes through the day. Contribution of the new water (water from snowmelt) was higher during the sunny hours in both SST1 and SST3, and hence the total water discharge was higher than that from the night hours. This trend was more remarkable in the SST1. Still, the fraction of Qn (new water) was very low, because the snowmelt was at its very beginning and the thawing processes were taking place slowly. The mean contribution of the snowmelt during the 24 hours of sampling was 2.16% in SST1 and 4.47% in SST3, and the maximum fractions were of 4.27% and 6.92% respectively. The SST3 subcatchment shows several zones that, because of their southwest exposition and their lack of trees, are the first in losing the snow cover. Instead, the forested areas of the catchment are all located between SST1 and SST3, and their shadow slows down the melting process. This is the reason why new water contribution was higher in SST3, nonetheless the higher altitude. The rapid rising of the water discharge in SST3 during the sunny hours of 8th is probably due to the quick melting of the snow cover of some area close to the channel.

Water discharge ranged from 0.67 m^3 s^{-1} to 0.785 m^3 s^{-1} in SST1 (Fig. 85). The maximum value was registered the first day of sampling at 19:00. After this peak, discharge decreased due to the falling temperatures during nigh hours, and raised again the day after due to the sunny weather. In SST3 (Fig. 87), the rising was more evident, because discharge raised from 0.15 m^3 s^{-1} to 0.446 m^3 s^{-1} at 17:45 of the first day of sampling. After this peak, values diminished perceptibly. The contribution of SST3 sub basin to the total water discharge ranged between 22.4% and 58.6%. The maximum fraction of water from SST3 sub basin corresponded to the water discharge peak at SST3 section.

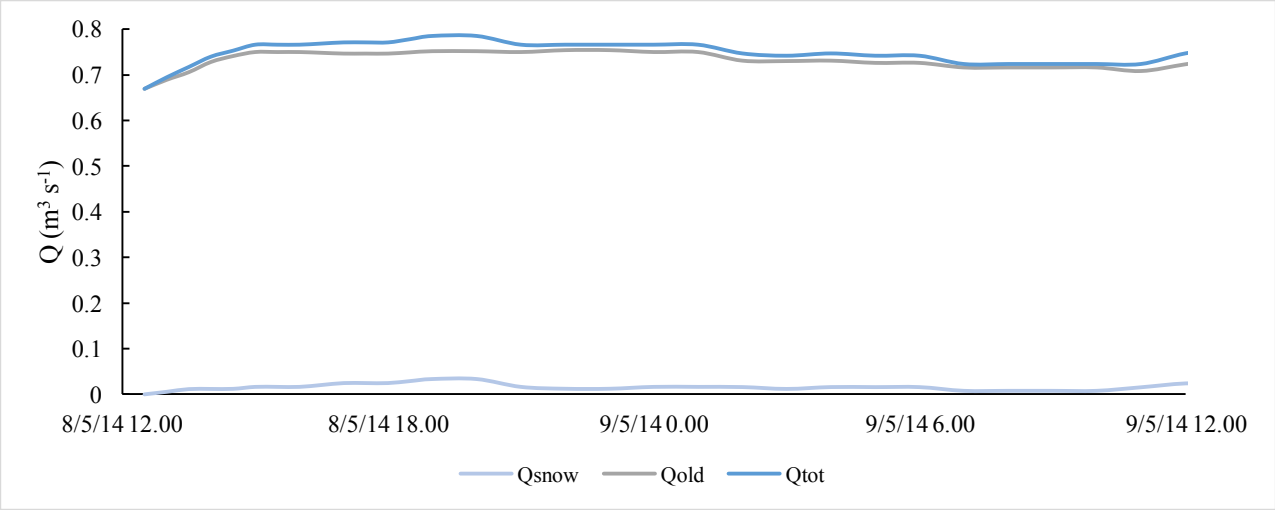

Figure 85: Hydrograph separation in SST1 in the first sampling campaign of May 2014.

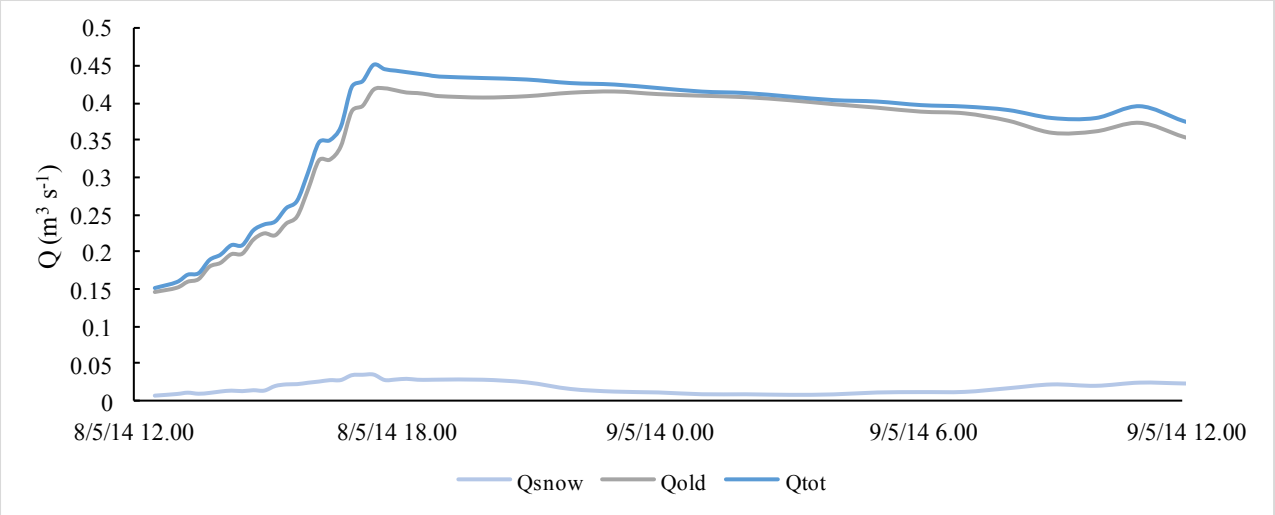

Figure 86: Hydrograph separation in SST3 in the first sampling campaign of May 2014.

The fact that the snowmelt processes were just starting is also revealed by the quantity of material mobilized. In fact, suspended sediment concentration values were quite low. The sedigraph showed several peaks, but ranged among quite low values during the whole field campaign (Fig. 87 and 88). The sequence of several low-value SSC peaks in both SST1 and SST3 leads to infer that the sediment sources were spread and material arrived from different areas. No significant sediment source was active during this event. The maximum value registered was 0.148 g l^{-1} in SST1, the 9th at 10:00 a.m., and 0.043 g l^{-1} in SST3, the 8th at 14:30 p.m. The total load during this 24 hour campaign was 4.48 t of suspended sediments. The load from the SST3 subcatchment was only 0.32 t, which represents the 7%

of the total suspended load. Bearing in mind that water contribution from SST3 subcatchment was up to 58.6%, differences between the upper and the lower part of the catchment turn out to be significantly marked: the catchment area downstream SST3 contributed 41.4% of the water volumes, but 93% of the solid budget. Therefore, the major suspended sediment budget came from sources located between SST1 and SST3 and no sediment source from the upper part of the catchment contributed significantly during these days of sampling.

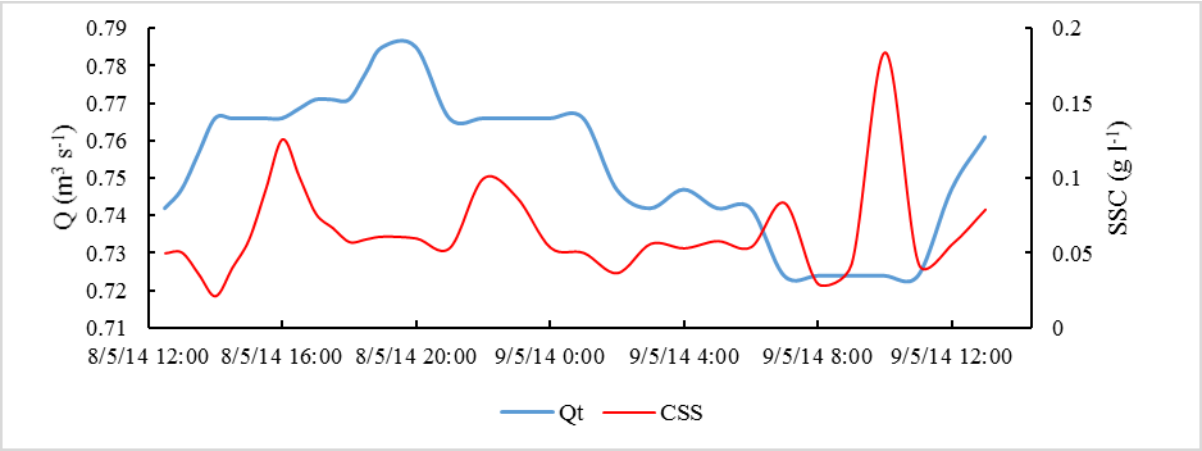

Figure 87: Hydrograph and sedigraph at SST1 during the first sampling campaign of May 2014.

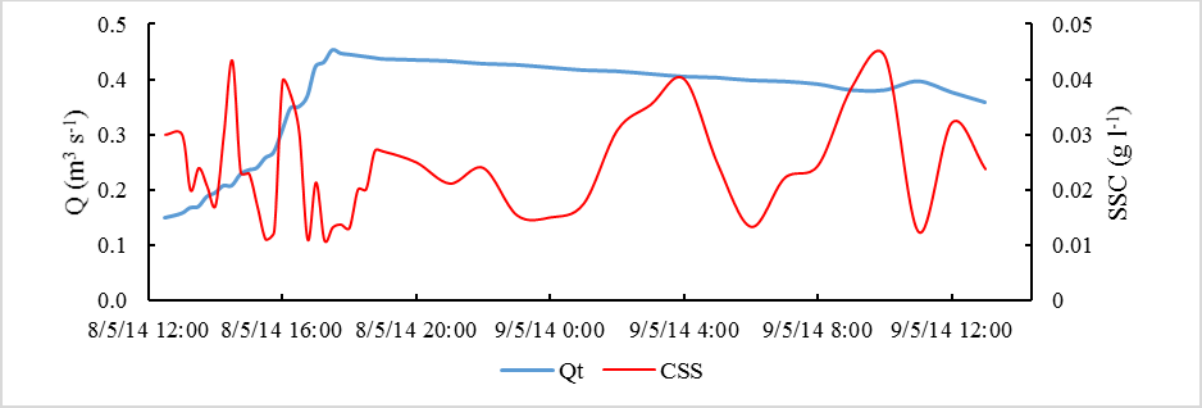

Figure 88: Hydrograph and sedigraph at SST3 during the first sampling campaign of May 2014.

Development of the snowmelt during 26-29th May

The second sampling campaign took place during the last days of the snowmelt. Snow cover was much diminished the first day of the field work (26th) and almost inexistent during the last day of sampling. During the first day of sampling, 8.6 mm of rainfall were registered. The 27th May precipitations were

equal to 11.2 mm. The mean intensity value during these 2 days of rains was 0.4 mm. The maximum intensity was equal to 3.4 mm. This low but continued rainfall during the 26th and 27th May contributed to the quick melting of the last remaining of snow. Because snowmelt was at its endings, hydrograph showed a continuous decreasing during those days. Runoff was induced by both rainfall and snowmelt, so the hydrograph separation was constructed by considering three components: old water (underground), new water from rainfall and new water from snowmelt. Once again, conductivity was used as tracer.

Figure 89: Medium part of the catchment the 27 of May 2014, at the end of the snowmelt.

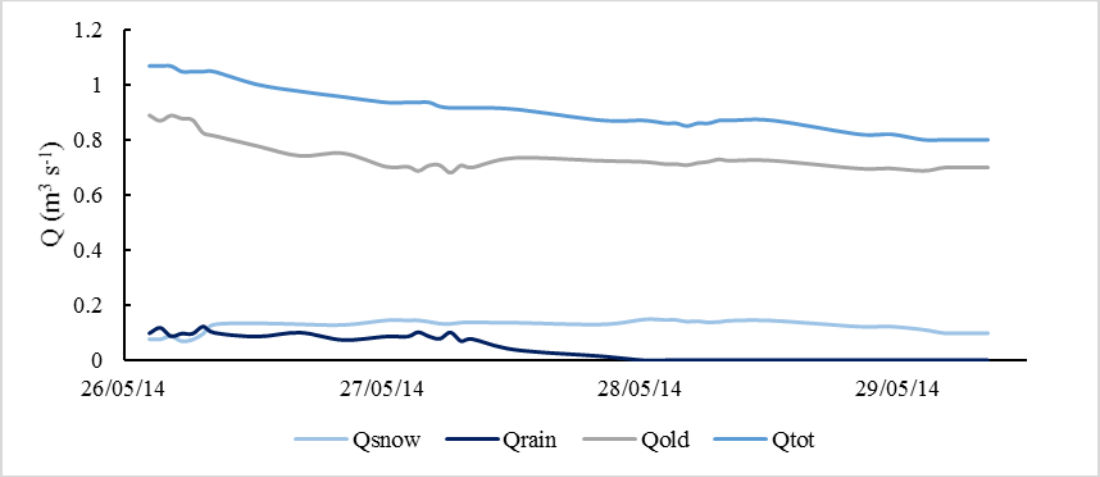

Figure 90: Hydrograph separation in SST1 in the second sampling campaign of May 2014.

The hydrograph separation of the water discharge registered in both SST1 and SST3 sections permits to understand the contribution of melting and rainfall to the surface runoff during the last days of this snowmelt (Figures 90, 91). In SST1, Q from rainfall contributed a maximum of 12.12% at 16:00 of the 27th of May, close to the moment in which rainfall registered its major intensity. The mean contribution

of precipitation during the rainfall hours was 9.14%. The mean contribution of snowmelt during the whole field campaign was 10.85%, with a maximum fraction of 21.35% at 10:00 of the 27th. Underground contribution increased during the 28th, probably due to the infiltration of the water resulting from the mixing of rainfall and the melting of the remaining snow cover.

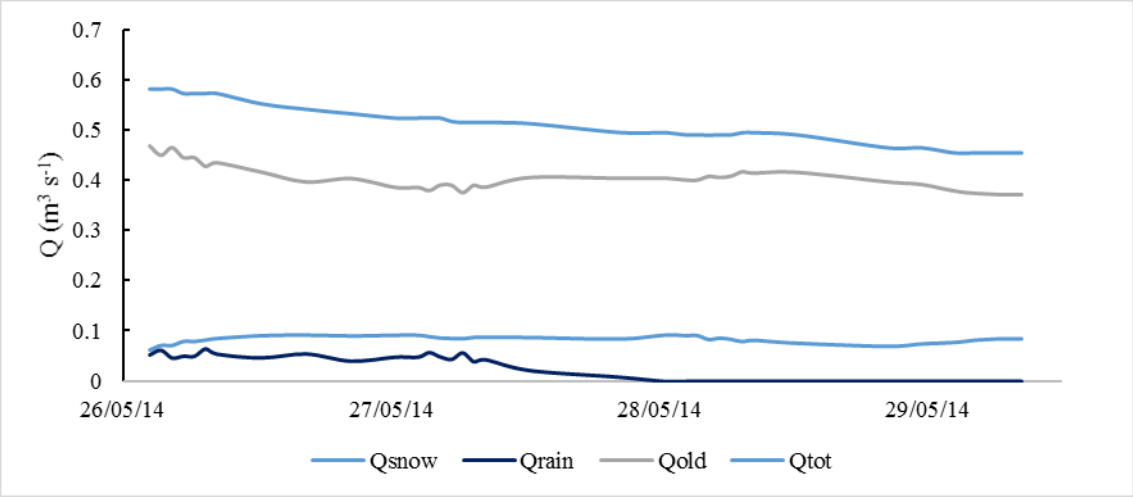

Figure 91: Hydrograph separation in SST3 in the second sampling campaign of May 2014.

In SST3, rainfall contributed in a lower percentage. Its major contribution, at the same time as in SST1, was of 6.19%, and its mean contribution was 4.84%, a bit lower than the fraction in SST1. On the other hand, the snowmelt contribution was higher than in SST1, due to the snow supply of some permanent shadowed areas that were still covered by snow and that lost their snow cover due to the continuous precipitation of the 26th and the 27th. Also in this section, the underground contribution increased during the second half of the campaign, still in a lower percentage than in SST1. Total water discharge was at the falling limb of the general snowmelt hydrograph. In SST1, values ranged between 1.07 m^3s^{-1} and 0.8 m^3 s^{-1}. This parameter was decreasing because of the end of the snowmelt: the availability of the water from thawing processes was ending. The falling limb of the hydrograph would have shown a more marked fall were it not for the rain, which buffered this tendency. The contribution of the SST3 subcatchment to the total water discharge ranged between 54.4% and 57.6%. The maximum fraction from SST3 was registered the 28th during the afternoon, that is to say, when no rainfall was taking place and the major fraction of the in-channel water was from the underground.

It is noticeable that the gentle slope of the falling limb is due to the rainfall registered. Without the precipitations that took place in de catchment during the first days of field works, the water discharge would have diminished much faster, because snowmelt process was at its very endings.

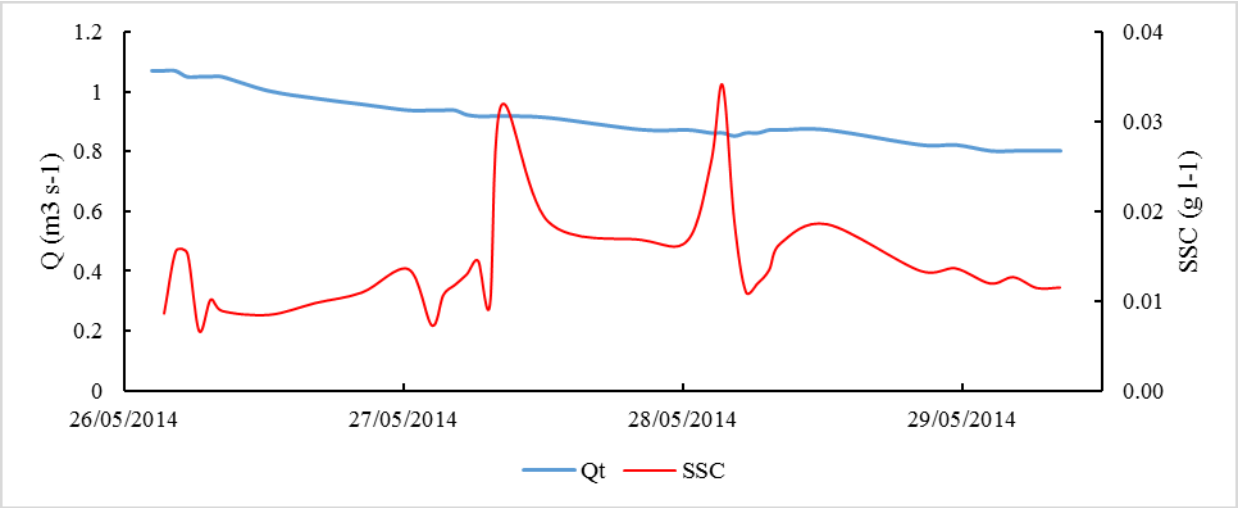

Figure 92: Hydrograph and sedigraph at SST1 during the second sampling campaign of May 2014.

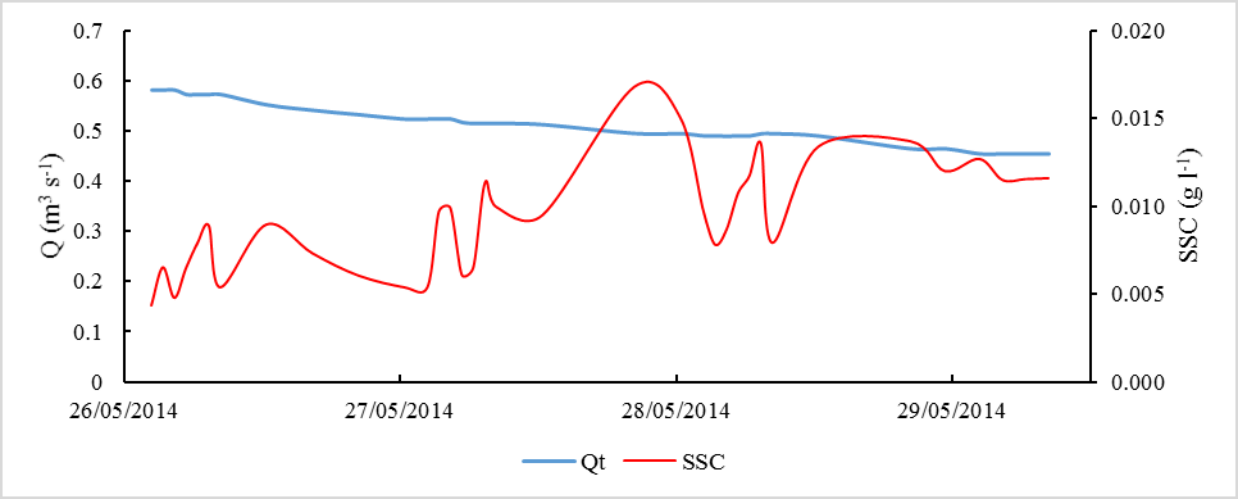

Figure 93: Hydrograph and sedigraph at SST3 during the second sampling campaign of May 2014.

Suspended sediment transport was quite low during this field campaign. Registered maximum values for SST1 and SST3 were 0.034 g l^{-1} and 0.017 g l^{-1} respectively (Figure 92 and 93). The total suspended load was 3.72 t, a quite low value considering that it was the end of the snowmelt mixed with a rainfall event. The load generated upstream the SST3 was 1.44 t, the 38.71% of the total load, a higher fraction than that registered during the first days of snowmelt. This solid fraction coming from the SST3 subcatchment is in concordance with the water discharge fraction.

Because fieldwork did not cover the whole snowmelt period, suspended sediment concentration data is missing. Hence, it was not possible to construct the whole hysteresis cycle for the 2014 snowmelt.

Snowmelt from 2014 was a quite extended process, considering the fact that started around 25th April and finished the last days of May. Usually, snowmelt process takes around 2 weeks in this catchment. Longer snowmelts are rare. The reason of this long duration was mainly the temperature. The sensors registered a maximum daily temperature of 9.5°C, and maximum hourly temperatures were always below 15°C. Besides, values below 0 during night were common. A quick rising of the temperatures, much common at the beginning of the spring in this part of the Alps, was lacking this year. Consequently, the snow cover melted slowly. Snow from the lower part of the basin turned into liquid volumes in the first days of the snowmelt event, whilst in the upper part the snow showed slow melting processes, characterized by an heterogeneous temporal and spatial distribution. Both campaigns corroborate this: snow contribution to the total water discharge was higher in SST1 during the first campaign, developed during the first days of snowmelt. Instead, during the second campaign SST3 featured a higher snow contribution. Because the slow melting velocities, this event did not transport a noticeable quantity of material. In fact, water showed low turbidity values during the fieldwork. It is presumable that suspended solids concentration remained low for the whole snowmelt period, apart from the beginning and the end of the process. Unfortunately, automatic recording of turbidity values did not work during this period, so only data from the field campaigns is available. Even so, results from these two field campaigns confirm what established in the previous analysis: the hydrograph separation and the differences in the liquid and solid contributions between SST3 subcatchment and the total catchment area support that runoff volumes are not the main factor affecting transport rates.

Rainfall event from May 2015

Sampling campaign was carried out from 14th to 16th May 2015, due to a small rainfall event that took place in the catchment area (Figure 94). This year, snowmelt was practically inexistent, due to the thin snowpack created during the winter months. Besides, the melting process took place slowly, and hence the water level of the main channel did not show a considerable increase. Therefore, we can consider that 2015 was characterized by a non-significant snowmelt.

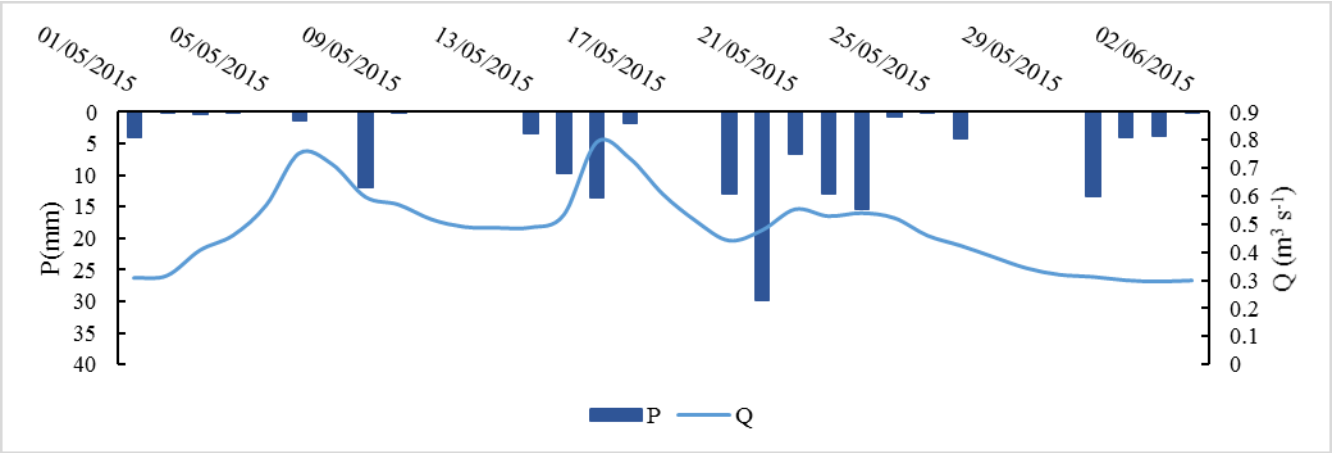

Figure 94: Hydrograph and pluviograph during May 2015.

The 14th of May, snow cover was missing all over the catchment area. The only residuals of snow can be considered insignificant, and hence the precipitation registered during that day and the following did not mix with any snowmelt. The total rainfall was around 25 mm, starting the 14th around 21:00, and it induced an increase of the water discharge from 0.475 $m^3 s^{-1}$ to 0.915 $m^3 s^{-1}$ at 11 a.m. of the 15th. The pluviographs from the catchment registered 9.6 mm from 20:00 to 23:59 of the 14th, 13,5 mm along the 15th and only 1,8 mm during the 16th. Two peaks of water discharge were registered before the maximum value, as showed in the hydrograph from SST1.

Figure 95: View of the upper part of the catchment from SST3, 14th May 2015.

The hydrograph separation of the water discharge registered in both SST1 and SST3 sections permits to understand the contribution of rainfall to the surface runoff during this event (Figures 96 and 97). The tracer used was the conductivity of the water. The only inputs were the water from rainfall and the underground water, so a two-component separation was performed. Water from rainfall (new water) mean contribution was around 7.77% in the downstream sampling station (SST1), whilst this value was lower in the SST3: 4.87% of new water mean contribution was registered in this section. Maximum

fractions of new water were registered at 21:00 of the 14th in both sections, coinciding with the maximum rainfall intensity. In this moment, rainfall contribution was 7.77% for SST1 and 9.68% for SST3.

Water discharge ranged between 0.47 and 0.83 m^3 s^{-1} in SST1. This parameter registered three consecutive peaks of 0.67, 0.71 and 0.83 m^3 s^{-1}, respectively. The evolution of the water discharge in SST3 was different, ranging between 0.35 and 0.45 m^3 s^{-1}. A small first peak (0.385 m^3 s^{-1}) matched with the first peak at the SST1, but the maximum value was registered during the falling limb of SST1 hydrograph. Water contribution from the SST3 subcatchment ranged between 41.9% and 80.0% to the total water discharge measured at SST1. This fraction was greater during the first hours of the event, and diminished through the event.

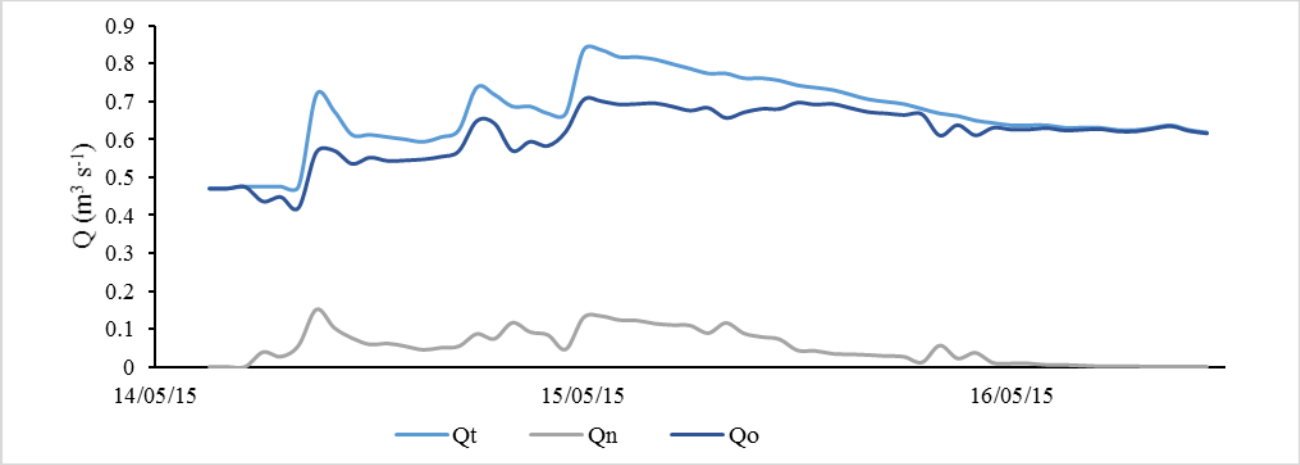

Figure 96: Hydrograph separation in SST1 during the sampling campaign of May 2015.

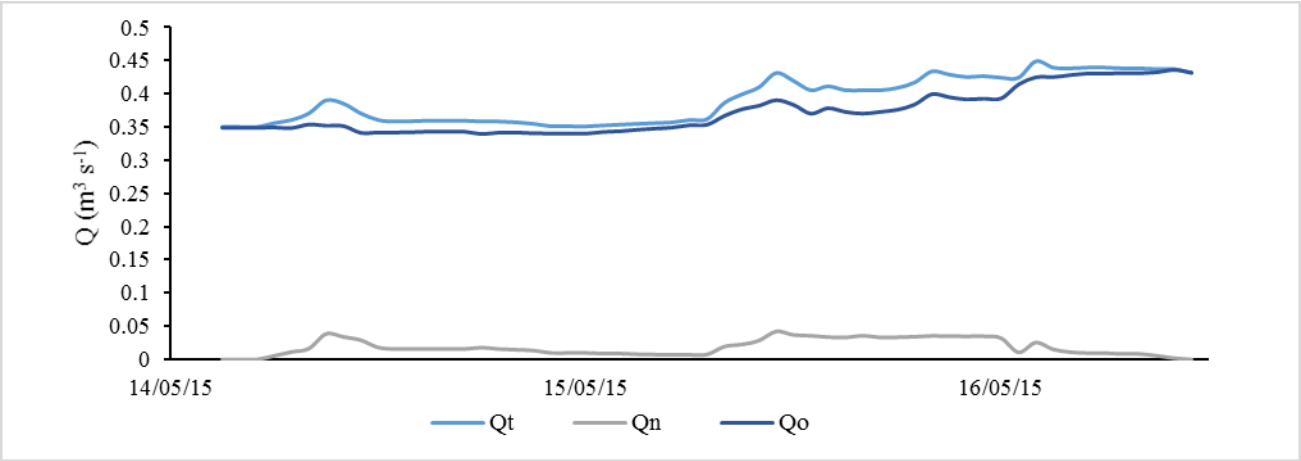

Figure 97: Hydrograph separation in SST3 during the sampling campaign of May 2015.

The evolution of the sedigraph was also different in SST1 and SST3. Whilst in SST1 the maximum value was registered at the beginning of the event, in the upstream sampling station the sediment concentration peak arrived more than 12 hours after the beginning.

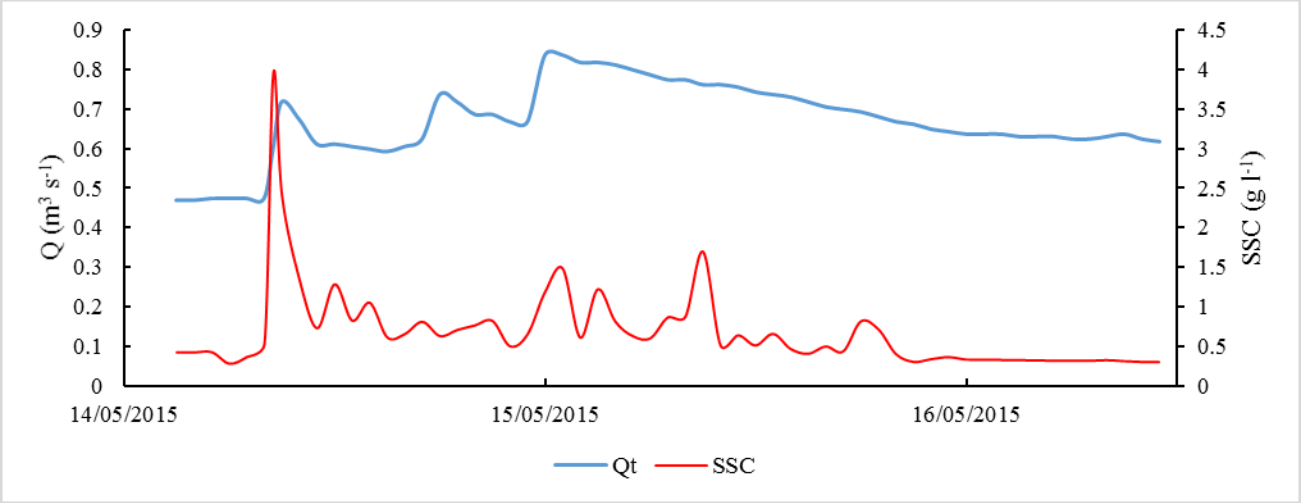

Figure 98: Hydrograph and sedigraph at SST1 during the sampling campaign of May 2015.

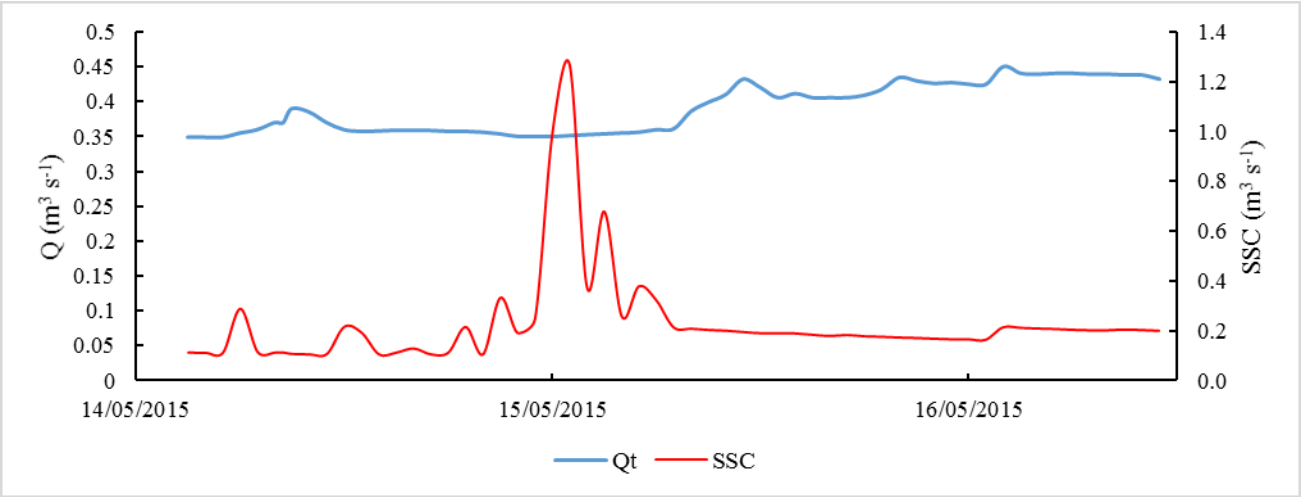

Figure 99: Hydrograph and sedigraph at SST3 during the sampling campaign of May 2015.

Suspended sediment transport was not as low as in the previous field campaigns. Registered maximum values for SST1 and SST3 were 3.94 g l^{-1} and 1.23 g l^{-1} respectively (Figures 98 and 99), and the total suspended load was 8.78 t, a remarkable value considering that the event took less than 48 hours in total and that the maximum water discharge was much below the bankfull discharge. The load generated upstream the SST3 was 1.31 t, the 18.17% of the total suspended load. No bedload transport was registered during this event.

Hysteresis cycles were assessed with the values registered in both sections. Both cycles showed clockwise behaviors (Fig. 100), indicating a short distance between the sections and their respective sediment sources.

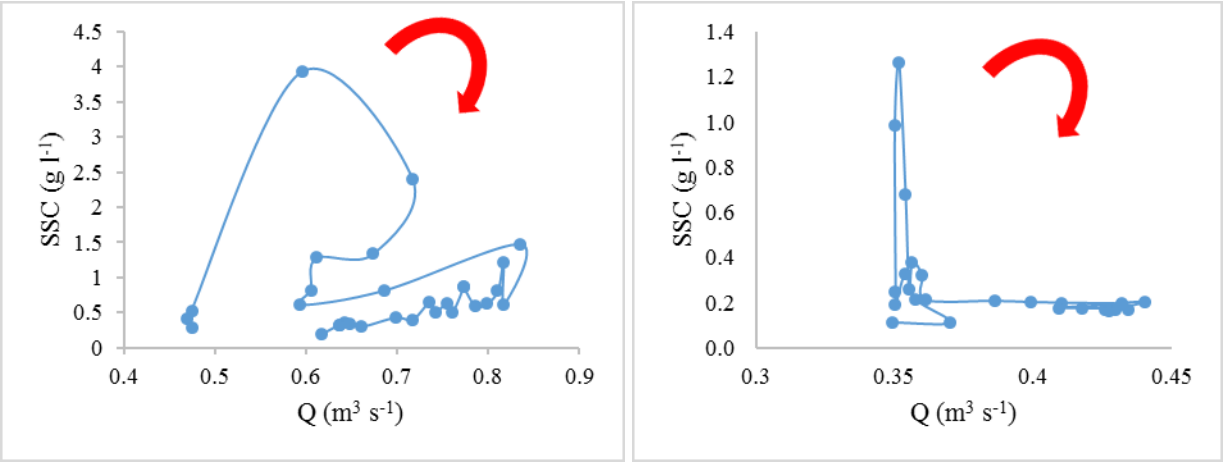

Figure 100: Hysteresis cycles registered in SST1 (a) and SST3 (b) during the campaign of May 2015.

It is noticeable that during this event a different response to the rainfall was found in SST1 and SST3. Whilst in SST1 the water discharge showed a clear response to different rainfall peaks, in SST3 it is not possible to identify different discharge peaks corresponding to the rainfall incomes. The reason of this might be the closeness to the snowmelt period. Despite of the thin snowpack characterizing 2015 winter and hence the low quantities of water inputs from snowmelt processes during 2015 spring, the soil featured still high moisture values due to the recent infiltration of water volumes coming from snowmelt. Results suggest that moisture content was heterogeneous in the basin area: the upper part featured drier soils in the areas that are more exposed to the sunlight and the wind. SST3 subcatchment did not show such a clear response to rainfall input as the lower area of SST1 catchment, and the proportion of new water was higher in the SST1 section. This, together with the higher suspended loads registered in SST1, suggest that the suspended sediment transport had its origin mainly in surface runoff of the rainfall water.

Rainfall event from October 2015

The intense rainfall of the 13th and 14th of October 2015 led in a small event in the Rio Cordon (Figure 101). Total precipitation was 78.4 mm, distributed among the 13th and the 16th. Water discharge values were quite low before the beginning of the rainfall event, because of the dry period registered in the previous weeks. Still, water discharge showed an initial value of 0,193 m^3 s^{-1} the day before the sampling, and reached 0,544 m^3 s^{-1}, which is an important increase, even if the hydrograph rising was not very steep and the maximum value is not high. In fact, a discrete but considerable suspended load was mobilized downstream during this event.

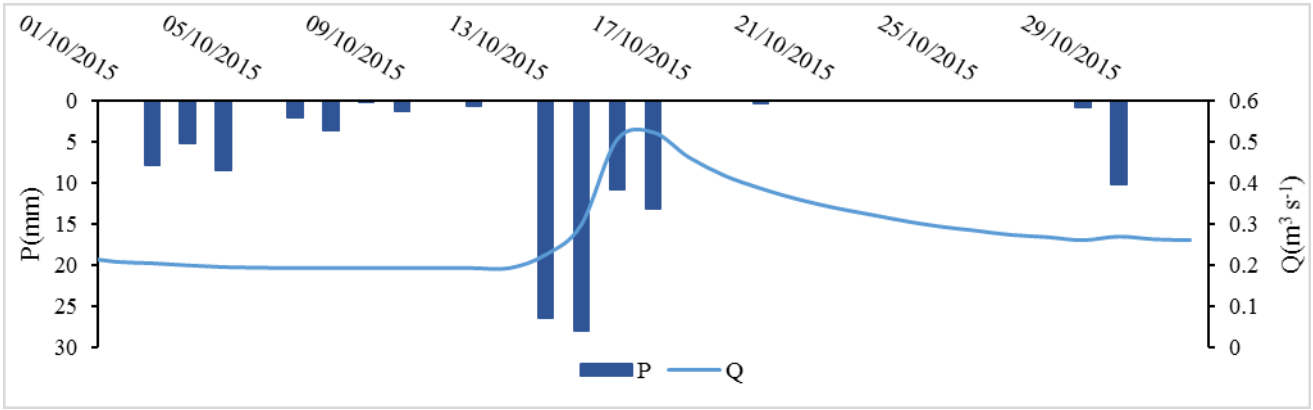

Figure 101: Hydrograph and pluviograph during October 2015.

Figure 102: The main channel at its medium reach the October 14th, 2015.

Rain was already falling since the previous day when the field campaign started. More than 26 mm fell during the last hours of the 13th, 28 mm were registered during the 14th, and the rest was distributed homogeneously among the 15th and the first hours of the 16th. The hydrograph separation of the water discharge registered in both SST1 and SST3 sections was used to assess the contribution of rainfall to the superficial runoff during this event (Figures 103 and 104). Conductivity was used as a tracer. The main hydrograph rising took place between the last hours of the 14th and the first hours of the following day in the outlet of the catchment (SST1). Here, the water discharge increased 81.9% its initial value, whereas in SST3 the hydrograph showed more homogeneity and the increase was of 28.9 %.

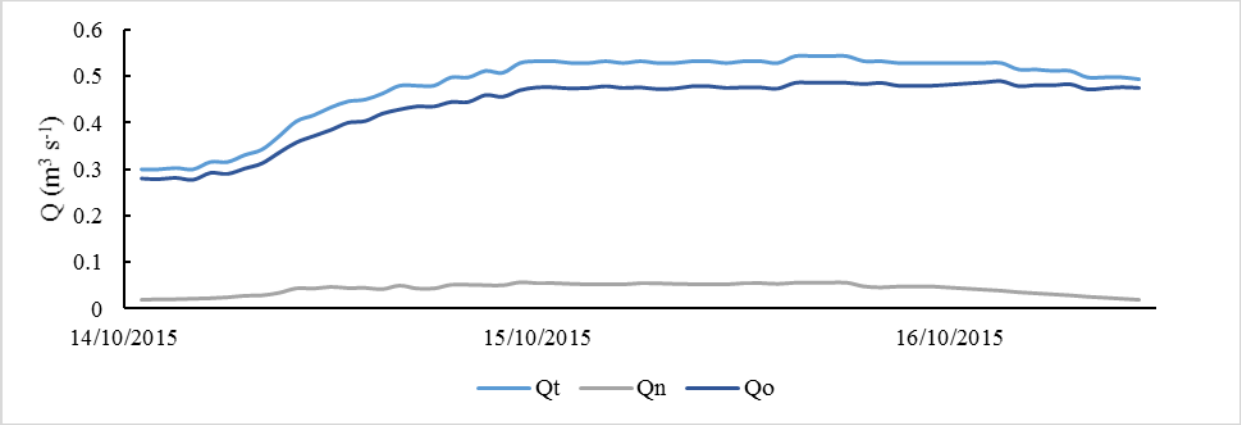

Figure 103: Hydrograph separation in SST1 during the sampling campaign of October 2015.

The mean contribution of new water to the main channel water discharge was of 8.84% in the SST1. The maximum fraction of water from rainfall registered during the field campaign was 10.92%. The contribution of rainfall water to the water discharge was lower in SST3. Here, the Qn mean fraction was 6.77%, while the maximum fraction was 10.33%.

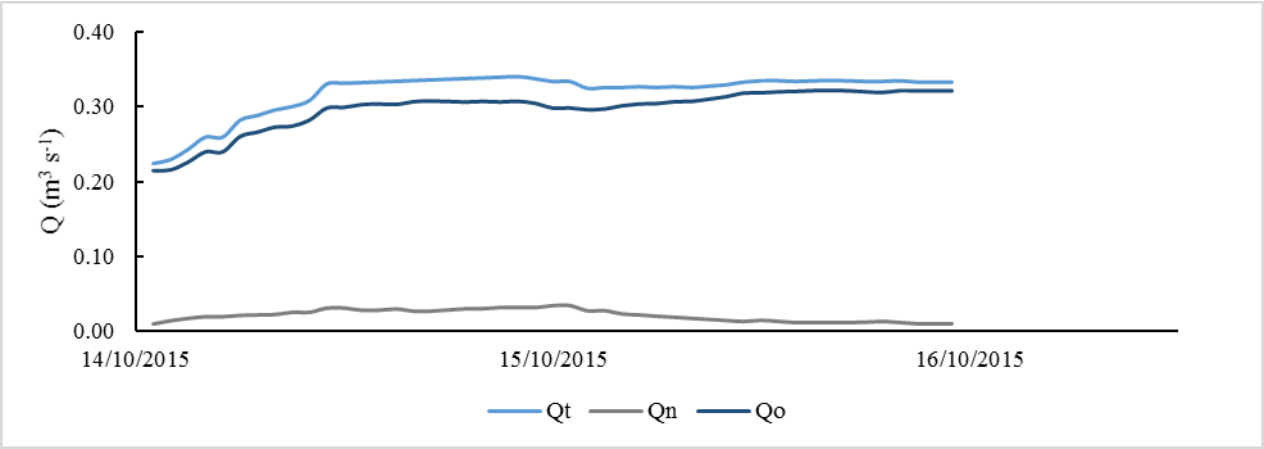

Figure 104: Hydrograph separation in SST3 during the sampling campaign of October 2015.

The water volumes that had their origin in the SST3 subcatchment were considerable. In fact, the fraction of water volumes from SST3 present at the SST1 section ranged between 89.4% and 60.9%. The mean contribution was 68.6%.

The evolution of the sedigraph was different in SST1 and SST3 (Figures 105 and 106). The maximum value of suspended sediment concentration registered was 4.32 g l^{-1} in SST1 and 0.515 g l^{-1} in SST3. During this event, 8.27 t of fine sediment were mobilized towards the outlet. In the SST3, 1.52 t were registered, so 18.41% of the total load was contributed by the SST3 subcatchment. These loads can be considered high, if we keep in mind that the water discharge did not show particularly high levels.

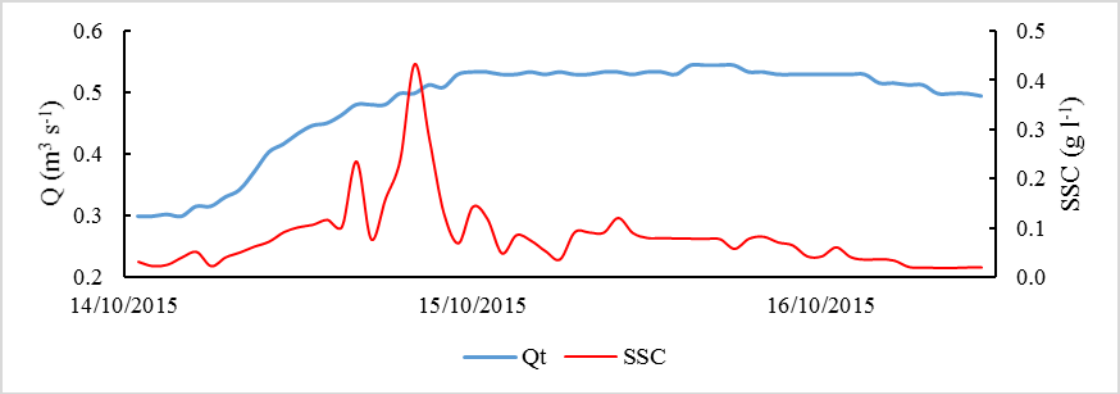

Figure 105: Hydrograph and sedigraph at SST1 during the sampling campaign of October 2015.

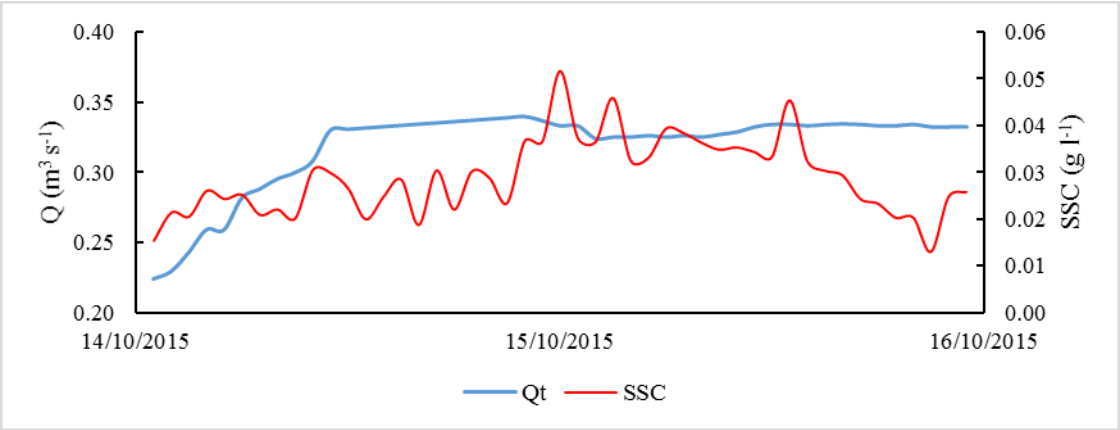

Figure 106: Hydrograph and sedigraph at SST3 during the sampling campaign of October 2015.

Hysteresis between Q and SSC values during the hours of the field campaign has been studied in both sections (Figure 107). In SST1, water discharge and suspended sediment concentration describe a clockwise loop, due to the highest peak of SSC arriving 19 hours before the highest value of Q. besides, the first SSC rising, that shows a maximum of 0.23 g l^{-1}, suggests that a resuspension process took place in the main channel during this event. The several peaks registered in the SST3 make the hysteresis loop between the two variables too complicated to be classified.

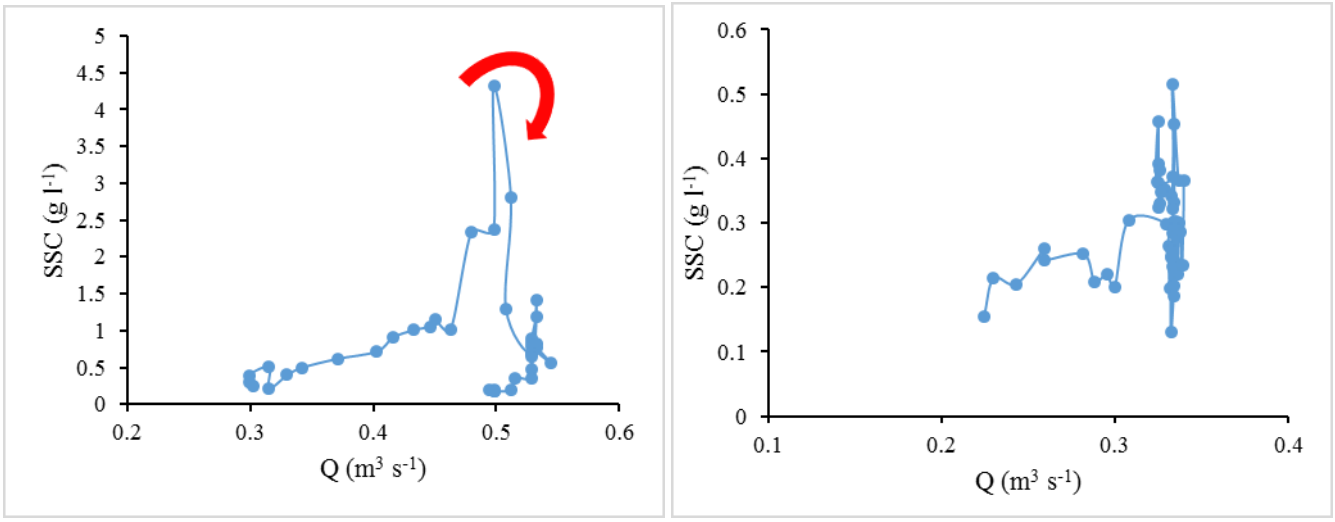

Figure 107: Hysteresis cycles registered in SST1 (a) and SST3 (b) during the campaign of October 2015.

The hydrological year 2015 was a quite dry year with low soil moisture content, specially in the upper part of the catchment. It is important to remember that upper areas of the Rio Cordon catchment are more exposed to the sun and the wind. Moreover, they do not feature trees or shrubs, but alpine

grasslands and bare lands. Because of these reasons, after the previous dry weeks, the upper part of the basin featured a drier soil than the lower part and its response to the rainfall inputs was minor than the response registered in SST1. This fact is reflected in the hydrograph separations from both sections. Because 2015 had featured only low intensity events that generated low volumes of surface runoff, the available fine sediments present in the sediment source areas of the catchment had not been washed downstream yet. Besides, the low water discharge values from the previous rainfall events probably induced the deposition of fine sediments on the channel bed. This material, with the rising of the discharge during this event, might have suffered a resuspension, as the first SSC peak of the sedigraph from Figure 106 suggests. For this reasons, the October event featured a considerable suspended sediment load respect to the previous events studied, even if water discharge did not show particularly high values.

4. CHAPTER FOUR- DISCUSSION

4.1. Thirty years of suspended sediment fluxes

Suspended sediment load and bedload were assessed for every year of the study period. The total sediment load of the three decades is 15100 t, of which 79% is fine material. Suspended sediment loads are more likely to exceed bedloads in unstable streams (Barsch et al. 1994). Still, sediment budget is not homogeneously distributed in time: both bedload and suspended sediment supplies are diminishing in the Rio Cordon, yet the suspended sediment fraction increased in the latest fifteen years. The observed suspended sediment fraction contribution results markedly higher than the predicted fractions calculated using the equations that predict the long-term SS fraction as a function of the catchment area proposed by Schlunegger and Hinderer (2003) and Turowski et al. (2010).

The first half of the study period registered higher mean annual suspendetd budget than the second. From 1986 to 1993, there was a slight diminishing trend of the suspended sediment supply, but in September 1994 the extraordinary rainfall event destroyed the bed armor layer and altered the channel bed morphology. The following years showed high values of annual suspended budget because of the high availability that this event generated. In 2001, the mud flow generated unlimited availability conditions that affected the dynamics of the following year. After 2002, the catchment showed a marked diminishing trend. Results suggest that this trend is not induced by a lower quantity of precipitation volumes (snow or rainfall) arriving to the catchment, because analyses show that runoff volumes did not change much from one year to another. The reason of the diminishing trend of the catchment is the depletion of the sediment sources and the armouring process affecting the streambed, which have been highlighted by previous works in the catchment (Lenzi, 2001; Mao, 2004; Rainato et al., 2016). It is also noticeable that the last decade of the study period lacked flood events shownt intensity enough to activate new source areas or reactivate the old ones. A high intensity flood event would probably increase the sediment availability of the catchment by the activation of the sediment sources and/or the breaking of the bed armour, but water discharge values have not gone beyond the bankfull value in the last 15 years. Therefore, the armoring processes affecting the channel bed are stronger year after year and the catchment does not feature the activation of new sediment sources. As a consequence, during the latest years the basin area was characterized by lower sediment supply than the 1994-2001 period.

Substantial differences in the annual behavior are observed among the years of the study period. The analysis of the seasonal suspended budget showed that the temporal variability of the sediment transport often leads into a heterogeneous contribution of the seasons in the annual suspended load. In fact, years with a marked prevalence of one season over the others are quite common, while years showing a homogeneous seasonal contribution are quite rare. This result is in line with the seasonal variability in the suspended sediment concentration found in previous studies in mountainous water courses (Collins, 1990; Bogen, 1995). The major contributors during the 1986-2000 period were summer or autumn, and the mean snowmelt contribution to the total suspended sediment load was 36%. Before 1994, summer contribution clearly prevailed, yet with marked differences between years. After the September 1994 flood, autumn budget was the major contribution for most of the years. A particularly high snowmelt budget was observed in 2001, due to the mud flow that released a large amount of sediment available for the subsequent floods (autumn 2002). After this, snowmelt has been the major suspended sediment load contributor in most of the years, with a mean snowmelt fraction of 58%. Nonetheless, the snowmelt budgets have not increased markedly in the last years.

In order to understand the annual dynamics, years were divided according to the shape described by the seasonal increase of sediment loads and water volumes. The years in which autumn is the major contributor are 1994, 1996, 1998, 1999 and 2000, and can be identified by their downward triangle shape. The years showing a marked higher summer contribution, characterized by an eight-shaped curve, are 1986, 1987, 1989, 1991, 1995, 2004 and 2015. The years in which the major contributor is the snowmelt show an upward triangle shape, and are 1988, 1990, 1992, 1993, 1997, 2001, 2002, 2006, 2007, 2008, 2009, 2010, 2011, 2013 and 2014. The years 1999, 2003 and 2005 are difficult to classify because their seasonal contribution is more homogeneous and hence their shape tends to be linear. Still, this method of classification turns out to be suitable for assessing a general idea of the annual behavior, and highlights that snowmelt is the main suspended load contributor in the Rio Cordon catchment. In fact, snowmelt dominates the hydrological processes of the catchment (Lenzi et al., 2003), and this fact turns evident during the 2001-2015 period. Before 2001 the years showing higher loads from snowmelt events than from rainfall events were rare: from 1986 to 2000, only 5 years of 15 showed this behavior. This is because during this period some intense rainfall events contributed to the seasonal load enough to overcome the snowmelt suspended load. This situation changed noticeably after 2000: from 2001 to 2015, 10 years showed an upward triangle shape, thus indicating that snowmelt was the main suspended sediment contributor of the year, and the period showing the higher SSL/R proportion. It is

important to notice, though, that apart from 2001 the snowmelt suspended load showed values that were not much above the mean value of the three decades. This corroborates that the reason of the snowmelt SSL fraction slight increase of the latest 15 years is not an increasing of the snowmelt sediment loads, but a diminution in the rainfall events contribution to the total annual SSL.

4.2. Study of the single events

Most to-date works suggest that clockwise loops are the most common in medium and small-size catchments (Brasington & Richards, 2000; Lenzi and Marchi, 2000; Seeger et al., 2004; Smith and Dragovich, 2009). It has been highlighted a greater presence of clockwise events in the Rio Cordon, that is to say, events in which the SSC reaches its peak before the Qp and the sedigraph starts diminishing when the hydrograph is still at its rising limb. This result, combined with the brief Δt characterizing counter-clockwise events, lead into believe that the sediment sources that contribute to the suspended load in the Rio Cordon event are mainly close to the main channel, or located in the lower part of the basin. Besides, the decoupling created by the low gradient belt (Lenzi and Marchi, 2000; Cavalli, 2009) prevents the sediment originated in the upper part of the channel to arrive to the lower reach of the channel and hence limits the number of counter-clockwise loops. The results from this analysis support what stated by other authors for the first 15 years of monitoring in the Rio Cordon (Lenzi and Marchi, 2000; Mao, 2004). The 4 snowmelt events had clockwise hysteresis probably because usually the lower part of the basin starts the thawing processes earlier, because it is exposed to higher temperatures. As sediment sources are located in the lower part, they contribute to the main channel during the melting of the lower part of the basin (beginning of the snowmelt), and are depleted at the final steps of the snowmelt, when the runoff from the upper areas arrive. Results permit us to subdivide clockwise events occurred in Rio Cordon catchment in two groups. The first shows the typical response to ordinary, continuous rainfall or a quick snowmelt process, confirming what exposed by Brasington and Richards (2000) and Eder et al. (2010), among others. The second group shows atypical clockwise characteristics as a response to interrupted snowmelt or high initial rainfall intensity. Resuspension may explain the atypical hysteresis in those cases in which the sedigraph shows a small peak located at the very beginning of the event, followed by a higher peak.

A quick reduction of the SSC values after the peak accompanied by a especially slow diminution of the Q values along the falling limb characterizes some clockwise events due to the

dilution of the suspended sediment concentrations caused by an increased proportion of the baseflow on the falling limb of the hydrograph. It is confirmed that suspended sediment concentrations during baseflow do not change with the discharge and remain low (Lenzi & Marchi, 2000; Picco et al., 2012). Thus, very low suspended concentrations resulted not only from a reduction of the quantity of available sediment, but also from dilution of suspended sediment concentrations by the baseflow.

Most of the events (76.5%) showed an anticipation of the BSSC respect to the BQ. This result supports that usually the sediment sources are located in a precise area of the catchment. In the Rio Cordon, the sediment sources are unlikely spread all over the basin area. In those few cases in which the hysteresis behavior suggested a spread distribution of the source areas, the barycenter of the hydrograph preceded the barycenter of the sedigraph or arrived some few minutes after it (events 14, 18 and 28, among others).

Results from the single events analysis support what stated in the annual analysis: a clear diminution of the sediment availability is taking place in the catchment. This is in accordance with the studies on multitemporal analysis of the sediment sources in the catchment (Cavalli et al., 2016). The Rio Cordon presented this behavior since the beginning of its monitoring, but it is important to bear in mind that some high-intensity events occurred through the years, interrupting the trend. The presence of the extraordinary events in the data series highlights the non-uniformity of the studied period. The last extraordinary event was registered in 2001, and its effects lasted for the following two years. Since 2004, a slow diminishing trend of the sediment loads can be observed, thus proving the reduction of the sediment supply in the catchment. The extraordinary events mentioned above, which released new material from the sources activated during the event and increased the availability during the following years, acted as interrupters of this trend during the previous period (1986-2003). The analysis of the suspended sediment transport through the events of the last three decades has highlighted that the September 1994 event influenced on the sediment production of the following floods. This event created new source areas and activated old ones, inducing into a higher transport activity during the following period. In fact, the decade after this event shows different conditions than the pre-1994 years, and is also clearly different than the 2005-2015 decade, as the SSL/Ru ratios demonstrate. This effect is called “memory effect” (Hinderer et al., 2013; Rainato, 2016). After 2004, when the effects of the 1994 and 2001 events are not so present, the catchment leads into low availability conditions. The sediment loads of the latest years are lower even if some intense events have been registered, because the sediment supply influences suspended sediment transport in a stronger way than the stream energy

(Walling and Webb, 1987). The long-term effect of the extraordinary events might be the main reason why a strong heterogeneity in the relationship between runoff Ru and the sediment transport is found when taking into account the three decades of data.

In order to understand whether the results found in Rio Cordon catchment were due to its particular hydrogeological characteristics or could be extrapolated to different basins, a similar analysis was developed in a Mediterranean medium-sized catchment, the Carapelle. The comparison between the results from both catchments was an attempt to understand which dynamics of the Rio Cordon catchment could be expected in catchments showing different hydrogeological characteristics. The analysis of the hysteresis patterns described by the studied rainfall events highlights differences between catchments. While clockwise loops are the most common in the Rio Cordon, confirming what said in literature (Lenzi and Marchi, 2000; Smith and Dragovich, 2009; Eder et al., 2010), a higher proportion of counter-clockwise loops characterizes Carapelle catchment. . This is probably due to the presence of large sediment sources distant from the zone of major runoff production, related to hillslope areas covered with winter wheat (Abdelwahab et al., 2014). The main difference between catchments seems to have its origin in the size of the catchment area and the distribution of the sediment sources, sometimes located far from the monitoring station in the case of the Carapelle. Neither the circular nor the eight-shaped loops are sharply predominant in none of the basins, despite a moderate prevalence of circular loops was found in both cases. Eight-shaped loops are usually related to multi-peak pluviographs.

Rainfall conditions were analyzed in both catchments. In the Carapelle, results show that flow generation features large times of response to the rainfall due to the medium-large size of the catchment. Antecedent precipitations determine the initial conditions of the flood event in this catchment, despite they do not affect the flow and sediment transport dynamics. Differently, in the Rio Cordon catchment antecedent and initial conditions do not show a clear correlation with the initial conditions of the flood. Nonetheless, they have an influence in the event dynamics, due to the rapid response of the catchment induced by its small size. The way in which the rainfall intensity affects sediment transport is different for each catchment. In the Carapelle catchment, the erosion capacity of the rainfall suffers the attenuation effect due to the large size of the catchment area, confirming what stated by Zabaleta et al. (2007), whereas in the Cordon, the intensity of the precipitations influences markedly the suspended sediment mobility.

The delay or anticipation of the suspended sediment concentration peak with respect to the water discharge peak determines the type of hysteresis between these two variables and gives additional information about the sediment sources and their location (Lenzi and Marchi, 2000; Jansson, 2002; Mao, 2004; Zabaleta et al., 2007). In this work, the study of the mass centers (i.e. the barycenters) of the hydrograph and the sedigraph and their relationship with the temporal variables gives additional information with respect to the arrival time of the peaks and highlights similarities between catchments. Peaks between SSC and Q barycenters and peaks between SSCp and Qp are usually both positive or negative, indicating that loop direction is in concordance with the relative position of the solid and liquid mass. In the Carapelle catchment, the delay or the advance between the hydrograph and sedigraph is determined by the intensity of the event. An increase in the delay between the mass of the rain and the mass of sediment transported leads into a rising of the lag between SSC peak and Q peak, suggesting the presence of some attenuation effects on the sediment transfer dynamics. Similar dynamics can be found in the Rio Cordon, where the time lag between the barycenter of the sedigraph and the barycenter of the hydrograph is closely linked to the runoff volumes and the total precipitation during the event. Therefore, the intensity of the event establishes the delay or the advance between suspended sediments and flow in both catchments.

In the Rio Cordon catchment neither the loop direction nor the loop shape are explained by the main components of the PCA. This result highlights the high heterogeneity of the events, thus suggesting that it is unlikely that the activation of the sediment sources follows a particular pattern. In fact, the transport dynamics of this catchment are more unpredictable than the dynamics occurring in the Carapelle catchment. As mentioned before, the Carapelle catchment registers a higher proportion of counter-clockwise loops, usually characterized by low intensity and a significant the lag between solid concentration and water discharge. When this kind of event takes place in this catchment, heterogeneous rainfall distribution and the decupling effects in the flow generation play a key role in the differences between the hydrograph and sedigraph shapes. Clockwise events usually occur in this catchment only under high intensity rainfalls that induce the mobilization of solids stored in the channel, divergently to what exposed by Seeger et al. (2004). These events show always eight-shaped loops and a reduced lag between SSC and Q.

The common PCA supported that the main factors affecting suspended sediment transport are related to the flood properties and to the precipitation characteristics in both study cases. The location of the sediment sources, the decoupling and the lamination effects are the main factors affecting

hysteresis patterns in each study area. Main differences found in the responses of each catchment to the flood events can be explained by the catchment size and the temporal and spatial distribution of the precipitations.

4.3. Field monitored events

The study of the transport dynamics during the 2014 snowmelt and the rainfall events of May 2015 and October 2015 was developed monitoring the different variables in two different sections located in the main channel. Those events were ordinary events, with average water discharge values, and hence average behavior. Hydrograph separation in both sections permitted to study the origin of the in-channel water and understand some of the runoff generation dynamics. Alpine catchments feature rapid hydrological processes, caused by high hydraulic gradients and high flow velocities, and therefore the time of residence of the water in these areas is quite short (Laudon and Slaymaker, 1997). Still, mean old water contribution ranged between 86 and 97% during the monitored events in the Rio Cordon. The low new water contribution in all the studied events suggests that the suspended sediment transport is not mainly induced by only surface runoff. New water fraction in the event water was spatially heterogeneous during a single event. Different responses to the water input (snowmelt or rainfall) were found in SST1 and SST3. New water contribution to the hydrograph was greater in SST1 than in SST3 during the rainfall events, whilst during snowmelt SST3 featured greater new water percentages than SST1. This result suggests that the superficial soils from the SST3 subcatchment are more affected by dry periods. The antecedent moisture has a strong influence on the sediment transport patters (Seeger et al. 2004; Soler et al., 2008). In the Rio Cordon catchment area, soils do not show homogeneous water content. Due to the geomorphology, the geological and hydrological settings, the vegetation cover characteristics and the exposure, the soil moisture of the upper part of the basin shows lower values than the soil moisture of the lower part. Hence, when a rainfall event takes place after a dry period, water contribution from underground is higher in the lower part of the basin. Results from the snowmelt campaigns suggest that when soil moisture content is higher, this difference is less significant. Besides, SST3 contribution to the total water volumes during the rainfall events was greater than the contribution registered during snowmelt. Concretely, water fraction from the SST3 subcatchment was 41% and 56% during the first and second snowmelt campaigns, respectively, whilst it rose up to 60% and 68% during the first and second rainfall campaigns, respectively.

The assessment of the different suspended sediment loads and the Q-SSC hysteresis patterns of both sections helped to identify the areas that contributed to the total sediment budget of the

event. The campaigns of 2014 snowmelt revealed low sediment loads (4.48 and 3.72 t, respectively). During 2014 snowmelt, thawing took several weeks and hence runoff generation processes took place slowly. As a consequence, sediment mobilization was weak. The hysteresis between Q and SSC could not be assessed because we did not monitor the whole snowmelt process. During 2015 rainfall events, rainfall intensity played a key role in the sediment mobilization. Suspended sediment transport was higher than the previous: May event registered 8.78 t of total load, and 8.27 t were transported during the October event. In both cases, the Q-SSC hysteresis was clockwise shaped in SST1. In SST3, Q and SSC featured clockwise behavior during the May event, and did not show a particular pattern during the October event. These results support that the main sediment sources that contribute during single events are usually close to the main channel. Moreover, results show that runoff volumes are not the main factor explaining the suspended sediment loads. Higher water contribution from the SST3 subcatchment to the total volumes is not followed by a higher sediment load fraction from SST3. In fact, suspended sediment concentration usually shows low values in SST3 section, and the mean contribution from SST3 subcatchment to the total sediment load is only 20.6%. This result supports the decoupling generated by the low gradient belt located in the medium part of the catchment, highlighted by previous works (Mao, 2004; Cavalli, 2009). This decoupling limits the contribution from the SST3 subcatchment. Hence, most part of the suspended sediments that arrive to the outlet is generated in the contributing areas of the catchment located between SST3 and SST1. In this area, sediment transfer is not limited by decoupling, and the quantity of material transported to the main channel seems to be linked to the previous moisture conditions and the intensity of the event.

The field campaigns described here helped in the assessment of the factors determining the suspended sediment transport during ordinary floods. Hydrograph separation of the events are a valuable tool in understanding whether the origin of the suspended sediments is the same as the water origin.

5. CHAPTER FIVE- CONCLUSIONS AND FUTURE RESEARCH DIRECTIONS

This work studies the sediment transport occurred in the Rio Cordon catchment through the last three decades, focusing on the suspended sediment fluxes. For analyzing the transport dynamics, the analysis approaches both long- and short-term analysis. Results have permitted to understand more about the factors influencing the mobilization of the fine materials during single events and the interannual transport dynamics.

In three decades, 15100 t of sediments were registered, of which 79% was fine material and the rest was bedload. Still, this budget was not homogeneously distributed in time: both bedload and suspended sediment supplies show a diminishing trend in the Rio Cordon. Analyses show that this trend in the sediment load is not induced by a lower quantity of precipitation volumes (snow or rainfall) arriving to the catchment, because runoff volumes did not change much from one year to another. Besides, the study of the transport behavior through three decades also permits us to infer that higher volumes of runoff do not obligatory induce into a higher total transport. The main factor explaining the sediment supply diminishing trend is the depletion of the active sediment sources and the lack of flood events strong enough to activate new source areas or reactivate the old ones. A high intensity flood event would probably change this situation, but water discharge values have not gone beyond the bankfull value in the last 15 years. Therefore, the armoring processes affecting the channel bed are stronger year after year. As a consequence, during the latest years the basin area was characterized by lower sediment supply than the fisrt years of the study period. Suspended sediment load overcomes bedload every year of the study period. The reason is that bedload takes place in the catchment only under treshold flow conditions that can be observed when a flood event takes place, whilst suspended sediment transport can happen also when the channel network features lower water discharges. Therefore, suspended sediment transport takes place in the catchment with more frequency than bedload transport. The long-term partitioning obtained in the Rio Cordon exhibits the clear prevalence of the suspended sediment loads, with a contribution of 79% to the total load.

The analysis of the seasonal behavior through the three decades leads to observe that snowmelt is the main suspended load contributor in the Rio Cordon catchment. In fact, snowmelt dominates the hydrological processes of the catchment and this fact turns evident during the 2001-2015 period. During the first half of the study period, some intense rainfall events contributed to the seasonal load enough to overcome the snowmelt suspended load, but his situation changed noticeably after 2000: from 2001 to 2015, that snowmelt was the main suspended sediment contributor of the year, and the

period showing the higher SSL/R proportion. It is important to notice, though, that apart from 2001 the snowmelt suspended load showed values that were not much above the mean value of the three decades. The reason why snowmelt loads are higher than the summer and autumn loads during the second half of the study period is that less quantity of material is mobilized during the last two seasons of the year. Though runoff volumes have not decreased considerably enough to explain this, the temporal distribution of the rainfall during the events has changed in the last fifteen years, showing longer durations and lower rainfall intensity. In fact, the 2002-2015 period has been characterized by the absence of high intensity events. As a consequence, the activation of the sediment sources during rainfall event has been weak or localized in a very constrained area. Hence, no sediment availability was released for the next floods, thus affecting, in the medium-term, the total seasonal load during summer and autumn.

The analysis of the single flood events recorded through the three decades supported what proposed after the annual and seasonal analysis. The three decades were divided in three periods characterized by different sediment transport dynamics: The 1986-1993 period featured medium-low availability but some high water discharge events. The second period corresponds to the years between 1994 and 2001, in which high transport efficiency characterized the catchment thanks to the sediment supply released by the 1994 event. In other words, the years following September 1994 were affected by the memory effect of this event. The sources activated during this extraordinary event released the available material during the events occurring the following years until their depletion, in which the registered events started featuring low values of suspended sediment load. In fact, the 2002-2015 period is characterized by both low water discharges and low transport rates. Results suggest that, if a new high intensity event should arrive, the temporal decreasing trend of the sediment supply would break and the years after the event would be characterized by high transport rates. Rio Cordon catchment tends to the stability, and the transport dynamics are modified by high intensity events, which release new material from the sources activated during the event and increase the availability during the following years, interrupting the trend. The long-term effect of the extraordinary events is the key factor of the strong heterogeneity that characterizes the transport efficiency in the catchment. The sediment transport at the event scale is markedly affected by the runoff generation and the sediment supply conditions released by the previous events. The rainfall conditions of the previous days affect less markedly than the rainfall characteristics during the event. The intensity of the precipitations influences markedly the suspended sediment mobility, establishing the delay or the

advance between solid sediments and the flow. Despite of the differences between periods, it is possible to assess the location of the sediment sources, the decoupling and the small size of the catchment as the main factors affecting hysteresis. The clockwise loop prevailed through the whole study period (68% of the cases). The sediment sources that contributed to the suspended load were close to the main channel, or located in the lower part of the basin, in most of the studied events. Moreover, it was possible to establish that in most of the cases the sediment sources were located in a precise area of the catchment. The low gradient belt located in the medium part of the basin created a decoupling that prevented the sediment originated in the upper part of the channel to arrive to the lower reach of the channel during the three decades (with the exception of the extraordinary event of September 1994), and hence limited the number of counter-clockwise loops.

The comparison between the Rio Cordon and the Mediterranean catchment of the Carapelle torrent permitted to assess differences and similarities in the transport dynamics of both catchments. Contrary to the Rio Cordon, the events in the Carapelle catchment were usually characterized by low intensity flows and significant lags between water discharge and solid concentration. A higher proportion of counter-clockwise loops was registered (88%), due to the medium size of this catchment and the distribution of the sediment sources, sometimes located far from the monitoring station. Antecedent precipitations had greater influence in the transport dynamics in the Carapelle than in the Cordon. The common PCA suggested that the main factors affecting suspended sediment transport are related to the flood properties and to the precipitation characteristics in both catchments.

Field campaigns performed in the Rio Cordon catchment highlighted different responses to the water input at different reaches of the main channel. Because of the vegetation cover characteristics and the exposure, the soil moisture shows heterogeneous values within the catchment, especially after dry periods. When this happens, the catchment area features differences in the runoff characteristics. Nonetheless, it is important to remember that, because of its small size and its Alpine characteristics, this catchment features rapid hydrological processes characterized by short times of residence, so the differences caused by a spatial heterogeneity of the soil moisture within the catchment are usually small. The low fraction of new water in the in-channel water found in the hydrograph separations suggests that superficial runoff does not play an important role in the sediment transport dynamics. In fact, the main sources in low-intensity floods seem to be the channel bed and the bank erosion. The main factor limiting the transport capacities is the decoupling between the upper and lower part of the basin.

Overall, Rio Cordon catchment shows a stability trend, which can be interrupted if a high intensity flood event takes place. If this happens, some source areas remain active for some time after the event, and the following events (both rainfall and snowmelt) show higher supply conditions. In the case of ordinary floods, the intensity of the rainfall and the sediment supply from the previous events play a key role in the sediment transport dynamics. The heterogeneity found between events and from year to year emphasizes the importance of performing studies based on long-term series to properly analyze and predict the dynamics of the suspended sediments in mountainous areas. The results of this work highlight the important role of long-term data series analyses in the study the suspended sediment dynamics.

As a final remark, the author would like to emphasize the necessity of intensive monitoring and extended analyses for understanding the dynamics of the fine sediment fluxes, interpreting the interactions of the factors influencing them and predicting the suspended sediment loads. Despite recent important advantages, the main limitation in sediment transport studies is the availability of long-term data. In fact, studies of the suspended sediment transport in mountain catchments with an extended monitoring period are rare in literature. This work takes advantage of data series collected through a long period, and combines them with information about the location of the sediment sources in the catchment. This has permitted to assess the high influence of the extraordinary events in the hydrological behavior of the following months and years. The analyses show also that the quantity of transported material is not directly correlated to the magnitude of the runoff volumes, highlighting the unpredictability of the sediment transport processes. These results evidence the need of further studies in the Rio Cordon catchment in order to find out which are the variables that we are missing that would better explain the high variability of the transport dynamics. The analysis of the continuous recorded data from the monitoring station should be combined with more field campaigns during flood events, in order to gather greater data series and assess more reliable results. It would be interesting to combine the extension of the methods explained in this work with new approaches. In particular, a quantitative approach based on sediment sources tophographic monitoring and on connectivity indicies would be very helpful in order to evaluate the real sediment supply within the catchment. Studies in the future should also focus on the role of the vegetation and the exposure in the soil moisture temporal and spatial variability in the hillslopes of the Rio Cordon catchment, and in the correlation between this moisture and the sediment transport dynamics.

CHAPTER FIVE- REFERENCES

- Abdelwahab O. M. M., Bisantino T., Milillo F., Gentile F., 2013. Runoff and sediment yield modeling in a medium-size Mediterranean watershed. Journal of Agricultural Engineering 44(s2): 31-40. DOI: 10.4081/jae.2013.s2.e7.

- Abdelwahab O. M. M. , Bingner R. L. , Milillo F., Gentile F., 2014. Effectiveness of alternative management scenarios on the sediment load in a Mediterranean agricultural watershed. Journal of Agricultural Engineering XLV(430): 125-136. DOI:10.4081/jae.2014.430

- Aich V., Zimmermann A., Elsenbeer, H., 2014. Quantification and interpretation of suspended-sediment discharge hysteresis patterns: How much data do we need? Catena 122, 120-129.

- Alexandrov Y., Laronne J. B., Reid I., 2007. Intra-event and interseasonal behaviour of suspended sediment in flash floods of the semiarid northern Negev, Israel. Geomorphology 85: 85-97. DOI: 10.1016/j.geomorph.2006.03.013

- Anderson C. W., 2005. Turbidity (version 2). U. S. G. S. Techniques of Water Resources Investigations Book 9, chapter A6, section 6.7, 64 pp.

- Arnborg L., Walker H. J., Peippo J., 1967. Suspended load in the Colville River, Alaska, 1962. Geogr. Ann., 49A, 131-144.

- Asselman N. E. M., 1999. Suspended sediment dynamics in a large drainage basin: the River Rhine. Hydrological Processes 13, 1437-1450.

- Asselman N. E. M., 2000. Fitting and interpretation of sediment rating curves. Journal of Hydrology 234, 228-248.

- Axelsson V., 1967. The Laitaure Delta- a study of deltaic morphology and processes. Geogr. Ann. 49A, 1-127.

- Banasik K., Bley D. (1994) An attempt at modeling suspended sediment concentration after storm events in an Alpine torrent. Lecture Notes in Earth Sci. 52, 161–170.

- Barsch D., Gude M., Mäusbacher R, Schujraft G, Sculte A., 1994. Sediment transport and discharge in a high arctic catchment (Liefdefjorden, NW Spitsbergen), in Dynamics and Geomorphology of Mountain Rivers, edited by P. Ergenzinger and K.-H. Schmidt, 225 – 237, Springer, Berlin.

- Bathrust J., Graf W. H., Cao H. H., 1987. Bed load discharge equations for steep mountain rivers. Sediment Transport in Gravel-Bed Rivers, edited by C.R. Thorne, J.C. Bathurst and R.D.Hey, John Wiley & Sons Ltd., 453–477

- Bathurst J. C., 2007. Effect of coarse surface layer on bed-load transport. Journal of Hydraulic Engineering ASCE 133 (11), 1192-1205.

- Benkhaled A., Higgins H., Chebana F., Necir A., 2013. Frequency analysis of annual maximum suspended sediment concentrations in Abiod wadi, Biskra (Algeria). Hydrological Processes(2013) 1-14.

- Berman E. S. F., Gupta M., Gabrielli C., Garland T., McDonnell J. J., 2009. High-frequency field-deployable isotope analyzer for hydrological applications. Water Resources Research 45 (10), W10201.

- Billi P., 1994. Morfologia dei corsi d'acqua. Verde Ambiente, 5, 61-70.

- Billi P., D'Agostino V., Lenzi M.A., Marchi L., 1998. Bedload, slope and channel processes in a high altitude Alpine torrent. In: Gravel-Bed Rivers in the Environment (ed. by P. C. Klingeman, R. L. Beschta, P. D. Komar & J. B. Bradley), 15–38. Water Resources Publication, LLC, Littleton, Colorado, USA.

- Bisantino T, Bingner R, Chouaib W., Gentile F., Trisorio Liuzzi, G. 2015. Estimation of runoff, peak discharge and sediment load at the event scale in a medium-size Mediterranean watershed using the AnnAGNPS model. Land Degradation & Development 26: 340-355. doi: 10.1002/ldr.2213.

- Bogen J., 1995. Sediment transport and deposition in mountain rivers. In Sediment and water quality in river catchments, I.D.L. Foster, A.M. Gurnell, B.W. Webb (eds.), J. Wiley, Chichester, 437-451.

- Borselli L., Cassi P., Torri D., 2008. Prolegomena to sediment and flow connectivity in the landscape: A GIS and fiend numetrical assessment. Catena, 75, 268-277.

- Brasington J, Richards K., 2000. Turbidity and suspended sediment dynamics in small catchments in the Nepal Middle Hills. Hydrological Processes 14, 2559–2574.

- Brummer C. J., Montgomery D. R., 2006. Influence of coarse lag formation on the mechanics of sediment pulse dispersion in a mountain stream, Squire Creek, North Cascades, Washington, United States. Water Resources Research 42, 1-16.

- Buchanan P.A., Schoellhamer D.H., 1998, Summary of suspended-solids concentration data, San Francisco Bay, California, Water Year 1996: U.S. Geological Survey Open-File Report 98-175, pp. 59.

- Buendia C., Vericat D., Batalla R. J., Gibbins, C. N., 2015. Temporal dynamics of sediment transport and transient in-channel storage in a highly erodible catchment. Land Degradation and Development, doi : 10.1002/ldr.2348.

- Buffington J.M., Montgomery D.R., 1997. A systematic analysis of eight decades of incipient motion studies, with special reference to gravel-bedded rivers. Water Resour. Res., 33(8), 1993-2029.

- Burger H. 1945. Der Wasserhaushalt im Valle di Melera von 1934/35 bis 1943/44, Mitteilungen der Eidgen¨ossischen Anstalt f¨ur dasforstliche Versuchswesen, 24, Heft 1, 133–218 (in German).

- Burt T. P., Gardiner A. T., 1982. Runoff and sediment production in a small peat covered catchment: Some preliminary results. In Catchment experiments in fluvial geomorphology, edited by T. P. Burt and D. E. Walling. Norwich: Geo Books, 133–51.

- Buttle J. M., 1994. Isotope hydrograph separations and rapid delivery of pre-event water from drainage basins. Prog. Phys. Geog. 18, 16-41.

- Caissie D., Pollock T. L., Cunjak R. A., 1996. Variation in stream water chemistry and hydrograph separation in a small drainage basin. Jouranl of Hydrology 178, 137-157.

- Cavalli M., 2009. Caratterizzazione idrologica e morfologica dei bacini montani mediante scansione laser da aeromovile. Ph.D thesis. University of Padua, TeSAF dipartment, pp. 186 (in Italian).

- Cavalli M., Trevisani S., Comiti F., Marchi L., 2013. Geomorphometric essassment of spatial sediment connectivity in small Alpine catchments. Geomorphology, 188, 31-41.

- Cavalli M., Tarolli P., Dalla Fontana G., Marchi L., 2016. Multi-temporal analysis of sediment source areas and sediment connectivity in the Rio Cordon catchment (Dolomites). Rendiconti online della Società Gelologica Italiana, 39, 27-30. Doi: 10-3301/ROL.2016.39.

- Collins D. N., 1990. Seasonal and annual variations of suspended sediment transport in meltwaters draining from an Alpine glacier. In: Hydrology in Mountainous Regions. I-Hydrological Measurements: The Water Cycle(eds. H. Lang & A. Musy) (Proc. Lausanne Symp, August 1900), 439-446. IAHS Publ. 193.

- Comiti F., Mao L., 2012. Recent Advances in the Dynamics of Steep Channels, in Gravel-Bed Rivers: Processes, Tools, Environments (eds. M. Church, P. M. Biron and A. G. Roy), John Wiley & Sons, Ltd, Chichester, UK. doi: 10.1002/9781119952497.ch26

- D'Agostino V., Lenzi M.A., Marchi, L., 1994. Sediment transport and water discharge during high flows in an instrumented watershed. In: Dynamics and Geomorphology of Mountain Rivers. Ed: Ergenzinger P. & Schmidt K.H., Lecture Notes in Earth Sciences, 52, Springer Verlag, Berlin-Heidelberg, 67-81.

- Dalla Fontana G., 1992. Caratteri salient dell'idrologia del bacino. In Il bacino attrezzato del Rio Cordon vol. 13 (ed. by L. Marchi), 144-158 Regione Veneto, Quaderni di Ricerca Italy (in Italian).

- Dalla Fontana G., Marchi L., 1994. Sediment source areas in a small alpine basin. In Forest Hydrology (Proc. International Symposium, Oct. 24-28, Tokyo, Japan), 455-462.

- Dalla Fontana G., Marchi L., 2003. Slope-area relationships and sediment dynamics in two alpine streams. Hydrological Processes 17, 73-87.

- DeBoer D. H., Campbell I. A., 1989. Spatial scale dependence of sediment dynamics in a semi-arid badland drainage basin. Catena 16, 277-290.

- De Girolamo A. M., Pappagallo G., Lo Porto A., (2015) Temporal variability of suspended sediment transport and rating curves in a Mediterranean river basin: The Celone (SE Italy). Catena 128, 135-143.

- Diplas P., Parker G. 1992. Deposition and removal of fines in gravel-bed streams. In: Dynamics of Gravel-bed Rivers (eds. P. Billi, R. D. Hey, C. R. Thorne & P. Tacconi), 313–329.

- Diplas P., Kuhnle R. A., Gray J. R., Glysson G. D., Edwards T. E., 2008. Sediment transport measuremens. In Sedimentation Engineering, American Society of Civil Engineering annuals and Reports on Engineering Practice, Manual 110, Chapter 5, 307-353.

- Duijsings J. J. H. M., 1986. Seasonal variation in the sediment delivery ratio of a forested drainage basin in Luxembourg. In Drainage Basin Sediment Delivery, ed. Hadley R.F.. IAHS Publication 159. IAHS Press, Wallingford, UK, 153-164.

- Dunne T., Black R., 1970. Partial area contributions to storm runoff in a small New England watershed. Water Resources Research 6, 1296-1331.

- Eads R. E., 2002. Continuous turbidity monitoring in streams of north-western California. In Turbidity and Other Sediment Surrogates Workshop, April 30- May 2, Reno, Nevada.

- Eder A., Strauss P., Krueger T., Quinton J. N., 2010. Comparative calculation of suspended sediment loads with respect to hysteresis effects (in the Petzenkirchen catchment, Austria). Journal of Hydrology 389, 168-176.
- Eder A., Exner-Kittridge M., Strauss P., Blöchl G., 2014. Re-suspension of bed sediment in a small stream-results from two flushing experiments. Hydrological Earth Sciences 18, 1043-1052.

- Engler A., 1919. Einfluss des Waldes auf den Stand der Gewässer. Mitteilungen der Schweizerischen Anstalt für das forstliche Versuchswesen, 12. Band: 1-626 (in German).
- Fang N. F., Shi Z. H., Chen F. X., Zhang H. Y., Wang Y. X., 2015. Discharge and suspended sediment patterns in a small mountainous watershed with widely distributed rock fragments. Journal of Hydrology 528: 238-248. doi: 10.1016/j.jhydrol.2015.06.046
- Fattorelli S., Keller H.M., Lenzi M.A. & Marchi L., 1988. An experimental station for the automatic recording of water and sediment discharge in a small alpine watershed. Hydrol. Sciences Journal 33(6), 607–617.
- Faulkner H., 2008. Connectivity as a crucial determinant of badland morphology and evolution. Geomorphology 100 (1–2), 91–103.
- Fritz P., Cherry J., Weyer K., Sklash M., 1976. Storm runoff analyses using environmental isotopes and major ions. In: Interpretation of Environmental Isotope and Hydrochemical Data in Groundwater, Panel Proceedings Series-International Atomic Energy Agency. International Atomic Energy Agency, Vienna, Austria, pp. 111–130.
- Fritz C., Gatto G., Silvano S., 1992. Caratteristiche geolitologiche, geomorfologiche e dissesti. In Il bacino attrezzato del Rio Cordon vol. 13 (ed. by L. Marchi), 144-158 Regione Veneto, Quaderni di Ricerca (in Italian).
- Fryirs K., 2013. (Dis)Connectivity in catchment sediment cascades: a fresh look at the sediment delivery problem. Earth Surface Processes and Landforms 38, 30-46.
- García-Rama A., Pagano S.G., Gentile F., Lenzi M.A., 2016. Suspended sediment transport analysis in two Italian instrumented catchments. Journal of Mountain Sciences 13 (6), doi:10.1007/s11629-016-3858-x.
- Genereux D., 1998. Quantifying uncertainty in tracer-based hydrograph separation. Water resources research, 34, 915-919.
- Gentile F, Bisantino T, Corbino R, Milillo F., Romano G., Trisorio Liuzzi G., 2008. Sediment transport monitoring in a Northern Puglia watershed. WIT Transactions on Engineering Sciences 60, 153-161.

- Gentile F., Bisantino T., Corbino R., Milillo F., Romano G., Trisorio Liuzzi G., 2010a. Monitoring and analysis of suspended sediment transport dynamics in the Carapelle torrent (Southern Italy). Catena 80, 1-8.

- Gentile F, Bisantino T, Trisorio Liuzzi G 2010b. Erosion and sediment transport modeling in Northern Puglia watersheds. WIT Transactions on Engineering Sc. 67, 199-212.

- Gippel C. J., 1995. Potential of turbidity monitoring for measuring the transport of suspended solids in streams. Hydrological Processes 9, 83-97.

- Gomi T., 2003. Bed load transport in managed steep-gradient headwater streams of southeastern Alaska. Water Resources Research 39 (12), 1336, doi: 10.1029/2003WR002440, 2003.

- Gray J. R., Gartner J. W., 2010. Technological advances in suspended sediment surrogate monitoring. Water Resources Research 45, W00D29, doi:10.1029/2008WR007063.

- Gray J. R., Glysson G. D., Turcios L. M., Schwarz G. E., 2000. Comparability of suspended sediment concentration and total suspended solids data. In U. S. G. S. Water Res. Investigations Report 00-4191, p. 14.

- Gray J. R., Glysson G. D., Edwards T. E., 2008. Suspended-sediment samplers and sampling method. In Sediment Transport Measurements, Sedimentation Engineering. American Society of Civil Engineers, Manual 110, 320-39.

- Gray J. R., Gartner J. W., Anderson C. W., Fisk G. G., Glysson G. D., Gooding D. J., Hornewer N. J., Larsen M. C., Macy J. P., Rasmussen P. P., Wright S. A., Ziegler A. C., 2010. Surrogate technologies for monitoring suspended sediment transport in rivers. Sedimentology of Aqueous Systems 1, (Ed by Gray J. R. &. & Garner J. W.) Blackwell Publishing, pp. 44.

- Hangen E., Lindenlaub M., Leibundgut Ch., von Wilpert K., 2001. Investigating mechanisms of stormflow generation by natural tracers and hydrometric data: a small catchment study in the Black Forest, Germany. Hydrological Processes 15, 183–199.

- He Q., Owens P., 1995. Determination of suspended sediment provenance using caesium-137, unsupported lead-210 and radium-226: a numerical mixing model approach. In: Sediment and Water Quality in River Catchments. (ed. By I. Foster, A. Gurnell & B. Webb), 207–227..

- Heckmann T., Schwanghart W., 2013. Geomorphic coupling and sediment connectivity in an alpine catchment- Exploring sediment cascades using graph theory. Geomorphology 182, 89-103.

- Heppell C. M , Chapman A. S., 2005. Analysis of a two-component hydrograph separation model to predict herbicide runoff in drained soils. Agricultural Water Management 79, 177–207.

- Herrmann, A., Stichler, W., 1980. Groundwater–runoff relationships. Catena 7 (1), 251–263.

- Hinderer M., Kastowski M., Kamelger A., Bartolini C., Schlunegger C., 2013. River loads and modern denudation of the Alps –A review. Earth-Science Reviews 118, 11–44.

- Hooke J., 2003. Coarse sediment connectivity in river channel systems: a conceptual framework and methodology. Geomorphology 56 (1–2), 79–94.

- Huth A. K., Leydecker A., Sickman J. O., Bales R. C., 2004. A two-component hydrograph separation for three high-elevation catchments in the Sierra Nevada, California. Hydrological processes 18, 1721-1733.

- Iovino F., Puglisi S., 1989. Il bacino strumentato Bonis tributario del torrente Cino nel versante Ionico Silano (Calabria). Quaderni di Idronomia Montana, 9, 159-169 (in Italian).

- Jansson M., 1992. Turbidimeter measurements in a tropical river, Costa Rica. Erosion and sediment transport monitoring programs in river basins (Oslo Symposium Proceedings, August 1992),IAHS Publ. 210, 71-78.

- Jansson M., 2002. Determining sediment source areas in a tropical river basin, Costa Rica. Catena 47, 63-84.

- Jeje L. K., Ogunkoya O. O., Oluwatimilehin J. M., 1991. Variation in suspended sediment concentration during storm discharges in three small streams in upper Osun basin, Central Western Nigeria. Hydrol. Processes 5, 361-369.

- Keller H. M. 1965. Hydrologische Beobachtungen im Flyschgebiet beim Schwarzsee (Kt. Freiburg), Mitteilungen der Eidgen¨ossischenAnstalt f¨ur das forstliche Versuchswesen, 41, Heft 2, 21–60 (in German).

- Kendall C., McDonnell J.J., 1998. Isotope Tracers in Catchment Hydrology. Elsevier Science Limited, Amsterdam.

- Klaus J., McDonnell J. J., 2013. Hydrograph separation using stable isotopes: Review and evaluation. Journal of Hydrology 505, 47-64.

- Klein M., 1984. Anti-clockwise hysteresis in suspended sediment concentration during individual storms. Catena 11, 251-257.

- Korup O., 2005. Geomorphic imprint of landslides on alpine river systems, southwest New Zealand. Earth Surface Processes and Landforms 30 (7), 783–800.

- Krueger T., Quinton J. N., Freer J., Macleod C. J. A., Bilotta G. S., Brazier R. E., Butler P., Haygarth P. M., 2009. Uncertainties in data and models to describe event dynamics of agricultural sediment and phosphorus transfer. Journal of Environmental Quality 38, 1137-1148.

- Laudon, H. Slaymaker O., 1997. Hydrograph separation using stable isotopes, silica and electrical conductivity: an alpine example. Journal of Hydrology 201, 82-101.

- Lenzi M.A., 2000. Variation in suspended sediment concentration during floods in the instrumented catchment of the Rio Cordon. In: Dynamics of Water and Sediments in Mountain Basins. Ed: Lenzi M.A., Quaderni di Idronomia Montana, 20, 53-67.

- Lenzi M. A., 2001. Step-pool evolution in the Rio Cordon, Northeastern Italy. Earth Surface Processes and Landforms, 26, 991-1008.

- Lenzi M.A., 2004. Displacement and transport of marked pebbles, cobbles and boulders during floods in a steep mountain stream. Hydrological Processes 18(10), 1899-1914.

- Lenzi M. A., Marchi L., 2000. Suspended sediment load during floods in a small stream of the Dolomites (Northeastern Italy). Catena, 39, 267-282.

- Lenzi M. A., Mao L., 2003. Analisi del contributo del trasporto solido in sospensione alla produzione di sedimento del bacino del Rio Cordon nel periodo 1986 – 2001. Quaderni di Idronomia Montana 21(1): 361-379 (in Italian).

- Lenzi M. A., Billi P., D'Agostino V., 1997. Effects of an extremely large flood on the bed of a steep mountain stream. Management of landscapes disturbed by channel incision, Stabilization, rehabilitation, restoration. (Ed by Wang S.S.Y., Langendoen E.J. & Shields F.D.Jr.), 19-23 Maggio 1997, Oxford, The University of Mississippi, 1061-1066.

- Lenzi M. A., D'Agostino V., Billi P., 1999. Bedload transport in the instrumented catchment of the Rio Cordon. Part I: Analysis of bedload recods, conditions and threshold of bedload entrainment. Catena, 36(3), 171-190.

- Lenzi M. A., Mao L., Comiti F. 2003. Interannual variation of suspended sediment load and sediment yield in an alpine catchment. Hydrological Sciences Journal, 48(6), 899-915.

- Lenzi M.A., Mao L., Comiti F., 2004. Magnitude-frequency analysis of bed load data in an Alpine boulder bed stream. Water Resour.Res. 40 (7), W072011-W0720112.

- Lenzi M. A., Mao L., Comiti F., 2006a. Effective discharge for sediment transport in a mountain river: Computational approaches and geomorphic effectiveness. J. Hydrol. 326 (1-4), 257-276.

- Lenzi M. A., Mao L., Comiti F., 2006b. When does bedload transport begin in steep boulder-bed streams? Hydrological Processes 20, 3517-3533.

- Lewis J., 2002. Estimation of suspended sediment flux in streams using continuous turbidity and flow data coupled with laboratory concentrations. In Turbidity and Other Sediment Surrogates Workshop, April 30- May 2, Reno, Nevada.

- Liu W., Lu H., Duan W., Li H., 2011. Runoff generation in small catchments under a native rain forest and a rubber plantation in Xishuangbanna, southwestern China. Water Environ. J. 25 (1), 138–147.

- López-Tarazón J. A., Batalla R. J., Vericat D., Francke T., 2012. The sediment budget of a highly dynamic mesoscale catchment: The River Isábena. Geomorphology 138, 15-28.

- Mao L. 2004. Analisi comparativa del trasporto solido di corsi torrentizi in diversi ambiti geografici. Ph.D thesis, University of Padua, TeSAF Department, p. 307 (in Italian).

- Mao L., Uyttendaele G. P., Iroumé A., Lenzi M. A., 2008. Field based analysis of sediment entrainment in two high gradient streams located in Alpine and Andine environments. Geomorphology 93, 368-383.

- Mao L., Cavalli M., Comiti F., Marchi L., Lenzi M. A., Arattano M., 2009. Sediment transfer processes in two Alpine catchments of contrasting morphological settings. Journal of Hydrology 364, 88-98.

- Mao L., Comiti F., Lenzi M. A., 2010. Bedload Dynamics in Steep Mountain Rivers: Insights from the Rio Cordon Experimental Station (Italian Alps). In: Bedload-surrogate monitoring technologies, edited by: Gray, J. R., Laronne, J. B., and Marr, J. D. G., 253–265.

- Marchi L., Arattano M., Deganutti A. M., 2002. Ten years of debris flow monitoring in the Moscardo torrent (Italian Alps). Geomorphology 46 (1/2), 1-17.

- Marks K., Bates P., 2000. Integration of high-resolution topographic data with floodplain flow models. Hydrological Processes, 14, 2109-2122.

- McHale M. R., McDonnell J. J., Mitchell M. J., Cirmo C.P., 2002. A field-based study of soil water and groundwater nitrate release in an Adirondack forested watershed. Water Resour. Res. 38 (4), 1031.

- McKean J., Roering J., 2004. Objective landslide detect on and surface morphology mapping using high-resolution airbone laser altimetry. Geomorphology, 57, 331-351.

- McNamara, J.P., Kane, D.L., Hinzman, L.D., 1997. Hydrograph separations in an Arctic watershed using mixing model and graphical techniques. Water Resour. Res. 33 (7), 1707–1719.

- Mitasova, H., Hofierka, J., Zlocha, M., Iverson, L. R., 1996. Modelling topographic potential for erosion and deposition using GIS. International Journal of Geographical Information Systems 10, 629-641.

- Montgomery D. R., Buffington R. 1997. Channel-reach morphology in mountain drainage basins. Geol. Soc. of Am. Bulletin 109, 596-611.

- Moore R. D., 1989. Tracing runoff sources with deuterium and oxygen-18 during spring melt in a headwater catchment, southern Laurentians, Quebec. Journal of Hydrology 112, 135-148.

- Mouri G., Ros F. C., Chalov S., 2014. Characteristics of suspended sediment and river discharge during the beginning of snowmelt in volcanically active mountainous environments. Geomorphology 213, 266-276.

- Muñoz-Villers L. E., McDonnell J. J., 2012. Runoff generation in a steep, tropical montane cloud forest catchment on permeable volcanic substrate. Water Resources Res. 48 (9), W09528.

- Navratil O., Lagout C., Gateuille D., Esteves M., Liebault F., 2010. Assessment of intermediate fine sediment storage in a braided river reach (southern French Prealps). Hydrological Processes 24, 1318-1332.

- Nitsche M., Rickenmann D., Turowski J.M., Badoux A., Kirchner J.W., 2011. Evaluation of bedload transport predictions using flow resistance equations to account for macro- roughness in steep mountain streams. Water Resour.Res. 47. W08513.

- Nolan K. M., Lisle T. E., Kelsey H. M., 1987. Bankfull discharge and sediment transport in northwestern California. In Erosion and Sedimentation in the Pacific Rim (Proceedings of the Corvallis Symposium, August, 1987). IAHS Publ. 165, 439-449.

- Pagano S. G., García-Rama A., Gentile F. 2016. Analisi del trasporto solido in sospensione a scala di evento: un confronto tra due bacini strumentati italiani. Quaderni di idronomia Montana, 34.

- Pagano S.G., García-Rama A., Gentile F., Lenzi M.A., (under review). Water discharge-suspended sediment concentration hysteresis patterns during single hydrologic events in two Italian experimental catchments Submitted to Catena.

- Paustian S. J., Beschta R. L., 1979. The suspended sediment regime of an Oregon Coast Range stream. Water Research Bulletin 15, 144-154.

- Pellerin A. B., Wollheim W. M., Feng X., Vörösmarty C. J., 2007. The application of electrical conductivity as a tracer for hydrograph separation in urban catchments. Hydrological Processes DOI: 10.1002/hyp.

- Penna D., Stenni B., Šanda M., Wrede S., Bogaard T. A., Gobbi A., Borga M., Fisher B. M. C., Bonazza M., Chárová Z, 2010. On the reproducibility and repeatability of laser absorption spectroscopy measurements for δ^2H and $\delta^{18}O$ isotopic analysis. Hydrology and Earth System Sciences 14, 1551-1566.

- Penna D., Stenni B., Šanda M., Wrede S., Bogaard T.A., Michelini M., Fisher B.M.C., Gobbi A., Mantese N., Zuecco G., Borga M., Bonazza M., Sobotková M., Čejková B., Wassenaar L.I., 2012. Technical Note: Evaluation of between-sample memory effects in the analysis of ^2H and ^{18}O water samples measured by laser spectroscopes. Hydrology and Earth System Sciences, 16, 3925–3933.

- Penna D., Oliviero O., Assendelft R., Zuecco G., van Meerveld I. (H. J.), Anfodillo T., Carraro V., Borga M., Dalla Fontana G., 2013. Tracing the water sources of trees and streams: isotopic analysis in a small pre-alpine catchment. Procedia Environmental Sciences 19, 106-112.

- Penna D., van Meerveld, H. J., Oliviero O., Zuecco, G., Assendelft, R. S., Dalla Fontana, G., Borga, M., 2015. Seasonal changes in runoff generation in a small forested mountain catchment. Hydrological Processes 29, 2017-2042.

- Picco L., Mao L., Rigon E., Moretto J., Ravazzolo D., Delai F., Lenzi M. A., 2012. An update of the magnitude-frequency analysis of Rio Cordon (Italy) bedload data after 25 years of monitoring. IAHS-AISH Publication, pp. 65-71.

- Pinder G., Jones J., 1969. Determination of the ground-water component of peak discharge from the chemistry of total runoff. Water Resources Research 5, 438-445.

- Rainato R., Picco L., Lenzi M.A., Mao L., Delai F., Rigon E., Moretto J., Cesca M., Vianello A., García-Rama A., 2013. Monitoring and analysis of the sediment transport event of November 2012 in the Rio Cordon station. Quaderni di Idronomia Montana 31, 323-338.

- Rainato R., Mao L., García-Rama A., Picco L., Cesca M., Vianello A., Preciso E., Scussel G. R., Lenzi M.A., 2016. Three decades of monitoring in the Rio Cordon instrumented basin: Sediment budget and temporal trend of sediment yield; doi: 10.1016/j.geomorph.2016.03.012

- Recking A., 2012. Influence of sediment supply on mountain streams bedload transport. Geomorphology, 175-176, 139-150.

- Recking A., Leduc P., Liébault F., Church, M., 2012. A field investigation of the influence of sediment supply on step-pool morphology and stability. Geomorphology, 139-140, 53-66.

- Rickenmann D., 1997. Sediment transport in Swiss Torrents. Earth Surface Processes and Landforms, 22, 937-951.

- Rickenmann D., 1999. Empirical relationships for debris flows. Natural Hazards. 19 (1), 47-77.

- Rigon E., Comiti F., Lenzi M. A., 2012. Large wood storage in streams of the Eastern Italian Alps and the relevance of hillslope processes. Water resources Research, 18, W01518, doi:10.1029/2010WR009854.

- Schlunegger F., Hinderer M. 2003. Pleistocene/Holocene climate change, re-establishment of fluvial drainage network and increase in relief in the Swiss Alps. Terra Nova, 15, 88–95.

- Seeger M, Errea M. P., Beguería S., Arnáez J., Martí, C., García-Ruiz, J. M., 2004. Catchment soil moisture and rainfall characteristics as determinant factors for discharge/suspended

sediment hysteretic loops in a small headwater catchment in the Spanish Pyrenees. Journal of Hydrology 288, 299-311.

- Simons D.B., Senturk F., 1977. Sediment Transport Technology. Water Resources Publications, Fort Collins, CO, pp. 807.
- Smith H.G., Dragovich D., 2009. Interpreting sediment delivery processes using suspended sediment-discharge hysteresis patterns from nested upland catchments, south-eastern Australia. Hydrological Processes 23, 2415-2426, doi: 10.1002/hyp.7357.
- Soler M., Latron J., Gallart F., 2008. Relationships between suspended sediment concentrations and discharge in two small research basins in a mountainous Mediterranean area (Vallcebre, Eastern Pyrenees). Geomorphology 98, 143-152.
- Straub L. S., 1936. Report of the committee on dynamics of streams. Transactions, American Geophysical Union 17, Issue 2, 334-334.
- Sueker J. K., Ryan J. N., Kendall C., Jarrett R. D., 2000. Determination of hydrologic pathways during snowmelt for alpine/subalpine basins, Rocky Mountain National Park, Colorado. Water Resour. Res. 36 (1), 63–75.
- Taylor S., Feng X., Williams M., McNamara J., 2002. How isotopic fractionation of snowmelt affects hydrograph separation. Hydrological processes 16, 3683-3690.
- Turowski J. M., Rickenmann D., 2009. Tools and cover effects in bedload transport observations in the Pizbach, Austria. Earth Surface Processes and Landforms 34, 26-37.
- Turowski J. M., Rickenmann D., Dadson S. J., 2010. The partitioning of the total sediment load of a river into suspended load and bedload: a review of empirical data. Sedimentology 57(4):1126–1146.
- Turowski J.M., Badoux A., Rickenmann D., 2011. Start and end of bedload transport in gravel bed streams. Geophysical Research Letters, 38.

- Uhlenbrook S., Hoeg S., 2003. Quantifying uncertainties in tracer-based hydrograph separations: a case study for two-, three- and five-component hydrograph separations in a mountainous catchment. Hydrol. Process. 17 (2), 431–453.

- Uhrich M.A., Bragg H.M., 2003. Monitoring instream turbidity to estimate continuous suspended-sediment loads and yields and clay-water volumes in the Upper North Santiam River Basin, Oregon, 1998–2000. U.S.G. S. Water-Resources Investigations Report 03–4098, 43 p.

- Wainwright J., Turnbull L., Ibrahim TG, Lexartza-Artza I., Thornton SF, Brazier RE. 2010. Linking environmental regimes, space and time: interpretations of structural and functional connectivity. Geomorphology 126, 387-404.

- Walling D.E. 1983. The sediment delivery problem. Journal of hydrology, 65. 209-237.

- Walling D. E., Webb, B. W., 1981. The reliability of suspended sediment load data. Erosion and Sediment Transport Measurement, 177–194, IAHS Publ. 133.

- Walling D. E., Owens P. N. , Leeks G. J. L., 1998. The role of channel and floodplain storage in the suspended sediment budget of the River Ouse, Yorkshire, UK. Geomorphology 22, 225-242.

- Whittaker J. G, Jaeggi M. N. R., 1982. Origin of step–pool systems in mountain streams. American Society of Civil Engineers, Journal of Hydraulic Division 108, 758–773.

- Whittaker J. G. 1987. Sediment transport in step–pool streams. Sediment transport in Gravel-Bed Rivers. Thorne CR, Bathurst JC,Hey RD (eds). Wiley: Chichester, 545–579.

- Wilcox A. C., Wohl E. E., 2006. Flow resistance dynamics in step-pool stream channels: 1. Large woody debris and controls on total resistance. Water Resour.Res. 42. W05418.

- Williams G. P., 1989. Sediment concentration versus water discharge during single hydrologic events in rivers. Journal of Hydrology 111, 89-106.

- Wolman M. G., Miller, J. P., 1960. Magnitude and frequency of forces in geomorphic processes. Journal of Geology, 68, 54-74.

- Wood P. A., 1997. Controls of variation in suspended sediment concentration in the River Rother, West Sussex, England. Sedimentology 24, 437-445.

- Wood M.S., 2014. Estimating suspended sediment in rivers using acoustic Doppler meters. U.S. Geological Survey Fact Sheet 2014-3038, 4 p., http://dx.doi.org/10.3133/fs20143038.

- Yager E.M., Turowski J.M., Rickenmann D., McArdell B.W., 2012. Sediment supply, grain protrusion, and bedload transport in mountain streams. Geophys. Res. Lett., 39, L10402.

- Yu G. A., Wang Z. Y., Zhang K., Chang T. C., Liu H., 2009. Effect of incoming sediment on the ransport rate of bedload in mountain streams. International Journal of Sediment Research 24, 260-273.

- Zabaleta A., Martínez M, Uriarte J. A., Antigüedad I., 2007. Factors controlling suspended sediment yield during runoff events in small headwater catchments of the Basque Country. Catena 71, 179-190.

AKNOWLEDGEMENTS

First of all, I would like to thank Professor M. A. Lenzi, who gave me the opportunity to develop this Ph.D, and has always guidden through this patway with his precious advices.

I would like to express my gratitude to the Arpav agency, in particular to Mateo Cesca, Alessandro Vianello and Walter Testor, for the collaborations and all their helpful work in the Rio Cordon.
I express my sincere gratitude to Stefano Pagano and Professor Francesco Gentile, from Bari University, for the enlightening collaboration we have performed through these three years.
I would also want to thank Lorenzo Picco and Riccardo Rainato for their help, and also Emanuel Rigon and Johnny Moretto, from whom I learned so much while they were still at the TESAF department. I am so grateful to Alessia Tonon, because it has been much easier to face the challenges having her help and company. Thanks also to all the staff of the TESAF department for being so problem-solving with all the paperwork.

Thanks to the Padova friends, especially Anna, Bledar, Miki, Enrico and Maurilia, for being my "Italian family" and make me feel protected and supported even in the worst periods.

A special thanks goes to my parents and my brother, who have always supported my decisions and have always given me their unconditional comprehension and love.

Finally, thanks to Ricardo for helping me raise the head and look further.